EFFECTS OF EXISTING SURFACE STRUCTURES ON SETTLEMENTS INDUCED BY TUNNELING

by

Charisis – Sotirios Th. Chatzigogos

Diploma in Civil Engineering (2001)
Aristotle University of Thessalonica

Submitted to the Department of Civil and Environmental Engineering
In Partial Fulfillment of the Requirements for the Degree of Master of Engineering
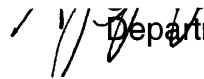in Civil and Environmental Engineering

at the

Massachusetts Institute of Technology

June 2002

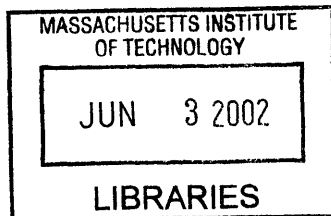© 2002 Massachusetts Institute of Technology

Signature of Author..

....

/ Department of Civil and Environmental Engineering
May 24, 2002

Certified by ....

....
Andrew J. Whittle
Professor of Civil and Environmental Engineering
Thesis Supervisor

Accepted by ....

....
Oral Buyukozturk
Chairman, Department of Committee on Graduate Students

EFFECTS OF EXISTING SURFACE STRUCTURES ON SETTLEMENTS INDUCED BY TUNNELING

By

CHARISIS SOTIRIOS TH. CHATZIGOGOS

ABSTRACT

Reliable prediction of potential structural damage caused by tunneling-induced ground movements is a very important factor in assessing the environmental impacts and costs of urban soft ground tunnel projects. Conventional practice relies on prior empirical data to estimate ground movements for "greenfield" conditions (no structures present) and then evaluates the effects of these displacements on overlying structures. This approach can be highly conservative (i.e., grossly overestimates the potential structural damage), imposing unrealistic or unnecessary constraints on the tunnel design or leading to unrealistic estimates for remedial costs. The alternative approach is based on predictions from non-linear finite element analyses that are highly sensitive to modeling of stress changes caused by tunnel construction and soil behavior. A recent design procedure presented by Potts and Addenbrooke (1997) has been used to evaluate effects of soil-structure interaction in the construction of the Jubilee Line Extension project in London. Their procedure uses simplified 2D FE models and simulates an overlying structure as a deep elastic beam (with equivalent axial and bending stiffness) with soil properties typical of conditions in London clay.

This thesis provides an independent assessment of the results presented by Potts and Addenbrooke (P&A). Underlying assumptions regarding the ground loss at the tunnel cavity, the initial K_0 stress state, the modeling of soil behavior and drainage conditions are all examined using the non-linear 2-D FE program Plaxis. Although these analyses confirm some key findings, such as the linearity between ground loss and centerline surface settlement, they also show that the initial K_0 value, drainage conditions and modeling of non-linear soil stiffness are all important factors in predicting the ground movements. Analyses using the Hardening soil model are successful in replicating the modification factors proposed by P&A for modeling effects of soil-structure interaction for a shallow tunnel in London clay. Although it is not possible to develop generic design methods for different ground conditions, the P&A design procedure offers a logical methodology that can be applied with other site-specific soil profiles. Further research is needed to address the underlying uncertainties in modeling 3-D stress changes around advancing tunnel headings for different methods of construction.

Thesis Supervisor: Andrew J. Whittle
Title: Professor of Civil and Environmental Engineering

TABLE OF CONTENTS   p.

TABLE OF FIGURES   p.

CHAPTER 1
INTRODUCTION AND GENERAL PRINCIPLES

1.1 GENERAL INTRODUCTION

In recent years, assessment of the environmental impact of major construction projects has become a normal and required procedure. While such projects may have significant short or long – term environmental benefits, they can also create significant environmental impacts. Impacts of construction include construction traffic, noise, vibration and dust as well as temporary restrictions on access to certain roads and other public areas. Longer-term impacts would include land and building acquisition, traffic and ventilation noise and vibration levels, and other impacts such as pollution, groundwater changes and effects on ecology.

An environmental impact of large urban tunneling projects, which is causing increasing public awareness and concern is that of subsidence and its effects on structures and services. Since construction of tunnels and deep excavations is inevitably accompanied by ground movements it is essential that both for engineering design and for planning and consultation, rational procedures are developed for assessing the risks of damage. Apparently the assessment of risk of potential damage is coupled with the requirement for implementation of effective protective measures, which can be deployed when predicted levels of damage are judged to be unacceptable.

The purpose of this thesis is focused mainly on the primary step in this sequence of assessments or implementation of protective measures, which concerns the assessment of the risk of potential damage to existing structures. This by itself is a rather broad topic as it will be presented later. In the attempt to assess the risk of damage to a structure due to a nearby tunneling operation a very important step is the determination of the deformation that the structure will undergo. Or else, if the movements of the foundations are known then the potential of damage for the structure can be evaluated. The calculation of these movements is a facet of a complicated phenomenon of interaction in which the structure, the underlying soil and the tunnel structure interact. Until relatively recently the interaction between soil, structure and tunnel was not taken into consideration. Ground movements were evaluated for "greenfield" conditions. These "greenfield" deformations are then assumed to act on the existing structure. Such an approach leads to unrealistically conservative interpretations of potential structural damage.

This thesis presents analyses of soil – structure interaction caused by shallow tunnel construction in soft ground. This is viewed as a contribution in obtaining a more accurate description of the movements that may develop in the foundation level of a structure and evidently in a more accurate prediction to whether and to what extent protective measures should be implemented. The following paragraphs of this first chapter present a general introduction to the basic principles that govern this problem as well as a brief discussion of the some well-accepted techniques and assessments used in conventional practice

1.2 SUGGESTED DEFINITIONS AND SYMBOLS FOR THE DEFORMATION OF FOUNDATIONS

The following definitions will be used throughout this thesis. They are bases on previous studies by Burland and Wroth (1974) and Boscardin and Cording (1989).

1. A change of length equal to δL over a length L gives rise to a <u>strain</u> $\varepsilon = \delta L/L$. A shortening of $-\delta L$ over a length L gives rise to a <u>compressive strain</u> $\varepsilon = -\delta L/L$. It is obvious, from the above definitions, that the tensile strain or simply strain is considered of positive sign whereas the compressive strain is considered of negative sign.
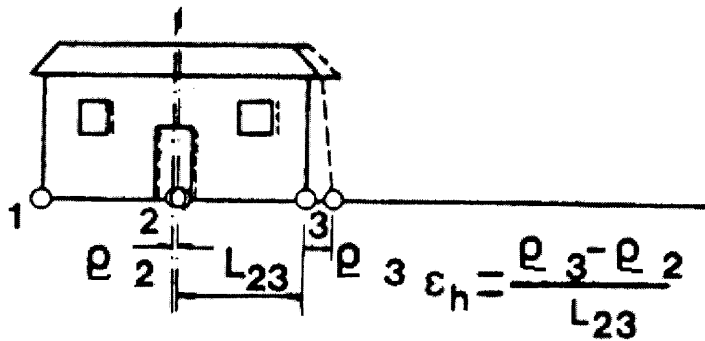
Figure 1.1. Definition of horizontal strain in the foundation of a structure (after Burland and Wroth, 1974)

2. <u>Settlement</u> is denoted by the symbol ρ and implies that the displacement is downwards. If the displacement is upwards it is termed heave and denoted ρ_h.

3. <u>Differential or relative settlement</u> is denoted by the symbol $\delta\rho$. <u>Differential or relative heave</u> is denoted by the symbol $\delta\rho_h$. In the figure below we define the settlement of C relative to D as $\delta\rho_{CD}$ and is taken to be positive. The settlement of B relative to A is denoted as $\delta\rho_{DC}$, which equals $-\delta\rho_{CD}$.

4. <u>Maximum differential settlement</u> is denoted by $\delta\rho_{max}$.

5. <u>Rotation</u> is denoted by θ and is used to describe the change in gradient of the straight line joining two reference points embedded in the foundation or ground.
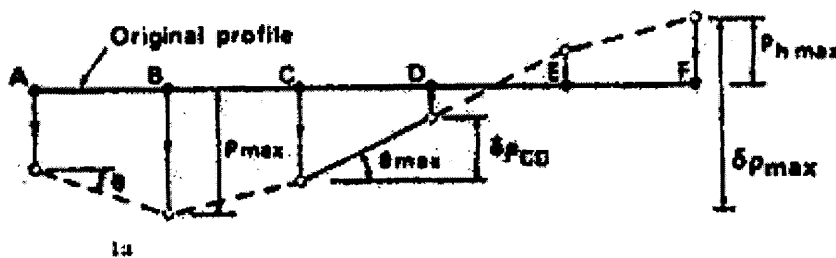
Figure 1.2. Definition of settlement ρ, relative settlement $\Delta\rho$ and rotation θ in the foundation of a structure (after Burland and Wroth, 1974)

6. Tilt is denoted by ω and normally describes the rigid body rotation of the whole superstructure or of a well – defined part of it. Normally it is not possible to ascertain the tilt unless details of the superstructure and its behavior are known. Even then it can be difficult when the structure itself flexes. The figure below shows diagrammatically the tilt ω of a building overlying points A, B and C.

7. Relative rotation is denoted by β and describes the rotation of the straight line joining two reference points relative to the tilt. The angular distortion as defined by many authors (e.g. Skempton and MacDonald, 1956) is identical to the relative rotation β.
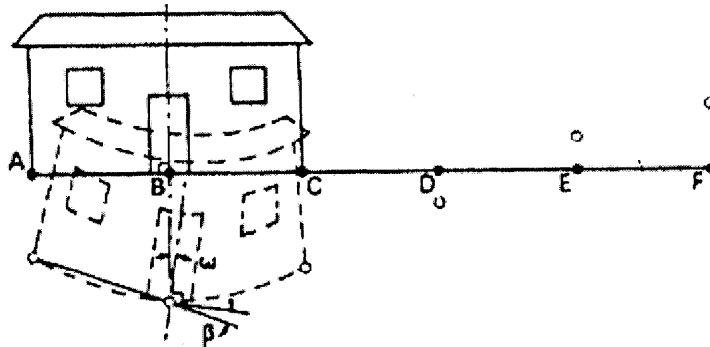
Figure1.3. Definitions of tilt ω and relative rotation (angular distortion) β (after Burland and Wroth, 1974)

8. Angular strain is defined by α. From the figure below it can be seen that the angular strain at B is given by the following expression:

$$\alpha_B = \frac{\delta\rho_{AB}}{l_{AB}} + \frac{\delta\rho_{BC}}{l_{AB}}$$

Angular strain is positive if it produces sag or upward concavity, as at B in the figure below, and negative if it produces hog or downward concavity as at E. The quantity of angular strain is very useful for predicting crack widths in buildings in which movement occurs at existing cracks or lines of weakness. Note that if the deformed profile between the three points ABC is smooth the average curvature is given by $2\alpha_B/L_{AC}$.
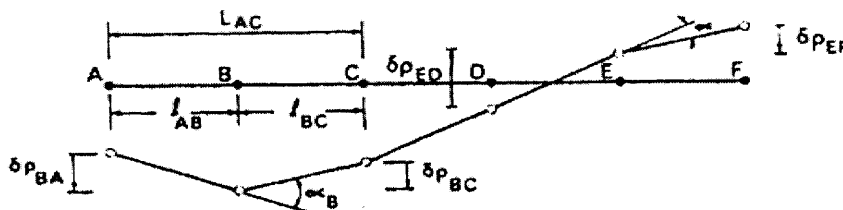
Figure 1.4. Definition of angular strain α (after Burland and Wroth, 1974)

3

9. <u>Relative deflection</u> (relative sag or relative hog) is denoted by Δ and is the maximum displacement relative to the straight line connecting two reference points a distance L apart. Relative sag produces upward concavity as at B for which Δ is positive. Relative hog produces downward concavity for which Δ is negative as at D.

10. <u>Deflection ratio</u> (sagging ratio or hogging ratio) is denoted by Δ/L or, in a simpler manner, by DR. The sign convention is the same as for the relative deflection. Note that when $l_{AB} = l_{BD}$ or the deformed profile is approximately circular then $\alpha = 4\Delta/L_{AD}$. In Figure 1.5 a sagging deflection ratio DR^{sag} is defined in the area of relative sagging L_{AD} as Δ_{AD} / L_{AD}. A hogging deflection ratio DR^{hog} is defined in the area of relative hogging L_{DF} as the ratio Δ_{DF} / L_{DF}. The deflections Δ_{AD} and Δ_{DF} are the maximum deflections in the areas L_{DA} and L_{DF} respectively.
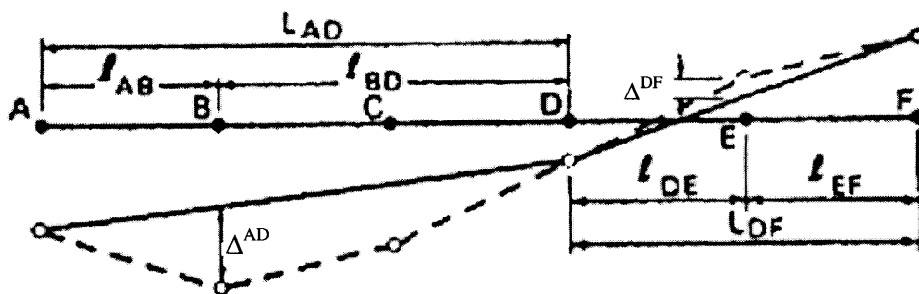
Figure 1.5. Definition of relative deflection (sag or hog) Δ and deflection ratio Δ/L (or more simply DR) (after Burland and Wroth, 1974)

- The preceding list of deformation parameters could be extended to describe three – dimensional effects. However, this list is considered to be adequate for interpreting in-plane predictions of soil – structure movement.

- For describing the deformation of the superstructure, we will apply the well – understood and defined physical quantities from the strength of materials.

1.3 GROUND MOVEMENT DUE TO TUNNELING

The construction of tunnels will inevitably be accompanied by movement of the ground around them. At the ground surface these movements manifest in what is called a "settlement trough". Figure 1.6 shows diagrammatically the surface settlement trough above an advancing tunnel. For "greenfield" sites, the shape of this trough transverse to the axis of the tunnel approximates closely to a normal Gaussian distribution curve – an idealization that has considerable mathematical advantages.
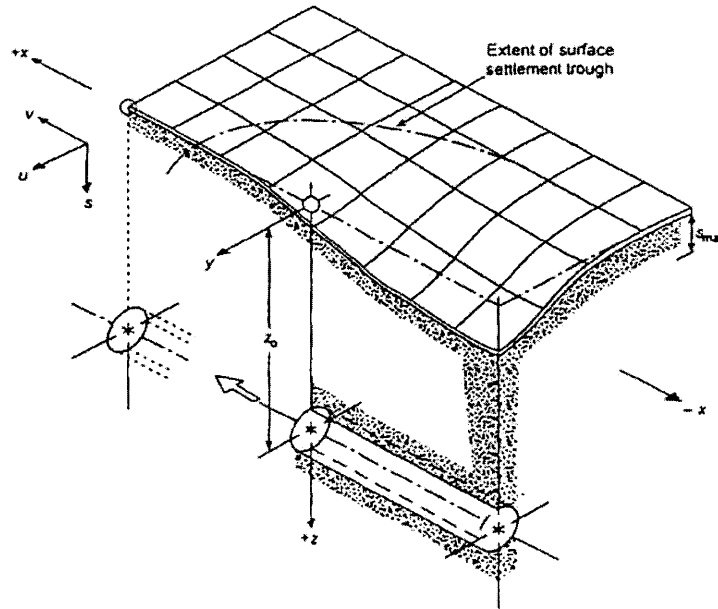
Figure 1.6. Surface settlement trough above an advancing tunnel (after Attewell et al., 1986)

Figure 1.7 shows such an idealized transverse settlement trough. Attewell et al. (1986) and Rankin (1988) have summarized the current widely used empirical approach to the prediction of immediate surface and near surface ground displacements. The settlement s in given by:

$$s = s_{max}e^{-\frac{y^2}{2i^2}}$$

(1.1)

where s_{max} is the maximum settlement and i is the value of y at the point of inflection. It has been found that, for most purposes, i can be related to the depth of the tunnel axis z_0 by the linear expression:

$$i = Kz_0 \qquad \qquad \text{(1.2)}$$

The trough width parameter K depends on the soil type. It varies from 0.2 to 0.3 for granular soils through 0.4 to 0.5 for stiff clays to as high as 0.7 for soft silty clays (Mair et al., 1993). As a general rule the width of the surfcace settlement trough is about three times the depth of the tunnel for tunnels in clay strata. It is important to note that, although the value of K for surface settlements in approximately constant for various depths of tunnel in the same ground, Mair et al. (1993) have shown that its value increases with depth for subsurface settlements.
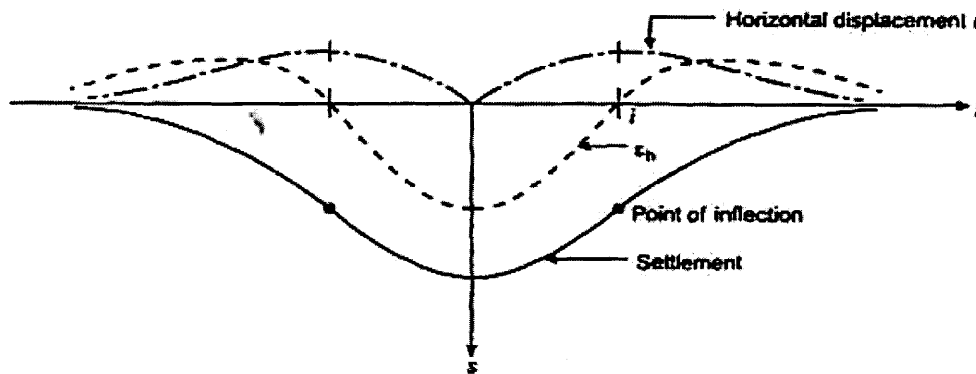
Figure 1.7. Transverse settlement trough (after Attewell et al., 1986)

The immediate settlements caused by tunneling are usually characterized by the "Volume Loss" V_L that is the volume of the surface settlement trough per unit length V_S expressed as a percentage of the notional excavated volume of the tunnel.

Integration of Equation 1.1 gives:

$$V_s = \sqrt{2\pi} i s_{max} \qquad \qquad \text{(1.3)}$$

so that

$$V_L = \frac{3.192\, i s_{max}}{D^2} \qquad \qquad \text{(1.4)}$$

where D is the diameter of the tunnel. Combining equations 1.1, 1.2 and 1.4, one obtains the surface settlement s at any distance y from the centerline:

$$s = \left[\frac{0.313V_L D^2}{K z_0} \right] \exp\left[\frac{-y^2}{2K^2 z_0^2} \right]$$

(1.5)

Horizontal displacements due to tunneling

Building damage can also result from horizontal extension of the ground and therefore predictions of horizontal movement are required. Unlike settlements, there are few case histories where horizontal movements have been measured. The data that do exist show reasonable agreement with the assumption of O' Reilly and New (1982) that the resultant vectors of ground movement are directed towards the tunnel axis. It follows that the horizontal displacement u can be related to the settlement s by the expression:

$$u = \frac{sy}{z_0}$$

(1.6)

Equation 1.6 is easily differentiated to give the horizontal strain ε_h at any location on the ground surface.

Figure 1.7 shows the relation between the settlement trough, the horizontal displacements and the horizontal strains occurring at ground level. In the region $i > y > -i$, the horizontal strains are compressive. At the points of inflection the horizontal displacements are a maximum and $\varepsilon_h = 0$. For $i < y$ the horizontal strains are tensile.
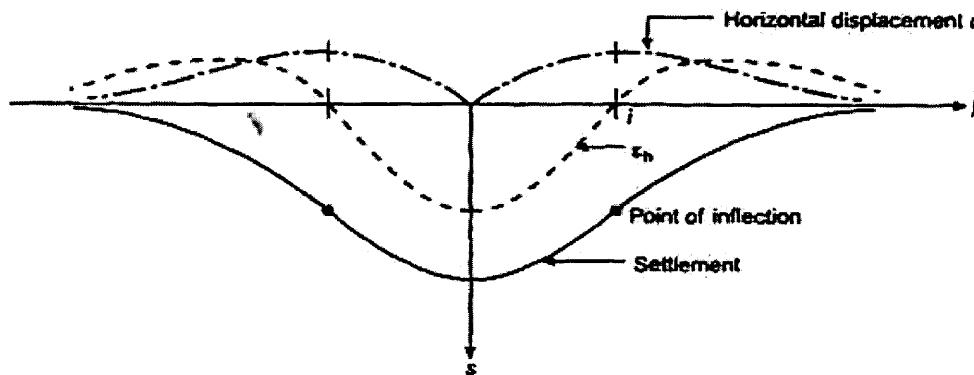
Figure 1.7. Transverse settlement trough and relation between the trough, the horizontal displacements and the horizontal strains (after Attewell et al., 1986)

7

Assessment of surface displacements due to tunneling

The above empirical equations provide a simple means for estimating the near surface displacements due to tunneling assuming greenfield conditions, i.e. ignoring the presence of the any building or structure.

A key parameter in this assessment is the volume loss V_L. This results from a variety of effects, which include movement of ground into the face of the tunnel and radial movement towards the tunnel axis due to reductions in supporting pressures. The magnitude of V_L is critically dependent on the type of ground, the ground water conditions, the tunneling method (EPB or slurry shield, NATM, etc.), the length of time in providing positive support and the quality of supervision and control. The selection of an appropriate value for V_L for design requires experience and is generally aided by well-documented case histories in similar conditions.

1.4 CLASSIFICATIONS OF BUILDING DAMAGE

Classification of building damage has been traditionally divided into three general categories after those employed by Skempton and MacDonald (1956) in their classic paper "The allowable settlement of buildings". These classifications, architectural damage, functional damage and structural damage are described as follows:

- Architectural damage affects the appearance of structures and is usually related to cracks or separations in panel walls, floors and finishes. Cracks in plaster walls greater than 0.5mm wide and cracks in masonry or rough concrete walls greater than 1mm wide are considered to be representative of a threshold where damage is noticed and reported by building occupants.
- Functional damage affects the use of the structure and is exemplified by jammed doors and windows, extensively cracked and failing plaster, tilting of walls and floors and other damage that would require nonstructural repair to return the building to its full service capacity.
- Structural damage affects the stability of the structure, usually related to cracks or distortions in primary support elements such as beams, columns and load bearing walls.

It is only a short step from the above three broad categories of damage to the more detailed classification given in Table 1.1. This defines six categories of damage, numbered 0 to 5 in increasing severity. Normally categories 0, 1 and 2 relate to aesthetic damage and 5 represents damage affecting "stability" as was first proposed by Burland et al. (1977) who drew on the work of Jennings and Kerrich (1962), the U. K. National Coal Board (1975) and McLeod and Littlejohn (1974). Since then it has been adopted with only slight modifications by BRE (1981 and 1990) and the Institution of Structural Engineers, London (1978, 1989, 1994 and 2000).

The system of classification in Table 1.1 is based on "ease of repair" of the visible damage. Thus, in order to classify visible damage it is necessary, when carrying out the survey, to assess what type of work would be required to repair the damage both internally and externally. The following important notes should be noted:

- The classification relates only to the visible damage at a given time and not to its cause or possible progression, which are separate issues.
- The strong temptation to classify the damage solely on crack width must be resisted. It is the ease of repair, which is the key factor in determining the category of damage.
- The classification was developed for brickwork or block work and stone masonry. It could be adapted for other forms of cladding. It is not intended to apply to reinforced concrete structural elements.
- More stringent criteria may be necessary where damage may lead to corrosion, penetration or leakage of harmful liquids and gases or structural failure.

Besides defining numerical categories of damage, Table 1.1 also lists the "normal degree of severity" associated with each category. These descriptions of severity relate to standard domestic and office buildings and serve as a guide to building owners and occupiers. In special circumstances, such as for a building with valuable or sensitive finishes, this ranking of severity may not be appropriate.

Category of damage	Normal degree of severity	Description of typical damage (Ease of repair in italics) Note: Crack width is only one factor in assessing category of damage and should not be used on its own as a direct measure of it.
0	Negligible	Hairline cracks less than about 0.1mm
1	Very Slight	*Fine cracks which are easily treated during normal decoration.* Damage generally restricted to internal wall finishes. Close inspection may reveal some cracks in external brickwork or masonry. Typical crack widths up to 1mm.
2	Slight	*Cracks easily filled. Re-decoration probably required. Recurrent cracks can be masked by suitable linings.* Cracks may be visible externally and *some repointing may be required to ensure weather-tightness.* Doors and windows may stick slightly. Typical crack widths up to 5mm.
3	Moderate	*The cracks require some opening up and can be patched by a mason. Repointing of external brickwork and possibly a small amount of brickwork to be replaced.* Doors and windows sticking. Service pipes may fracture. Weather-tightness often impaired. Typical crack widths are 5 to 15mm or several greater than 3mm.
4	Severe	*Extensive repair work involving breaking-out and replacing sections of walls, especially over doors and windows.* Windows and door frames distorted, floor sloping noticeably[1]. Walls leaning[1] or bulging noticeably, some loss of bearing in beams. Service pipes disrupted. Typical crack widths are 15 to 25mm but also depends on the number of cracks.
5	Very severe	*This requires a major repair job involving partial or complete rebuilding.* Beams lose bearing, walls lean badly and require shoring. Windows broken with distortion. Danger of instability. Typical crack widths are greater than 25mm but depends on the number of cracks.

NOTE. Local deviation of slope, from the horizontal or vertical of more than 1/100 will normally be clearly visible. Overall deviations in excess of 1/150 are undesirable.

Table 1.1. Classification of visible damage to walls with particular reference to ease of repair of plaster and brickwork or masonry (after Burland, Standing, Jardine, 2002)

The division between categories 2 and 3

The dividing line between categories of damage 2 and 3 is particularly important. Studies of many case records shows that damage up to category 2 can result from a variety of causes, either from within the structure itself (e.g. shrinkage or thermal effects) or associated with the ground. Identification of the cause of damage is usually very difficult and frequently it results from a combination of causes. If the damage exceeds category 2, the cause is usually much easier to identify and it is frequently associated with ground movement. Thus the division between categories of damage 2 and 3 represents an important threshold, which will be referred to later.

1.5 THE CONCEPT OF LIMITING TENSILE STRAIN

Onset of visible cracking – Critical tensile strain

Cracking in masonry walls and finishes usually, but not always, results from tensile strain. Following the work of Polshin and Tokar (1957), Burland and Wroth (1974) investigated the idea that tensile strain might be a fundamental parameter in determining the onset of cracking. A study of the results from numerous large scale tests on masonry panels and walls carried out at the U.K. Building Research Establishment showed that, for a given material, the onset of visible cracking in associated with a reasonably well defined value of average tensile strain which is not sensitive to the mode of deformation. They defined this as the critical tensile strain ε_{crit}, which is measured over the gauge length of a meter or more.

Burland and Wroth (1974) made the following important observations:
- The average values of ε_{crit}, at which visible cracking occurs are very similar for a variety of types of brickwork and are in the range of 0.05% and 0.1%.
- For reinforced concrete beams the onset of visible cracking occurs at lower values of tensile strain in the range 0.03% to 0.05%.
- The above values of ε_{crit} are much larger than the local tensile strains corresponding to tensile failure.
- The onset of visible cracking does not necessarily represent a limit of serviceability. Provided the cracking is controlled, it may be acceptable to allow deformations well beyond the initiation of visible cracking.

Burland and Wroth (1974) showed how the concept of critical tensile strain could be used in conjunction with simple elastic beams to develop deflection criteria for the onset of visible damage. This work will be discussed in more detail later.

Limiting tensile strain – a serviceability parameter

Burland *et al.* (1977) replaced the concept of critical tensile strain with that of limiting tensile strain ε_{lim}. The importance of this development is that ε_{lim} can be used as a

serviceability parameter, which can be varied to take account of differing materials and serviceability limit states.

Boscardin and Cording (1989) developed this concept of differing levels of tensile strain. Seventeen case records of damage due to excavation-induced subsidence were analyzed. This subsidence was actually described by two characteristic quantities that are assumed to cause damage to a building, the angular distortion and the horizontal strain. A variety of building types were involved and they showed that the categories of damage given in Table 1.1 could be broadly related to ranges of ε_{lim}. These ranges are tabulated in Table 1.2. This table is important as it provides the link between estimated building deformations and the possible severity of damage. It should be noted that Boscardin and Cording (1989) describe the damage corresponding to $\varepsilon_{lim} > 0.3\%$ as severe to very severe. However, none of the cases quoted by them exhibit severe damage for this range of strains. There is therefore no evidence to suggest that tensile strains $> 0.3\%$ will result in severe damage.

Category of damage	Normal degree of severity	Limiting Tensile Strain (ε_{lim})(%)
0	Negligible	0 - 0.05
1	Very Slight	0.05 - 0.075
2	Slight	0.075 - 0.15
3	Moderate	0.15 - 0.3
4 to 5	Severe to very severe	>0.3

Table 1.2. Relationship between category of damage and limiting tensile strain (after Boscardin and Cording, 1989)

1.6 STRAINS IN SIMPLE RECTANGULAR BEAMS – DESIGN CURVES FOR DAMAGE

Burland and Wroth (1974) and Burland *et al.* (1977) used the concept of limiting tensile strain to study the onset of cracking in simple elastic beams undergoing sagging and hogging modes of deformation[1]. This simple approach gives considerable insight into the mechanisms controlling cracking. Moreover, it was shown that the criteria for initial cracking of simple beams are in good agreement with the case records of damaged and undamaged buildings undergoing settlement. Therefore, in many circumstances, it is both reasonable and instructive to represent the façade of a building by means of a simple rectangular beam.

The approach adopted by Burland and Wroth (1974) is illustrated in Figure 1.8.
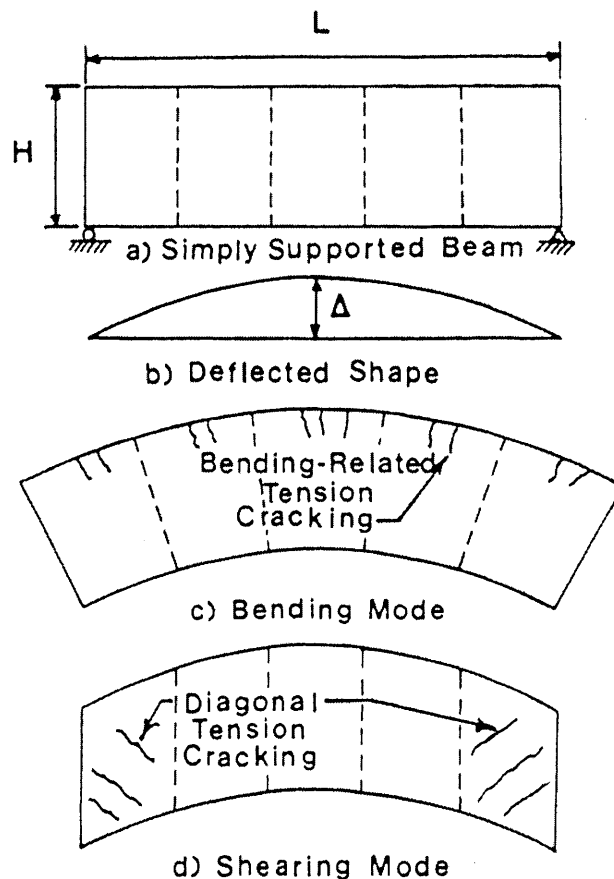
Figure 1.8. Cracking of a simple beam in bending and shear (after Burland and Wroth, 1974)

---

[1] The self – weight of the structures is included as a central point load at top – center of the structure.

The building is represented by a rectangular beam of length L and height H. The problem is to calculate the tensile strains in the beam for a given deflected shape of the building foundations and hence obtain the sagging or hogging ratio Δ/L at which cracking is initiated. It is immediately obvious that little can be said about the distributions of strains within the beam unless we know its mode of deformation. Two extreme modes are bending only about a neutral axis at the center and shearing only (Figure 1.8 (c) and (d) respectively). In the case of bending only, the maximum tensile strain occurs in the upper fiber (bottom fiber for sagging) and that is where cracking will initiate as shown. In the case of shear only, the maximum tensile strains are inclined at 45° giving rise to diagonal cracking. In general both modes of deformation will occur simultaneously and it is necessary to calculate both bending and diagonal tensile strains to ascertain which type is limiting.

The expression for the total mid span deflection Δ of a centrally loaded beam having both bending and shear stiffness is given by Timoshenko (1957) as:

$$\Delta = \frac{PL^3}{48EI}\left[1 + \frac{18EI}{L^2 HG}\right] \tag{1.7}$$

where E is the equivalent Young's modulus and G is the equivalent shear modulus[2]. I is the moment of inertia and P is the point load. The above equation can be written in terms of the deflection ratio Δ/L and the maximum extreme fiber strain ε_{bmax} as follows:

$$\frac{\Delta}{L} = \left[\frac{L}{12t} + \frac{3I}{2yLH}\frac{E}{G}\right]\varepsilon_{b\,max} \tag{1.8}$$

where t is the distance of the neutral axis from the edge of the beam in tension. Similarly for the maximum diagonal strain ε_{dmax} the following equation is obtained:

$$\frac{\Delta}{L} = \left[1 + \frac{HL^2}{18I}\frac{G}{E}\right]\varepsilon_{d\,max} \tag{1.9}$$

Similar expressions are obtained for the case of a uniformly distributed load with the diagonal strains calculated at the quarter points. Therefore, the maximum tensile strains are much more sensitive to the value of Δ/L than the distribution of loading (Burland and Wroth, 1974).

By setting $\varepsilon_{max} = \varepsilon_{lim}$, the above equations define the limiting values of Δ/L for the deflection of simple beams. It is evident that for a given value of ε_{lim} the limiting value of Δ/L (which ever is the lowest for bending and shearing) depends on L/H, E/G and the position of the neutral axis. For example, Burland and Wroth (1974) showed that hogging

---

[2] E and G are not material properties in this case but they are used to simply represent the structural idealization.

with the neutral axis at the bottom edge is much more damaging than sagging in which the neutral axis is in the middle of the structure.

The influence of horizontal strain

It is well accepted that ground surface movements associated with tunneling not only involve sagging and hogging profiles but significant horizontal strains as well. Boscardin and Cording (1989) included horizontal tensile strain ε_h in the above analysis using simple superposition, i.e. it is assumed that the deflected beam is subjected to uniform extension over its full depth. The resultant extreme fiber strain ε_{br} is given by:

$$\varepsilon_{br} = \varepsilon_{bmax} + \varepsilon_h \tag{1.10}$$

In the shearing region, the resultant diagonal tensile strain ε_{dr} can be evaluated using the Mohr's circle of strain. The value of ε_{dr} is then given by:

$$\varepsilon_{dr} = \varepsilon_h \left[\frac{1-v}{2}\right] + \sqrt{\varepsilon_h^2 \left[\frac{1+v}{2}\right]^2 + \varepsilon_{d\,max}^2} \tag{1.11}$$

where v is the Poisson's ratio. The maximum tensile strain is the greater of ε_{br} and ε_{dr}. Thus, for a beam of length L and height H, it is a straightforward matter to calculate the maximum value of tensile strain ε_{max} for a given value of Δ/L and ε_h in terms of t, E/G and v. This value of ε_{max} can then be used in conjunction with Table 2 to assess the potential associated damage. The calculations are easily automated on a computer and the results are presented in Figure 1.9.
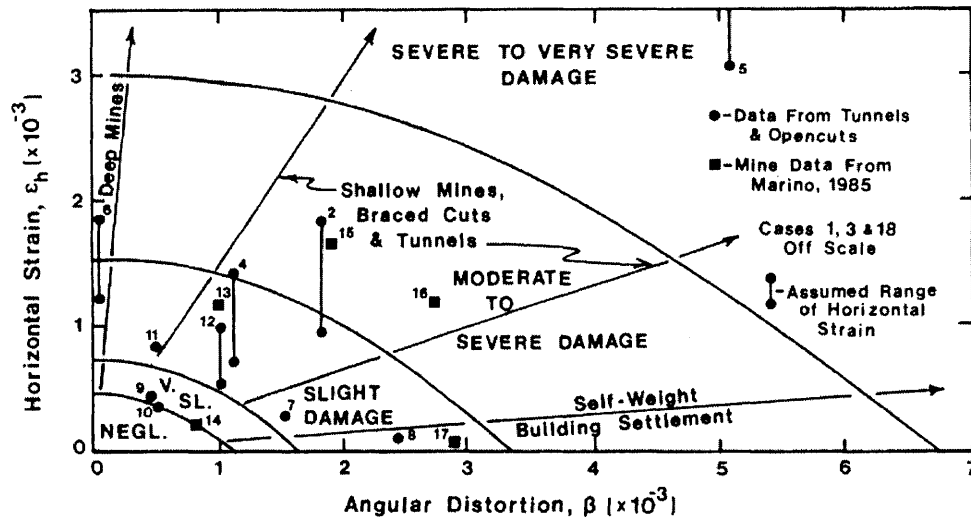
Figure 1.9. Relationship of Damage for Angular Distortion and Horizontal Extension Strain (after Boscardin and Cording, 1989)

Some comments on Figure 1.9 would be revealing:
- At very small angular distortions the curves become horizontal representing the condition where horizontal strains equal critical tensile strains for various levels of damage. (The degree of damage is inserted in the deep beam model assuming that every damage category corresponds to a specific value of critical tensile strain).
- At very low levels of horizontal extension strain, the curves are inclined nearly 45° representing the condition where diagonal tension strains equal the critical tensile strains.
- The different values of critical tensile strengths were obtained by the work of other researchers (Data compiled by Polshin and Tokar (1957), Skempton and MacDonald (1956), Bjerrum (1963), Burland and Wroth (1974)).
- The rays extending out of from the origin of Figure 1.9 indicate the region of the figure where data from various types of excavations are likely to plot.
- The database, which supports the figure, is extremely small, especially in the area near the origin.
- The green field distortions can be selected as input parameters for the use of figure 1.9.The figure below suggests a sound way to do this for the case of a tunnel settlement trough.

Relevant building dimensions

An important consideration is the definition of the relevant height and length of the building. A typical case of a building affected by a single tunnel settlement trough is shown in figure 1.10. The height H is taken as the height from the foundation to the eaves. The roof is usually ignored. It is assumed that a building can be considered separately either side of a point of inflection, i.e. points of inflection of the settlement profile (at foundation level) will be used to partition a building. The length of the building is not considered beyond the practical limit of the settlement trough. In a calculation of building strain, the building span length is required and is defined as the length of building in a hogging and sagging zone and limited by a point of inflection or extent of settlement trough.
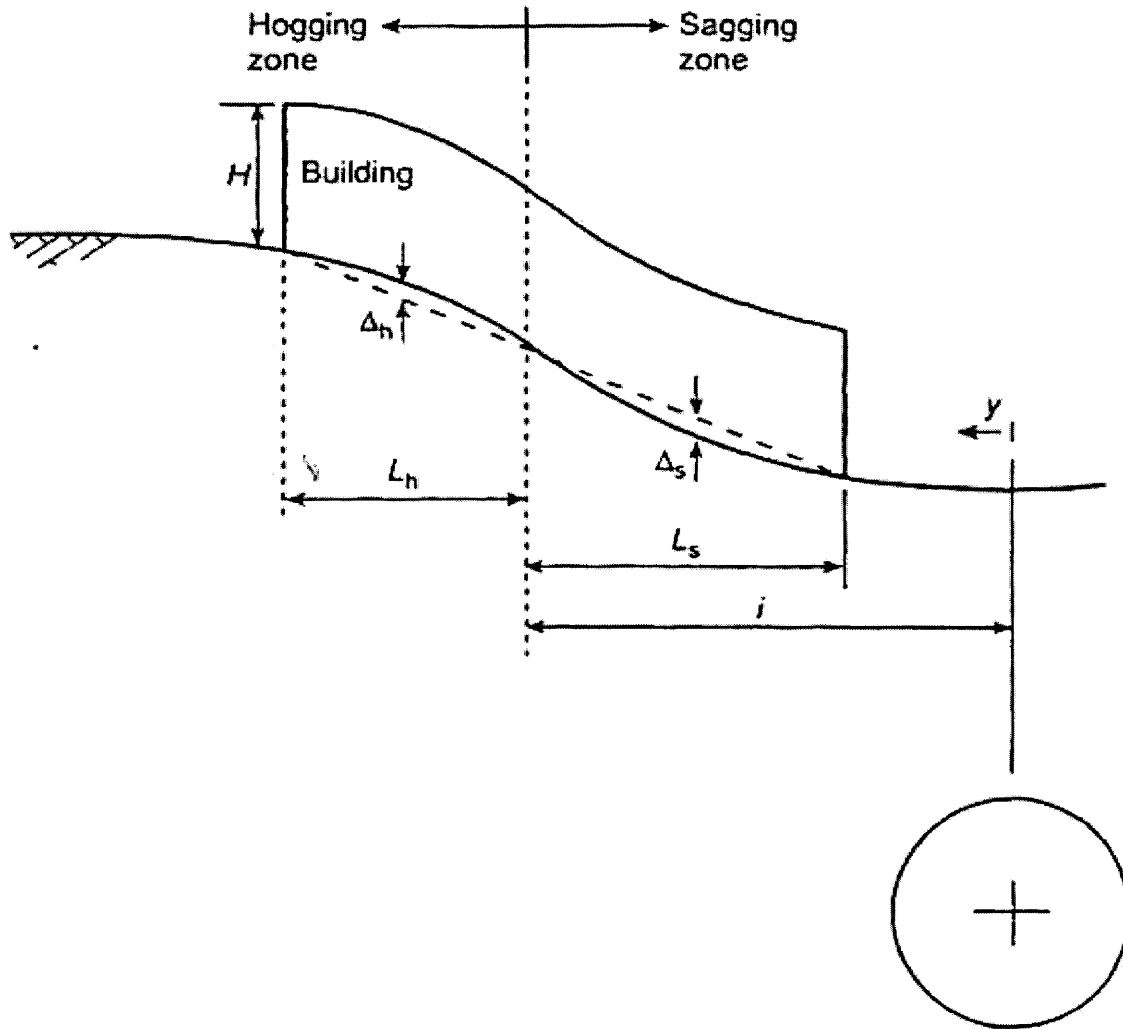
Figure 1.10. Building deformation (after Burland, Standing, Jardine, 2002)

In figure 1.10, the following definitions can be done:

- The deflection ratio in hogging $DR^{hog} = \Delta_h / L_h$
- The deflection ratio in sagging $DR^{sag} = \Delta_s / L_s$

Burland (1995) showed how the aforementioned equations could be used to develop simple charts showing the relationship between the limiting values of Δ/L and horizontal strain for different categories of damage and for various values of L/H. Figure 1.11 shows such a chart for L/H = 1 for a hogging mode of deformation. Other charts would be needed for different ratios of L/H and for different modes of deformation.

There are similarities between Figure 1.11 and Boscardin's and Cording's Figure 1.9 of angular distortion β against ε_h. However, Boscardin's and Cording's chart has the following limitations:
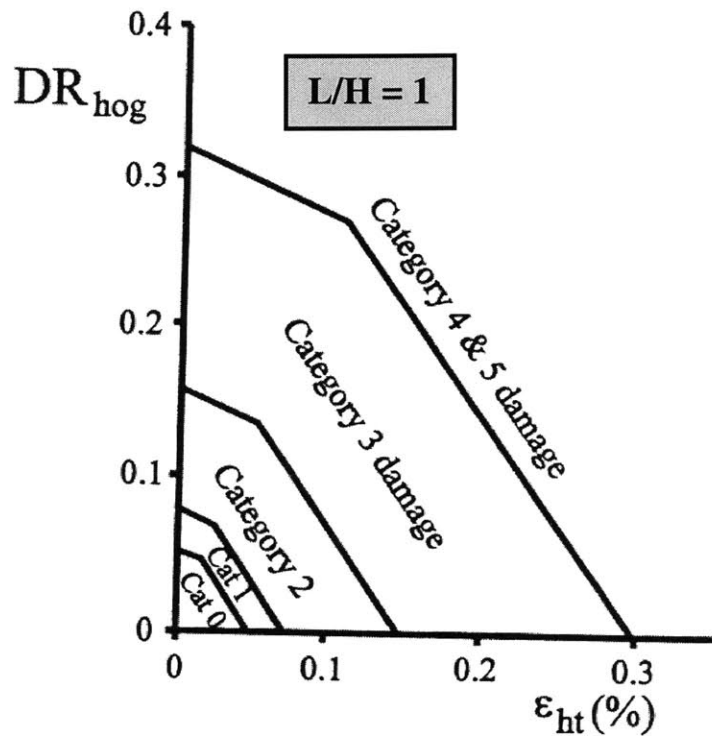
Figure1.11. Relationship of damage category to deflection ratio and horizontal strain for hogging and L/H = 1(after Burland, 1995)

- Maximum bending strains ε_{bmax} are ignored.
- The angular distortion β was assumed to be proportional to Δ/L whereas the relationship is in fact very sensitive to the load distribution.
- The evaluation of β is not always straightforward to compute.

18

1.7 EVALUATION OF THE POTENTIAL OF DAMAGE TO BUILDINGS DUE TO SUBSIDENCE

The various concepts discussed in the previous sections can be combined to develop a rationale for the assessment of damage to buildings due to the soil subsidence during and after tunneling. The following broadly describes the approach that was adopted during the planning and enquiry stages for the Jubilee Line Extension subway in London and the proposed Cross rail project by Burland, Standing and Jardine (2002).

Level of risk

The term "level of risk" or simply "risk", of the damage refers to the possible degree of damage as defined in Table 1. Most buildings are considered to be at "low risk" if the predicted degree of damage falls into the first three categories 0 to 2 (i.e. negligible to slight). At these degrees of damage structural integrity is not at risk and damage can be readily and economically repaired. It will be recalled that the threshold between categories 2 and 3 is a particularly important one. A major objective of design and construction is to maintain the level of risk below this threshold for all buildings. It should be noted that special consideration has to be given to buildings judged to be of particular sensitivity such as those in poor condition, containing sensitive equipment or of particular historical or architectural significance. For such buildings the thresholds given in Table 2 may need to be redefined.

Because of the large number of buildings involved, the method of assessing risk is a staged process as follows; preliminary assessment; second stage assessment; detailed evaluation. These stages will be briefly described now.

Preliminary assessment

So as to avoid a large number of complex and unnecessary calculations, a very simple and conservative approach is adopted for the preliminary assessment. It is based on a consideration of both maximum slope and maximum settlement of the ground surface at the location of each building. According to Rankin (1988) a building experiencing a maximum slope θ of 1/500 and a settlement of less than 10mm has negligible risk of any damage. By drawing contours of the expected ground surface settlement along the route of the proposed tunnel and its associated excavations it is possible to eliminate all buildings having negligible risk. This approach is conservative because it uses ground surface, rather than foundation level, displacements. Also it neglects any interaction between the stiffness of the buildings and the ground. For particularly sensitive buildings it may be necessary to adopt more stringent slope and settlement criteria.

Second Stage Assessment

The preliminary assessment described above is based on the slope and settlement of the ground surface and provides a conservative initial basis for identifying those buildings along the route requiring further study. The second stage assessment makes use of the

work described in the previous sections of this chapter. In this approach, the façade of a building is represented by a simple beam whose foundations are assumed to follow the displacements of the ground in accordance with the greenfield site assumption. The maximum resultant tensile strains are calculated from equations as 1.7 to 1.11. The corresponding potential category of damage, or similarly the level of risk is then obtained from Table 1.2.

The above approach, though considerably more detailed than the preliminary assessment is usually very conservative. Thus the derived categories of damage refer only to possible degrees of damage. In the majority of cases the likely actual damage will be less than the assessed category. The reason for this is that, in calculating the tensile strains, the building is assumed to have no stiffness so that it conforms to the "greenfield" site subsidence trough. In practice, however, the inherent stiffness of the building will be such that its foundations will interact with the supporting ground and tend to reduce both the deflection ratio and horizontal strains.

Detailed Evaluation

Detailed evaluation is carried out on those buildings that, as a result of the second stage assessment, are classified as being at risk of category 3 damage or greater (see Table 1.1). The approach is a refinement of the second stage assessment in which the particular features of the building and the tunneling and/or excavation scheme are considered in detail. Because each case is different and has to be treated on its own merits, it is not possible to lay down detailed guidelines and procedures. Factors that are taken more closely into account include:

Tunneling: The sequence and method of tunnel and excavation construction should be given detailed consideration with a view to reducing volume loss and minimizing ground movements as far as practical.

Structural Continuity: Buildings possessing structural continuity such as those of steel and concrete frame construction are less likely to suffer damage than those without structural continuity such as load bearing masonry and brick buildings.

Foundations: Buildings on continuous foundations such as strip footings and rafts are less prone to damaging differential movements (both vertical and horizontal) than those on separate individual foundations or where there is a mixture of foundations. (e.g. piles and spread footings).

Orientation of the building: Buildings oriented at a significant skew to the axis of a tunnel may be subjected to warping or twisting effects. These may be accentuated if the tunnel axis passes close to the corner of the building.

Soil/Structure Interaction: The predicted greenfield displacements will be modified by the stiffness of the building. The detailed analysis of this problem is exceedingly complex and resort is usually made to simplified procedures some of which are described in the

report published by the Institution of Structural Engineers (1989). The beneficial effects of building stiffness can be considerable, as demonstrated by some recent measurements on the Mansion House during tunneling beneath and nearby in Figure 1.12 (Frischmann et al., 1994). Note that the recorded movements are in the order of millimeters.
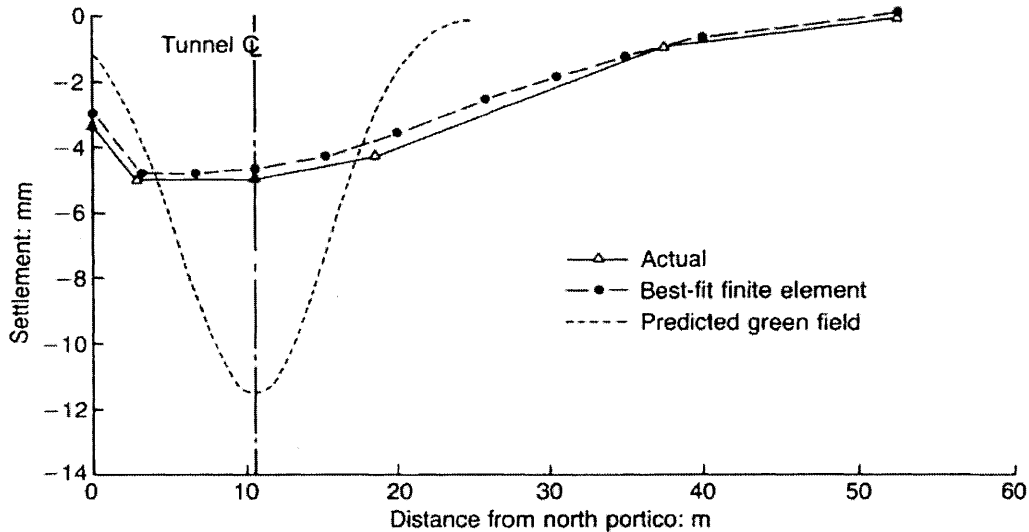
Figure 1.12. Comparison of actual and predicted settlements at west wall of the Mansion House due to 3.05m internal diameter tunnel. (after Frischmann et al., 1994)

As this is the main topic of this thesis, other case records of measured settlement of buildings due to tunneling will be presented later.

Previous movements: The building may have experienced movements due to a variety of causes such as construction, settlement, ground water lowering and nearby previous construction activity. It is important that these effects be assessed as they may reduce the tolerance of the building to future movements.

As many factors are not amenable to precise calculations, the final assessment of possible degree of damage requires engineering judgment based on informed interpretation of available information and empirical guidelines. Because of the inherently conservative assumptions used in the second stage assessment, the detailed evaluation will usually result in a reduction in the possible degree of damage. Following the detailed evaluation, consideration is given as to whether protective measures need to be adopted. These will usually only be required for buildings remaining in damage categories 3 or higher as presented in Table 1.

1.8. PROTECTIVE MEASURES

The range of possible protective measures is summarized briefly below:

- Tunneling: Before considering near surface measures, consideration should be given to measures that can be applied from within the tunnel to reduce the

volume loss. There are a variety of such measures such as increasing support at or near the face, reducing the time to provide such support, the use of fore poling, soil nailing in the tunnel face or the use of a pilot tunnel. These approaches tackle the root cause of the problem and may prove much less costly and disruptive and can have a significant environmental impact.

The main forms of protective measures currently available fall into the following six broad groups:

- Strengthening of the ground by means of ground injection (cement or chemical) or by ground freezing. Its primary purpose is to provide a layer of increased stiffness below foundation level or to prevent loss of ground at the tunnel face during excavation.
- Strengthening of the building in order that it may safely sustain the additional stresses or accommodate deformations induced by ground movements. Such measures include the use of tie – rods and temporary or permanent propping.
- Structural jacking to compensate for settlement.
- Underpinning by introducing an alternative foundation system, which eliminates of minimizes differential movements caused by tunneling.
- Installation of a physical barrier between the foundation of the building and the tunnel. Such a barrier is not structurally connected to the building's foundation and therefore does not provide direct load transfer. The intention is to modify the shape of the settlement trough and minimize ground displacements adjacent to and beneath the building.
- Compensation grouting that consists in the controlled injection of grout between the tunnel and the building foundations in response to observations of ground and building movements during tunneling as illustrated in Figure 1.13. As its name implies, the purpose is to compensate for ground loss. The process involves injecting grout in a controlled way at chosen locations using tubes – a – manchette (TAM) as illustrated in Figure 1.14. A TAM consists of a steel tube with ports at regular intervals along it, which are covered by rubber sleeves that act as one-way valves. The TAM is grouted into a borehole. Grout is injected by inserting the grout delivery probe into the tube and isolating the port to be injected by inflating packers on either side of the injection nozzle. Sufficient pressure is then applied to open the port and initiate flow of grout into the ground. A great advantage is that ports can be re – used a number of times. Successful application of the process requires detailed instrumentation to monitor the movements of the ground and the building. The technique has been recently used with success to projects in London and elsewhere (see for example, Harris et al., 1994)

It cannot be emphasized too strongly that all of the above measures are expensive and disruptive and should not be regarded as a substitute for good quality tunneling practice aimed at minimizing settlement.
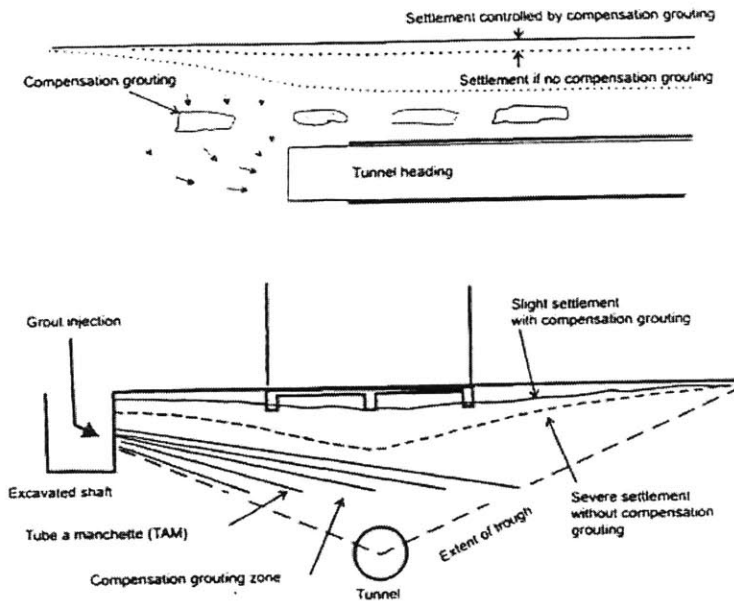
Figure 1.13. The principle of compensation grouting (after Burland, Standing, Jardine, 2002)
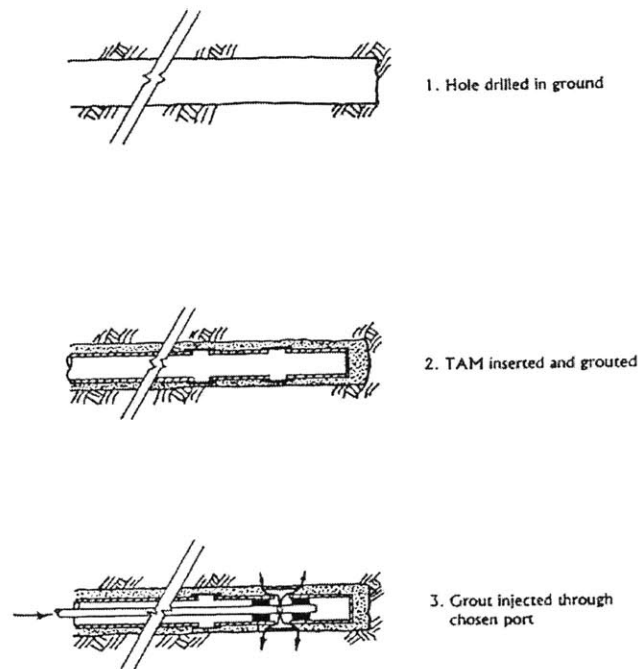
Figure 1.14. The use of TAMs (after Burland, Standing, Jardine, 2002)

CHAPTER 2

THE APPROACH OF POTTS AND ADDENBROOKE ON THE INFLUENCE OF A STRUCTURE ON TUNNELING – INDUCED GROUND MOVEMENTS

2.1 INTRODUCTION

This chapter summarizes the results of numerical studies reported by Potts and Addenbrooke (1997) concerning the influence of an existing structure on tunneling – induced ground movements. This is essential for the understanding of the calculations and the investigations performed in the framework of this thesis, as the work presented by Potts Addenbrooke served as the initial motivation but also as the criterion for comparisons and attempts for validation all through the stage of performing any calculations for this thesis.

The main parameters considered in the Potts and Addenbrooke (1997) study are the width of the structure, its bending and axial stiffness, the building location relative to the tunnel and the depth of the tunnel. The soil structure interaction is shown through the analyses by reference to commonly used building damage parameters, namely the deflection ratio and the maximum horizontal strain. The introduction of relative stiffness parameters, which combine the bending and axial stiffness of the structure with its width and the stiffness of the soil, is essential in establishing design curves for a quantitative assessment of the influence of the structure on the ground movements and more specifically on the settlement trough that will be developed below the building. This modified profile (modified with respect to the supposedly well known "greenfield" profile) can be used to give an initial estimate of likely building damage.

The interest in assessing the influence of tunneling on buildings and vice versa was instructed by the construction of the Jubilee Line Extension in London (e.g. Burland, Standing, Jardine, 2002). It is interesting to note that the majority of the petitions against the Jubilee Line Extension were settlement – related. The problem is apparently an interactive one – not only do tunneling settlements affect existing structures, but existing structures affect tunneling settlements.

Conventional design practice (Peck, 1969 or O'Reilly and New, 1982) consider that if the effect of ground movements are to be assessed on a surface structure, then the building is assumed to be infinitely flexible and will follow the "greenfield" settlement profile. The translations, rotations, strains and deformations so predicted are then compared with limiting criteria to estimate the likely damage to the building. This approach is clearly very conservative but further refinement clearly depends on capabilities to model the effects of existing surface structures reliably.

This thesis considers only the influence of an existing surface structure on the ground movements due to tunneling. A series of 2D numerical analyses have been performed for tunnel construction in the "greenfield" scenario with effects of surface beams of varying stiffness (representing coupling structures). The well established and accepted building

damage parameters of deflection ratio and horizontal strain are considered in modifying the greenfield ground movements. A unifying framework is then developed to account for the relative soil/structure stiffness when predicting levels of building damage. A design approach is thereby proposed which gives an improved assessment of the magnitude of building damage in response to tunneling induced ground movements.

2.2 PARAMETRIC STUDY (Potts and Addenbrooke, 1997)

The geometry of the problem under investigation is shown in Figure 2.1. The tunnel diameter was fixed at D = 4.15m and the depth from the soil surface to the tunnel axis was either Z = 20m or Z = 34m (typical London Underground values for D and Z). A beam of width B, resting on the ground surface with its center at an offset distance e, from the tunnel centerline was used to represent the effect of a surface structure. The fundamental work of Burland and Wroth (1974) lies behind these considerations (see also Chapter 1). Quantities that were changed the parametric study of Potts and Addenbrooke (1997) were:

- The axial stiffness of the beam EA
- The bending stiffness of the beam EI
- The beam width B
- The eccentricity with respect to the tunnel centerline e
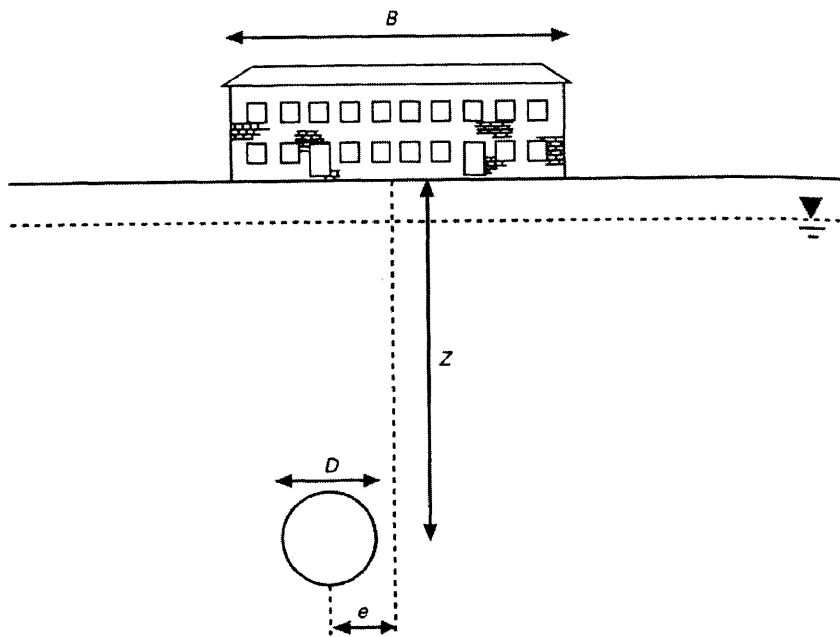
Figure 2.1. Problem Geometry (after Potts and Addenbrooke, 1997)

Soil Profile. Potts and Addenbrooke (1997) consider a typical London Clay profile, which is represented by a nonlinear elastic perfectly plastic constitutive model. The empirical equation proposed by Jardine et al. (1986) was used to represent the nonlinear pre-yield behavior of the soil and a Mohr Coulomb yield surface with flow at a constant

dilation angle were used to model the plastic behavior. This model will be presented in more detail later. The soil was saturated with a unit weight $\gamma = 20$ KN/m^2. The hydrostatic water table located 2m below ground surface and a coefficient of earth pressure at rest, $K_0 = 1.5$ was considered. These values are representative of conditions in London.

Only the short-term response was investigated and therefore the soil was assumed to respond in an undrained fashion[1].

Model for the beam. The overlying structure was represented by an elastic beam founded on the surface of the ground and the interface between the beam and the soil was considered to be rough. This means that no slippage was allowed between the beam and the soil. The bending and axial stiffness of the beam were varied independently over a wide range to investigate limits of soil – structure interaction. In addition to the bending and axial stiffness, there was also an effort to model some more realistic cases of buildings. A single slab and a 1, 3 and 5 – story building cases were modeled. For example the single slab had the following characteristics:

- Thickness = 150mm
- $E = 23 \times 10^6$ kN/m^2

For the calculation of the bending (EI) and axial (EA) stiffness of the beams for the cases of 1, 3 and 5 – story buildings, a rational but simplistic methodology was followed. According to this approach, the building is modeled as a series of slabs and the axial and bending stiffness of the building as a cross – section comprising of many slabs is calculated. The reader can find more on this topic on Potts and Addenbrooke (1997). Also in the Appendix at the end of this thesis, this topic is further discussed.

In all cases, it should be emphasized that no vertical loads were applied to the surface beam, i.e. dead or live load of the superstructure were not considered. This is a rather significant deviation from a realistic description of the problem of interaction. The reason is that the weight of the building will change the stress state in the soil. At the same time, the stiffness of the soil is stress level – dependent and it is essential to take this feature into account when modeling problems of this sort, otherwise the results make no sense. For example, only a stress dependent soil model can predict realistic "greenfield" settlement troughs. This is proven by the results presented later. Thus, by not considering the weight of the structure, a first approximation to the actual problem is considered and further refinement may be needed to account for the self weight of the structure.

At this point, it is important to define the so-called relative stiffness parameters, which account for the stiffness of both the beams and the soil. They are useful in the sense that they provide with a quantitative description of the stiffness of the system beam – soil. They are defined by the following equations:

---

[1] This was modeled in the analysis by assigning a high bulk modulus to the pore water, namely 100 times the effective bulk modulus of the soil skeleton.

- The relative bending stiffness $\rho^* = \dfrac{EI}{E_s H^4}$ [1/L] (2.1a)

- The relative axial stiffness $\alpha^* = \dfrac{EA}{E_s H}$ (2.1b)

In the above equation H is half the width of the beam and E_s is representative soil stiffness. The problem will be dealt as plane strain, so the relative axial stiffness α^* is dimensionless whereas the relative bending stiffness ρ^* has dimensions of [1/L]. The value of E_s adopted is the secant stiffness that would be obtained at 0.01% axial strain in a triaxial compression test performed on a sample retrieved from a depth of Z/2. This was chosen, as a measure that could be obtained from a practical site investigation. As the depth of the tunnel Z varies, the parameter E_s changes too. This arises from the fact that the applied soil model entails a stress – dependent soil stiffness. In the study of Potts and Addenbrooke (1997) two different values of Z were considered: Z = 20m and Z = 34m. For Z = 20m it turns out by application of the empirical equations of Jardine et al. (see Appendix) that value of depth, E_s = 103MPa. When Z = 34m, E_s = 163MPa. In this thesis, only the first case (Z = 20m) was considered. It can be noted that the quantity E_s can be considered varying linearly with depth.

The building damage parameters adopted are deflection ratio and horizontal strain. The definitions have been given at the introduction of this thesis, but in case of a tunneling induced settlement trough, they can be defined in the following Figure 2.2. An interesting observation is that the point of inflection of the settlement trough may or may not occur below the foundation of the building. If it does, then it separates the building in two zones: a sagging zone and a hogging zone. If not, then the building only suffers in either sagging or hogging mode only. In the numerical analyses the point of inflection is determined by numerical differentiation of the predicted model settlements[2]. Accurate determination of this point is in general very important. A slight change in the settlement trough may change dramatically the position of the inflection point because second derivatives control the calculation of the position of i. Other interesting remarks may arise from this observation. For example, a normal Gaussian curve may be able to satisfactory describe the settlement trough in terms of magnitudes of settlements or width of trough. But how good can it be in describing the second derivative of a real trough? It is true that the need for evaluating the second derivative in order to assess the potential for damage is an inherent disadvantage of this whole methodology since it is very difficult to achieve good accuracy in the level of second derivatives in curve fitting.

---

[2] The inflection point corresponds to the case where $\dfrac{d^2\Delta}{dx^2} = 0$, where Δ is the vertical displacement and x is the lateral coordinate. Numerical differentiation of nodal point displacements in the FE analyses is carried out and the second derivative at point x_i is evaluated according to the relationship:

$\dfrac{d^2\Delta}{dx^2}(x_i) = \dfrac{2\Delta_i - \Delta_{i-1} - \Delta_{i+1}}{(x_{i+1} - x_i)(x_i - x_{i-1})}$, taking account three consecutive points x_{i-1}, x_i and x_{i+1}.

The horizontal strain however can be obtained directly from the computer output. The strain is referred to the neutral axis of the beam, so any effects of bending are eliminated.

The goal always remains to assess the influence of an existing structure to the tunneling – induced ground movements. The reference deformation state is the one originating from a "greenfield" problem. It is thus convenient to define the following modification factors for the deflection ratio and the horizontal strains.
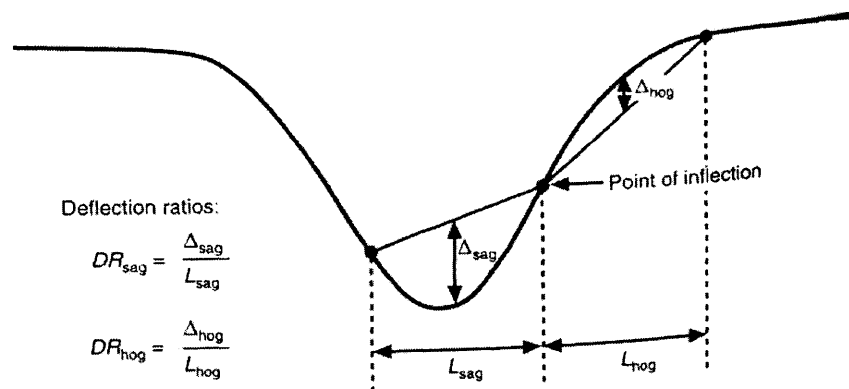
Figure 2.2. Definition of Deflection ratios (after Potts and Addenbrooke, 1997)

$$M^{DRsag} = \frac{DR_{sag}}{DR_{sag}^g} \tag{2.2a}$$

$$M^{DRhog} = \frac{DR_{hog}}{DR_{hog}^g} \tag{2.2b}$$

$$M^{\varepsilon_{hc}} = \frac{\varepsilon_{hc}}{\varepsilon_{hc}^g} \tag{2.3a}$$

$$M^{\varepsilon_{ht}} = \frac{\varepsilon_{ht}}{\varepsilon_{ht}^g} \tag{2.3b}$$

where DR^g_{sag} and DR^g_{hog} are the deflection ratios for that portion of the greenfield settlement trough, which lies directly beneath the structure. The subscripts *sag* and *hog* denote sagging and hogging respectively and the superscript *g* denotes greenfield conditions. Similarly, ε^g_{hc} and ε^g_{ht} are the maximum horizontal compressive and tensile strains of the ground surface for that portion of the greenfield settlement trough, which lies directly beneath the structure.

28

Modeling the excavation of the tunnel. The tunnel excavation was modeled by the incremental removal of stresses around the tunnel boundary. For each increment of the analysis the displacements of the tunnel cavity were recorded and used to calculate the volume of the soil moving into the tunnel. This was then divided by the original cross – section of the circular tunnel ($\pi D^2/4$) to obtain the volume loss parameter V_L. It should be recalled from chapter 1 that the volume loss parameter V_L is defined as the difference between the original and final cross sectional area of the tunnel over the original cross sectional area of the tunnel. For the analyses representing "greenfield" conditions (no surface structure) ground volume loss = 1.5% (representing average tunnel performance in London)[3]. For analyses with a surface structure, excavation was carried out by application of the same procedure such that all results apply for a standard volume loss of 1.5%.

From the numerical analyses that have been performed settlement troughs for different combinations of axial and bending stiffness were produced. Of special interest are two cases. In the first case, the relative bending stiffness of the system ρ^* is kept constant and the relative axial stiffness changes, in the second, the relative axial stiffness α^* is constant while ρ^* is varied. These specific two scenarios will be of special interest, since they are on whom the basic calculations for this thesis were performed. The beam is considered to be centrally positioned and exhibits a width of 60m. The tunnel is located 20m below the ground.

Figure 2.3 presents key results from Potts and Addenbrooke (1997) that can be summarized as follows:

- For the first scenario of relatively high relative bending stiffness $\rho^*(\rho^*=0.518m^{-1}$ within a range from 5.18×10^{-8} to $5.18\times10^{-1})$, it can be said that structures with low axial stiffness will eventually follow a trough very close to the greenfield trough as they deform in shear. It is evident that the greater the axial stiffness, the greater the modification to the "greenfield" settlement. (Figure 2.3a)
- For the second scenario, it turns out that the stiffer the beam, the greater the modification factor to the "greenfield" settlement. For high values of ρ^* ($\rho^* > 0.518\times10^{-3}$) the results show minimal differential settlement beneath the structure. (Figure 2.3b). It is also interesting to note that for low bending stiffness ($\rho^* = 5.18\times10^{-8}m^{-1}$ to $\rho^* = 5.18\times10^{-6}m^{-1}$) but with large axial stiffness ($\alpha^*=48.6$), the maximum settlements are greater than those from the "greenfield" analysis. This is a consequence of the fact that the analysis is being considered in undrained conditions. The volume defined by the settlement trough has to be the same for all scenarios since the volume loss is the same. Now, the beam, which exhibits very high axial stiffness, will greatly reduce the horizontal movements at the surface of the ground. This is proved by the modification factors for the horizontal tensile

---

[3] The assessment of the Volume Loss Parameter during planning and design of tunneling projects is a wide topic. This parameter depends on a list of factors such as the method of tunneling, the soil conditions, the level of workmanship etc. For further information see (Mair et al., 1993). The value of V_L = 1.5% was chosen for the design of the Jubilee Line Extension in London and is also applied here.

and compressive strains. Potts and Addenbrooke quote values being equal to zero or very close to zero. So the deformation of the beam will be governed strictly by bending and since the bending stiffness is very small and the condition for zero volume change has to be satisfied, a trough even steeper than the "greenfield" reference case is obtained. This is one of the few cases where it turns out that the "greenfield" assumption would give less conservative settlement troughs acting on the foundation of the structure (see also Chapter 4).

- It is thus evident that both the bending and axial stiffness affect the settlement trough. It can also be seen that the structure only influences the settlements over a limited extent beyond its edge. The greenfield settlement curve is recovered within a horizontal distance equal to 15% of the beam width. One can notice that the change in the settlement profile is very severe in the area close to the edge of the beam. In reality this may be interesting from the point of view that sensitive structures in the vicinity of very rigid structures may suffer significant damage exactly because they are positioned in this area of transition from the green field trough to the modified – due to the rigid structure's stiffness trough.

Similar remarks and conclusions can be extracted for the horizontal movements. The results are presented in Figure 2.4.
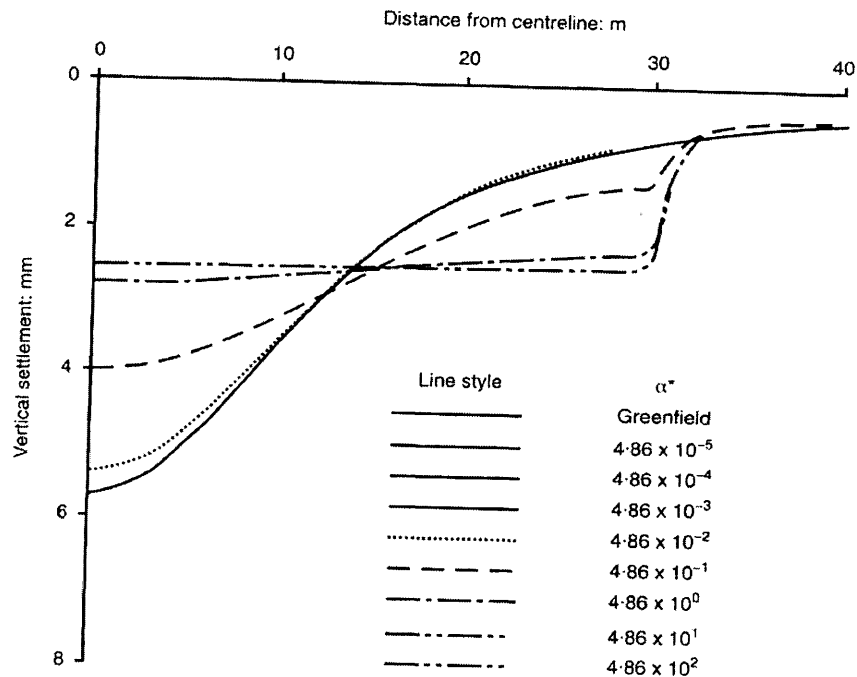
Figure 2.3a. Surface settlement troughs for a 20m deep tunnel excavated beneath beams 60m wide with zero eccentricity: Effect of relative axial stiffness α^* when building has a relatively high flexural stiffness ($\rho^* = 0.518m^{-1}$) (after Potts and Addenbrooke, 1997)
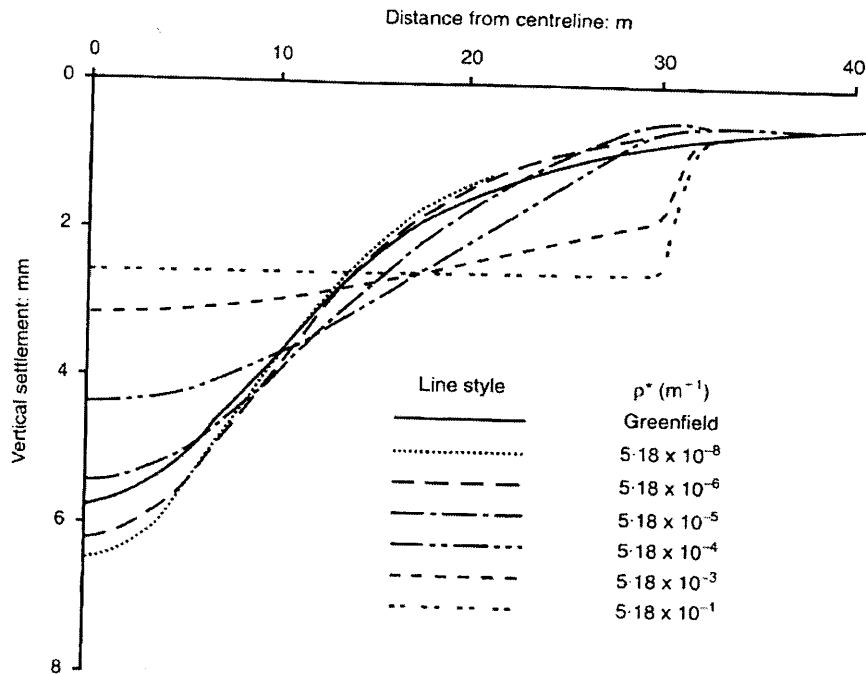
Figure 2.3b. Surface settlement troughs for a 20m deep tunnel excavated beneath beams 60m wide with zero eccentricity: Effect of the relative flexural stiffness parameter ρ^* for a high relative axial stiffness parameter ($\alpha^* = 48.6$) (after Potts and Addenbrooke, 1997)

As far as the horizontal movements are concerned, Figures 2.4a and 2.4b present some results. When the relative bending stiffness remains constant, the greater the relative axial stiffness α^*, the more severely restricted the horizontal movement. If on the other hand, the relative axial stiffness is kept constant, the variation in the relative bending stiffness seems to leave unaffected the profiles of horizontal movements. This can be very well depicted for the case $\alpha^* = 48.6$, for which all the range of values for ρ^* does not affect the profile of horizontal movements. In all cases, the horizontal movements beyond the edge of the beam are influenced by its presence. The "greenfield" curve is being recovered at a horizontal distance from the edge of the beam approximately equal to 30% of the beam width.
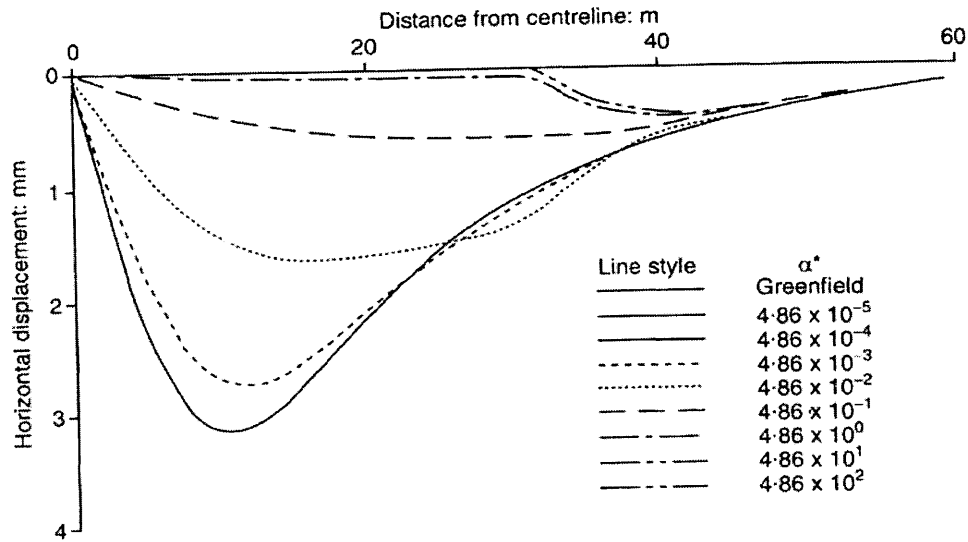
Figure 2.4a. Horizontal ground surface movements for a 20m deep tunnel excavated beneath beams 60m wide with zero eccentricity: Effect of α* for ρ* = 0.518m⁻¹ (after Potts and Addenbrooke, 1997)
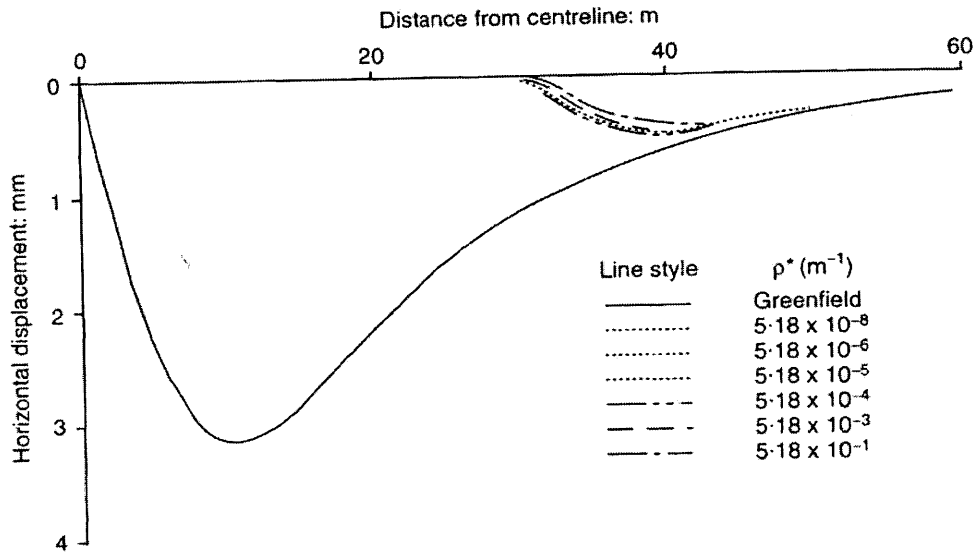
Figure 2.4b. Horizontal ground surface movements for a 20m deep tunnel excavated beneath beams 60m wide with zero eccentricity: Effect of ρ* for α* = 48.6 (after Potts and Addenbrooke, 1997)

Tunnel Support removal and Volume loss. As noted above, the same percentage of tunnel support removal was assumed for all analyses. The term "tunnel support removal" can be defined as one minus the ratio of the final stress in the tunnel boundary over the initial stress in the tunnel boundary. This was determined by the "greenfield" analysis so that it gave a volume loss of 1.5%. As a consequence of this procedure, all analyses with structure had slightly different volume losses. This is illustrated in figure 2.5. In this figure two scenarios are being examined; the scenario of greenfield conditions and the scenario of a five story building, which can be considered as the one modifying the most the greenfield settlement trough. The basic conclusion is that although the existence of a structure may affect dramatically the shape of the settlement trough it seems it has a minimal effect on the volume loss around the tunnel border for a specific stress release level at least for the case of this relatively deep tunnel. This is expected since the existence of the structure being weightless does not change the stress state with respect to the greenfield conditions. This is very important in order to allow comparisons between different analyses, since the case of undrained conditions is examined, and the volume defined by the settlement trough is equal to the Volume loss in the tunnel. All analyses have to exhibit the same amount of Volume Loss. So as a first remark one can say that if the level of stress release in the tunnel remains the same, the impact of an existing surface structure on the observed Volume Loss is very small and can be considered negligible.
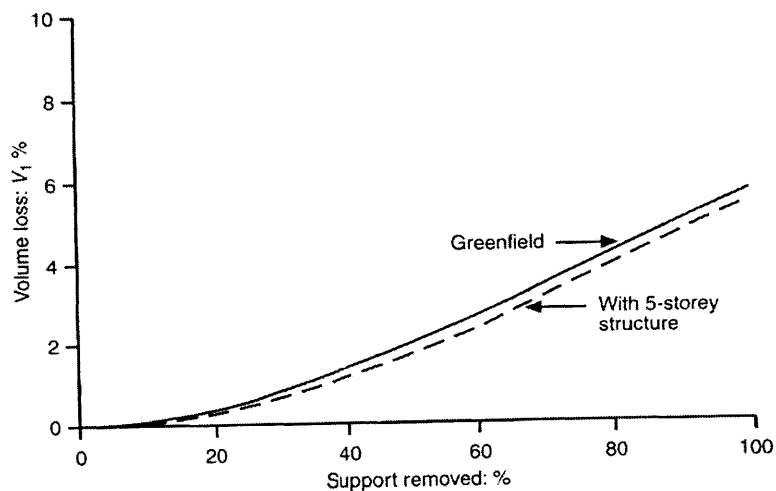
Figure 2.5. Variation of Volume Loss with Percentage Support removed (after Potts and Addenbrooke, 1997)

A second interesting conclusion can be made by examining the variation of a specific displacement in the model versus Volume Loss in the tunnel. For example, the vertical displacement at the center of the beam may be examined, which is also the maximum vertical displacement in all cases. It turns out that this relationship is linear. This is depicted in Figure 2.6. Even more important is the generalization of this observation for every displacement in the model. So if the state of deformations is known for two specific values of Volume Loss, it is a matter of elementary algebra to obtain the state of deformations for any other value of Volume Loss by simply interpolating linearly. This observation is very important. Of course, the essential detail is to keep the Volume Loss

constant for all the analyses. If however, a specific value of stress release percent is used and gives rise to a value of Volume Loss, which is not equal to the reference value, a simple correction in the basis of the aforementioned linear relationship of the deformations versus Volume Loss can be implemented and it is not at all necessary to repeat the analysis for a new stress release that will correspond to the desired Volume Loss. Even more important is the fact that an immediate consequence of this linear relationship is that the modification factors are independent of the value of Volume Loss. Of course among the analyses a constant Volume Loss has to be fixed. But the selection of this value can actually be arbitrary. No matter what value is selected for the Volume Loss, the modification factors will always be the same!
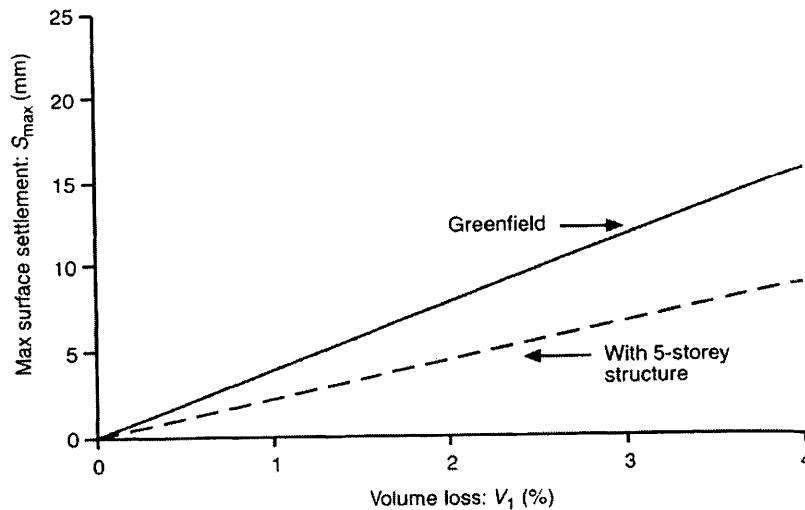
Figure 2.6. Variation of maximum surface settlement with volume loss (after Potts and Addenbrooke, 1997)

In Figure 2.6, the linear relationship is depicted but devoid of data points that could help in determining "how much" linear this relationship really is. In chapter 3, a similar calculation is being performed and there it is shown that the correlation factor R^2 can be as high as 0.99! So, one can say that the relationship between a displacement in the model and the volume loss in the tunnel is strictly linear, at least for the given soil conditions.

2.3 BUILDING DAMAGE

In terms of assessing the potential for building damage, the parameters that need to be examined and identified are the deflection ratio (sagging and hogging mode) and the horizontal strain (compressive and tensile).

a. **Deflection ratio**. Figure 2.7a presents the variation of the Modification Factors for both sagging and hogging against the relative axial stiffness α^* for a constant relative bending stiffness ρ^*. This Figure corresponds to a 60m wide beam centrally positioned with respect to the tunnel. It can be observed that for beams with low values of relative axial stiffness the modification factors for both sagging and hogging are equal to 1.0 for all values of relative bending stiffness. As the axial stiffness increases, then the value of the bending stiffness affects the results. Thus, for high values of bending stiffness the modification factors are reduced as the axial stiffness increases whereas for low values of relative bending stiffness, the modification factors increase. This means that values larger than unity are obtained for low values of relative bending stiffness combined with large values of relative axial stiffness. This means that the presence of the structure causes greater hogging and/or sagging than the "greenfield" curve. The soil structure interaction can sometimes cause settlement troughs below the structure that lead to more severe damage than the "greenfield" settlement trough. This is a rather interesting result since it contradicts the very broadly used principle that assuming greenfield conditions for assessing the potential of damage is a conservative assumption. Nevertheless, the combination of relative bending and axial stiffness that gives rise to such a result is a rather non realistic one for a real structure. In order to obtain modification factors larger than unity the relative axial stiffness has to be unrealistically large with respect to the relative bending stiffness. It should be stated that realistic ranges for the relative bending and axial stiffness are the following:

- Relative axial stiffness $\alpha^* = 0.5$ to 26
- Relative bending stiffness $\rho^* = 1.69 \times 10^{-7}$ m^{-1} (but this value corresponds to a simple slab) to 10^{-1} m^{-1} (5 – story building). (The order of magnitude or ρ^* for a 1-story building reaches an order of 10^{-4} m^{-1}).

Another interesting remark concerns the deflection ratios in hogging. There is actually a reversal in trend. For any axial stiffness $\alpha^* > 10^{-2}$ the modification factor initially decreases as the relative bending stiffness ρ^* increases until $\rho^* = 5 \times 10^{-4}$ m^{-1}. Any further increase in ρ^* causes a slight increase in the modification factor for hogging.

Figure 2.7b shows the modification factors against relative bending stiffness ρ^*, for a range of fixed relative axial stiffness α^*.The data is derived from Figure 2.3 and replotted here. This plot highlights the fact that for beams with $\alpha^* < 5 \times 10^{-3}$ to 5×10^{-4}, an increase in ρ^* does not cause the modification factors to fluctuate from unity. Beams with a higher relative axial stiffness α^* show the greatest variation in the modification factors with increase in relative bending stiffness (from 1.2 to 0). The plot also highlights the reversal in trend for the hogging modification factor as the relative bending stiffness increases for beams with high relative axial stiffness.
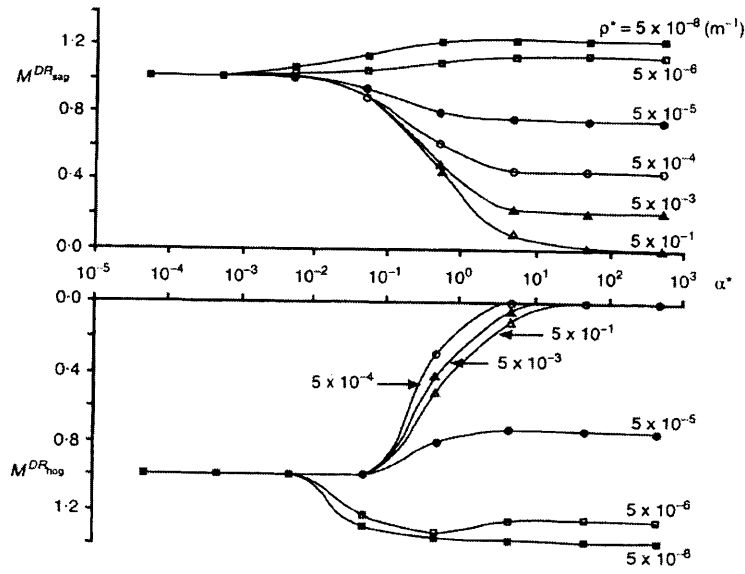
a) Variation in relative axial stiffness α^*
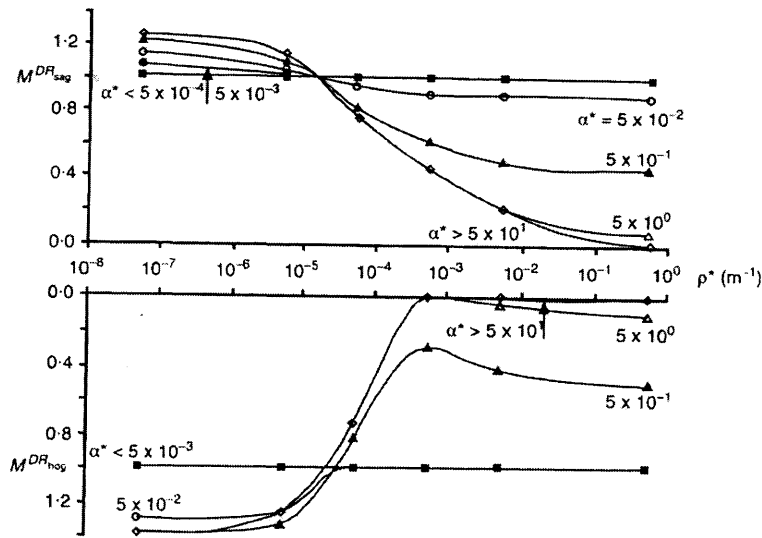
b) Variation with relative bending stiffness ρ^*

Figure 2.7. Variation of modification factors for deflection ratio with relative beam stiffness (after Potts and Addenbrooke, 1997)

36

b. Horizontal Strain. Figure 2.8 presents the variation of the modification factors for compressive and tensile maximum horizontal strain, over a range of relative bending stiffness values ($\rho* = 10^{-8}$ to 10^{-1} m^{-1}). The beam is again considered to be centrally positioned relative to the axis of a 20m deep tunnel. The width of the tunnel is assumed to be 60m as before. An immediate conclusion is that only the relative axial stiffness $\alpha*$ affects the horizontal strain, since the curves for different values of the relative bending stiffness plot on top of each other. This is an interesting result and leads to the conclusion that there are unique curves for the variation of the horizontal strain modification factors with relative axial stiffness. Figure 2.9 shows further modification factors for tensile and compressive horizontal strains for more realistic cases of buildings, beam widths and tunnel depths. For all cases (single slab to 5 – story building) the relative axial stiffness is $\alpha* > 0.5$. A first observation is that, there is little scatter in the data indicating that unique relationships between the modification factors and the axial stiffness. Values of the tensile strains extracted from these data are small whereas those of compressive strains are less than 10% of those calculated from "greenfield" analyses. The conclusion that unique curves of the variation of the modification factors of horizontal strain as a function of relative axial stiffness, independent of the relative bending stiffness, is valid for all building eccentricities considered in the study.
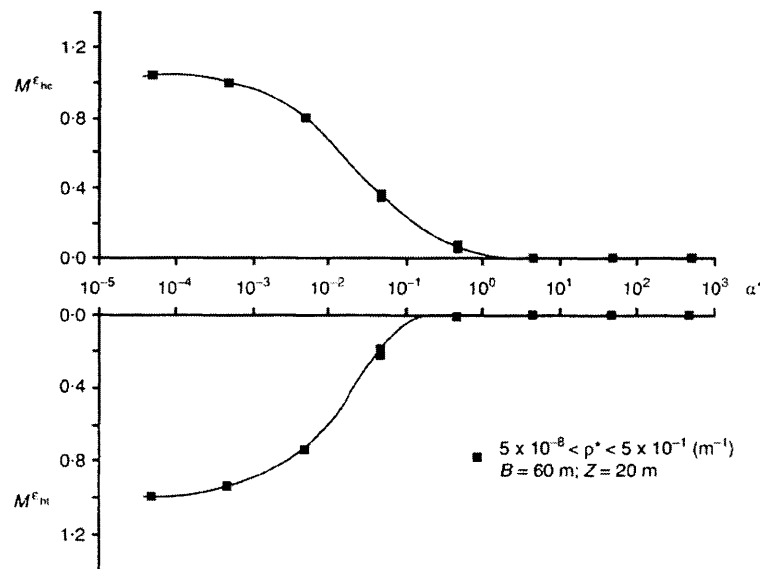
Figure 2.8. Variation of modification factors for horizontal strain with relative beam stiffness. The curves for different values of relative bending stiffness coincide (after Potts and Addenbrooke, 1997)
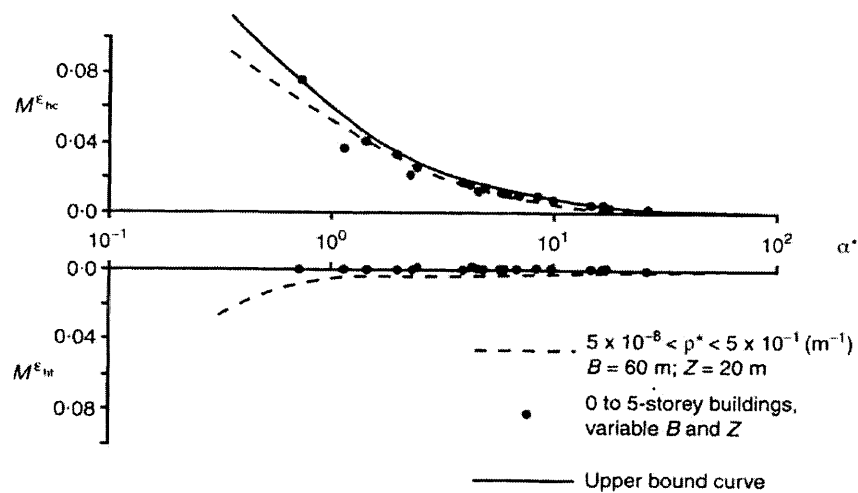
Figure 2.10. Variation of modification factors for horizontal strain with relative axial stiffness for beams with zero eccentricity and likely values of relative axial stiffness ($\alpha^* >$ 0.5), (after Potts and Addenbrooke, 1997)

2.4 DESIGN RECOMMENDATIONS

The final part of Potts and Addenbrooke (1997) paper is actually a set of design recommendations for the prediction of the damage potential to an existing surface structure located above a new tunneling operation. The approach is based on the numerical results obtained by the parametric study described above and the established methods for greenfield ground movement prediction and building damage category assessment.

The initial step in the recommended methodology is the establishment of the "greenfield" surface settlement trough and the horizontal ground movements in the area around the building. This is done through the geometry of the tunneling problem (depth of the tunnel axis, cross – section and dimensions of tunnel) and from the assumed Volume loss during construction without reference to any surface structure. The position of the existing surface structure is then considered. Over the region of the ground surface beneath the structure, the settlement and horizontal movements are used to calculate the maximum hogging and sagging deflection ratios, and the maximum compressive and tensile strains. These define the greenfield values of the building damage parameters. As a next step, the relative bending and axial stiffness of the system soil – structure α^* and ρ^* are evaluated. An initial estimation of these parameters could only consider the contribution of the foundation system of the building before taking into account the contribution of slabs, beams and vertical elements. Having an estimate of the relative stiffness parameters α^* and ρ^* for the specific problem, the engineer can then use design curves, based on the results of numerical analyses to obtain modification factors for sagging and hogging deflection ratio, as well as for tensile and compressive tensile horizontal strain. These

38

modification factors are applied to the previously calculated values of deflection ratio and horizontal strain. The newly obtained combinations of modified deflection ratio and horizontal strain imposed on the structure (in the sagging and hogging regions of the settlement trough and in the compressive and tensile region of horizontal displacements) can be used to estimate the likely damage category and classification.

The basic steps of the methodology described, concerning the prediction of the greenfield movements, the greenfield building damage parameters and the building damage assessment have been discussed extensively in Chapter 1.

2.5 CONCLUSIONS

The finite element study by Potts and Addenbrooke (1997) can be summarized as follows: The analyses consider 2D plane strain conditions. The surface structure is represented by a deep elastic beam with equivalent bending and axial stiffness. The tunnel is constructed with a single soil profile representing average conditions found in London Clay and modeled using a nonlinear elastic perfectly plastic material model. The authors assume undrained shearing within the clay mass. The principal parameters considered in the study are presented in the following table:

Parameter	Symbol	Units	Values
Tunnel Depths	Z	[m]	20 and 34
Tunnel Diameter	D	[m]	4.15
Beam Widths	2H	[m]	16 to 60
Eccentricity ratios	e/H	-	0 to 0.64
Range of relative bending stiffness	ρ^*	[m^{-1}]	5.18×10^{-8} to 5.18×10^{-1}
Recommended values of relative bending stiffness	ρ^*	[m^{-1}]	$>5.18 \times 10^{-4}$
Range of relative axial stiffness	α^*	-	5×10^{-5} to 500
Recommended values of relative axial stiffness	α^*	-	>0.5

The basic conclusions of their work can be summarized as follows:

1. Both the axial and bending stiffness of the surface structure will influence the ground surface movements and these movements can be very different from the ones predicted for a greenfield site. In the majority of cases, the effect of a surface

structure is to reduce the ground surface movements compared to the greenfield scenario. This confirms the assumption that "greenfield" conditions are conservative for assessing the potential structural damage.

2. If the structure has a low bending stiffness but a realistic axial stiffness then the surface settlements can be greater than those when no structure is present. At first sight this may seem to be a surprising result but it arises because the structure imposes a restriction on lateral surface movements.

3. Just beyond the edge of the structure, high gradients of ground movements can be induced. These could have severe implications for any adjacent services.

4. The relationship between an arbitrary deformation in the finite element model and the Volume Loss in the Tunnel is linear for the parameters chosen in this study.

5. There are unique curves describing the variation of the modification factors versus the relative axial stiffness α^*, independent of the relative bending stiffness.

As an epilogue of this chapter it would be interesting to present some case studies from the research program undertaken in London for the Jubilee Line Extension project. These are cases, where the methodology presented by Potts and Addenbrooke was directly applied (combined with the Damage assessment criteria presented earlier) to assess the potential of damage due to tunneling operations.

2.6 CASE STUDIES ON THE INFLUENCE OF BUILDING STIFFNESS TO TUNNELING INDUCED SETTLEMENTS (*After Burland, Standing and Jardine, 2002*)

As outlined before, the current methods of assessing the potential for damage in buildings influenced by tunnels and excavations adopt the very conservative assumption of neglecting the influence of building stiffness. In other words, the equivalent beam, which is used to represent the building, is assumed to conform to the "greenfield" site and not to modify it in any way. Moreover, the horizontal strains at the ground surface, which are associated with the Greenfield subsidence trough, are assumed to transfer directly into the building. Although this approach would seem to be very conservative, there have been very few case histories of measurements on buildings experiencing subsidence, which can be used to judge the degree of conservatism involved. In particular, there are almost no case records, which trace the passage of the subsidence trough through a building so that the maximum distortions can be identified.

A number of case records have been produced, which can be used to assess the extent to which the stiffness of a building modifies the "greenfield" ground surface movements. Of particular interest are those buildings for which class A (see Chapter 1) predictions were made prior to construction of the tunnel. These are the cases of Elizabeth House and Murdoch, Clegg and Neptune Houses from the Jubilee Line Extension Project.

Elizabeth House

Elizabeth House is a seven and ten-story reinforced concrete frame building founded on a 1.4m thick raft on a thin layer of gravel overlying London Clay (Figure 2.11). In plan the building is 18m wide and over 100m in length. The ten-story section is 50m long and is separated from the seven-story section by an expansion joint, which does not extend

through the raft. Based on the Potts and Addenbrooke method, the class A calculations concluded that in the longitudinal direction the building is almost perfectly flexible ($\rho^* < 5\times10^{-5}$) whereas in the transverse direction the building is almost rigid ($\rho^* > 5\times10^{-2}$). Using "greenfield" site settlement predictions (modified to take account of the building stiffness in the transverse direction) the response of the building was predicted for the construction of two 5.6m diameter running tunnels and a crossover tunnel running skew about 21.5m beneath the founding level of the building. The agreements are remarkable and in particular the "fully flexible" and fully rigid behavior, in the longitudinal and in the transverse direction respectively are fully confirmed. The measurements also showed that significant twisting around the longitudinal axis of the building occurred. (Figures 2.12, 2.13).

The measurements on the building included precise horizontal taping within the basement of the building. A most important observation is that the subsidence induced horizontal strains close to the foundations were negligible and those induced by thermal effects far exceeded them. Subsurface horizontal displacements were measured by means of electrolevel inclinometers installed in a vertical borehole adjacent to one of the running tunnels.
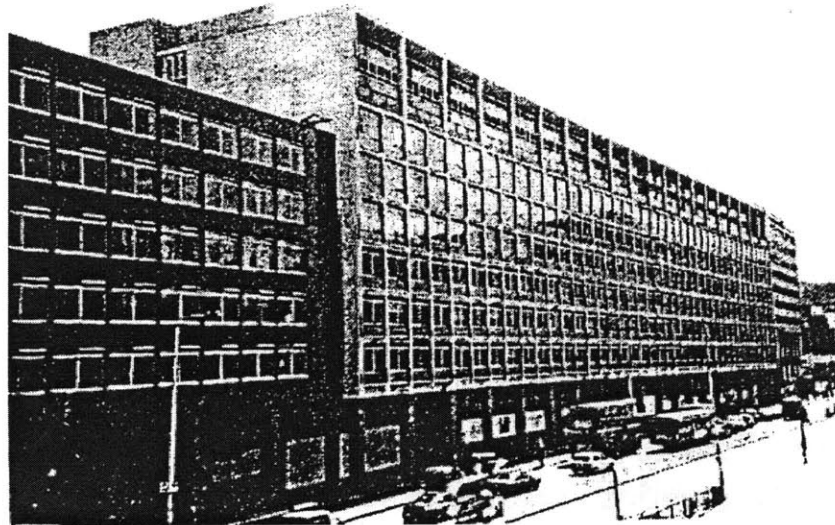
Figure 2.11 Elizabeth house from York Road in London

These measurements showed that horizontal displacements developed in the ground a few meters beneath the raft were consistent with the measurements made at the at the greenfield control site at St. James 's Park. However, these displacements reduced rapidly just beneath the raft due to the restraining action of the horizontal stiffness of the raft and building. It is possible that horizontal slip occurs at the interface between the ground and the foundation.
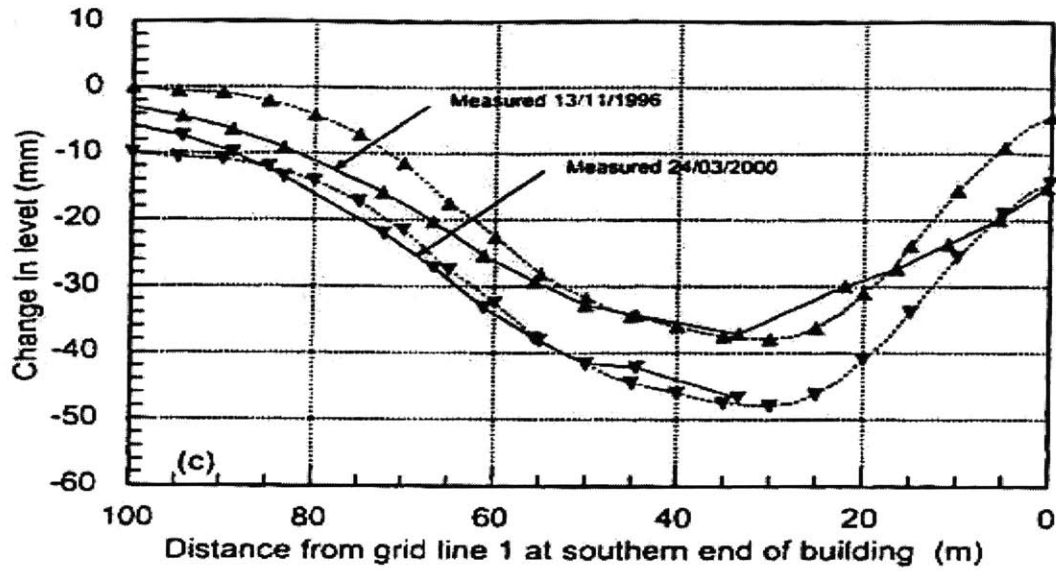
Figure 2.12. Elizabeth House: Predicted (via Potts and Addenbrooke (1997) methodology) and measured longitudinal settlements from crossover construction (after Burland, Standing, Jardine, 2002)
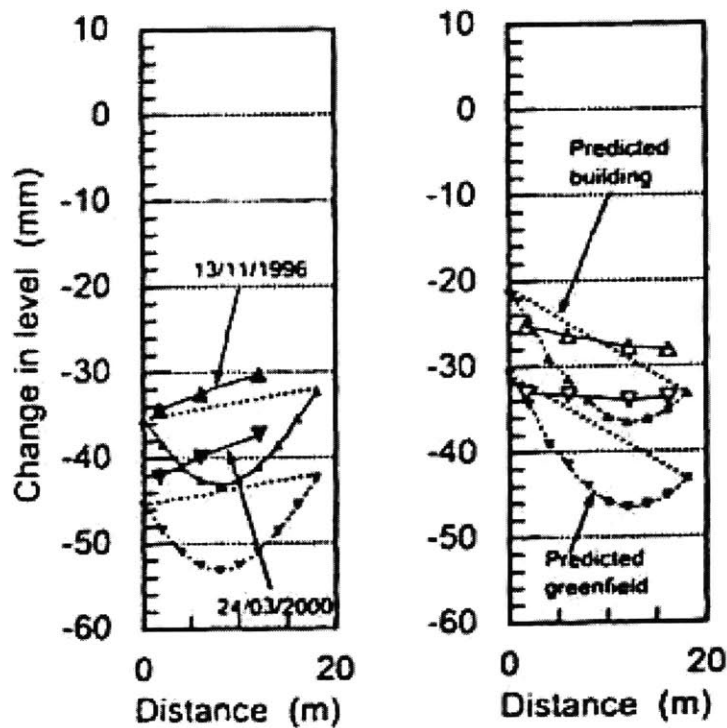
Figure 2.13. Elizabeth House: Predicted (via Potts and Addenbrooke (1997) methodology) and measured transverse settlements from crossover construction (after Burland, Standing, Jardine, 2002)

Neptune House, Murdoch House and Clegg House

These three buildings are small three story blocks of flats of load – bearing brick founded on concrete strip footings (Figure 2.14). Neptune House and Murdoch House are approximately 40m x 8m in plan dimension and Clegg House is about half the length of the other two (Figure 2.15). As this location the east and west bound tunnels of the Jubilee Line Extension run beneath the three buildings in the Lambeth Group at a depth below the ground level of about 18m and a separation of about 22m.

Figure 2.14. Murdoch House at Moodkee Street in London
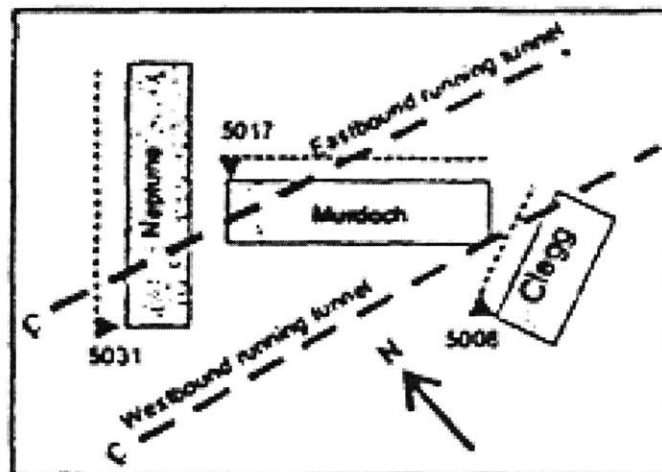
Figure 2.15. Plan view of Murdoch, Neptune and Clegg House (after Burland, Standing, Jardine, 2002)

43

Based on the Potts and Addenbrooke method, the Class A calculations were performed and it was concluded that the walls of the buildings are almost rigid relative to the stiffness of the underlying soil. Using the "greenfield" site settlement predictions suitably modified for the calculated building stiffness and with the volume loss and K values measured at the Southwark Park control site, the responses of the three buildings were predicted.

Figures 2.16 and 2.17 show the comparison between the predicted and measured settlements of the buildings. Considering the very small settlements involved in the agreements are remarkable. A particularly important observation is that those walls, which were subjected to a sagging mode of subsidence behaved in a more rigid manner than those subjected to a hogging mode, which appeared to be completely flexible.

The measurements on the buildings include precise horizontal taping. These measurements showed that the horizontal strains in the walls were negligible.
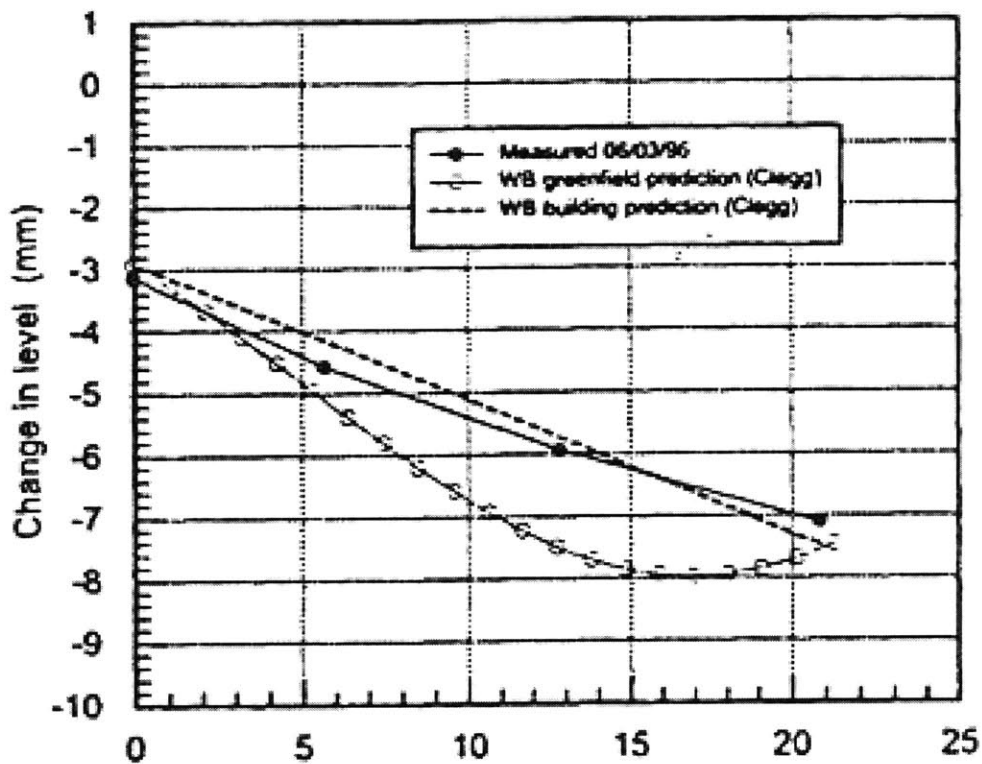
Figure 2.16. Comparison of measured settlement with predicted building (according to Potts and Addenbrooke (1997)) and "greenfield" surface settlement for a façade of Clegg House (after Burland, Standing, Jardine, 2002)
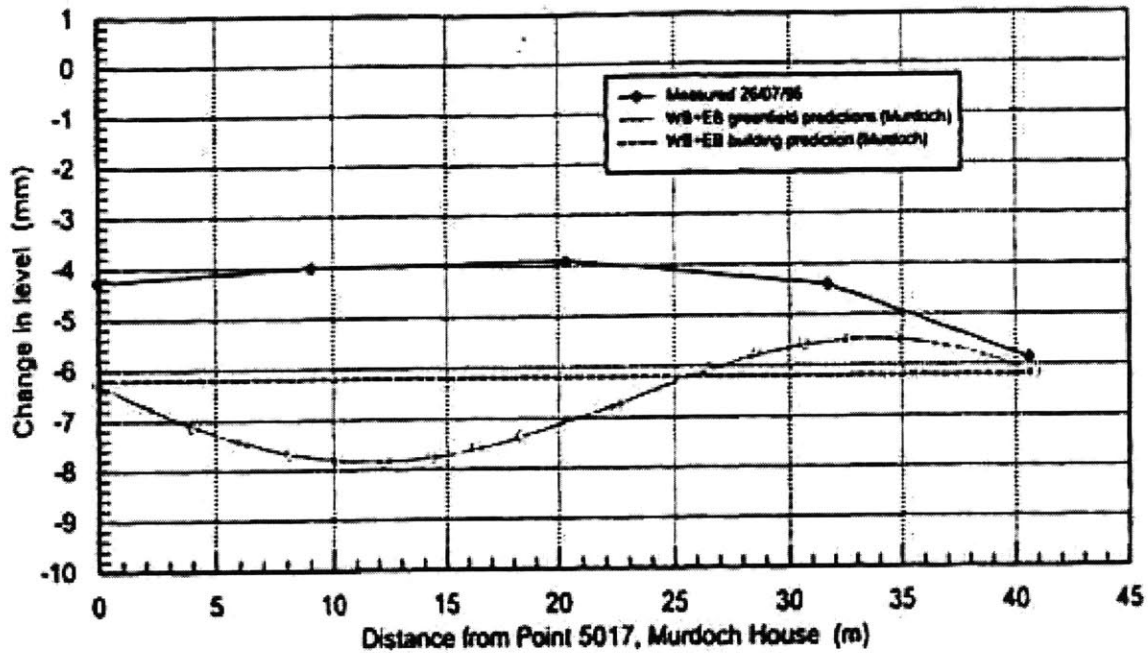
(a)
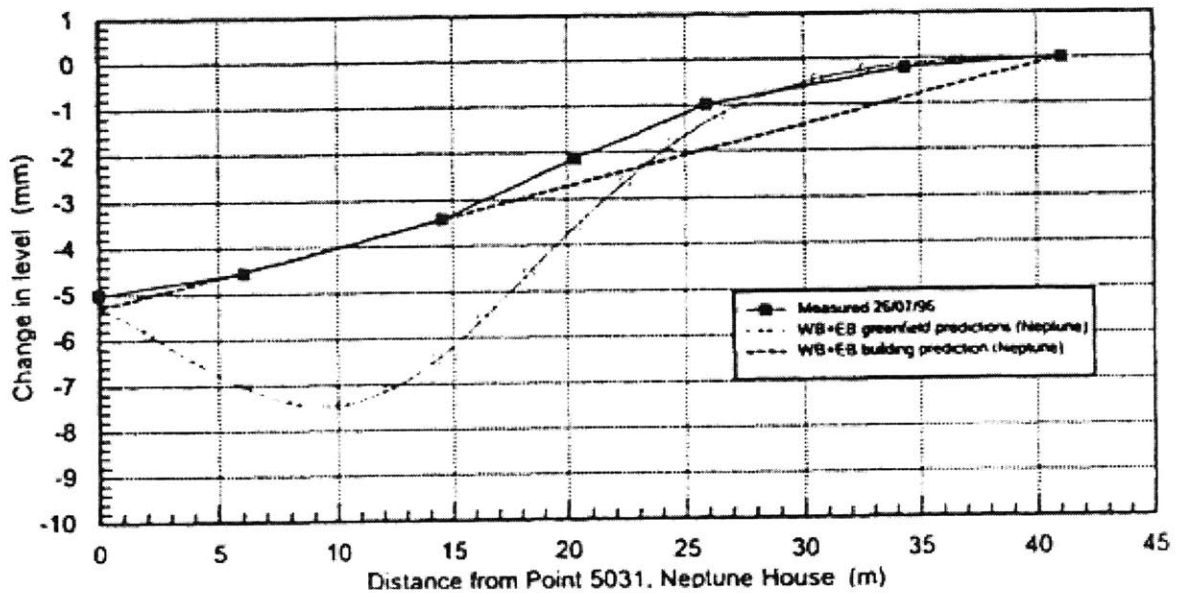
(b)

Figure 2.17. Comparison of the measured with the predicted building and greenfield surface settlements for facades of (a) Murdoch House, (b) Neptune House (after Burland, Standing, Jardine, 2002)

The Treasury

The Treasury is a massive stone – clad masonry building and it provides another important example of the influence of the building stiffness on the shape of the subsidence trough. The building has four stories above the ground level and its foundations consist of a light concrete slab with localized pads and strip footings on the Terrace gravel, which in turn overlies the London Clay.

The measurements plotted in Figure 2.18 show a comparison between the progressive subsidence of the west façade of the Treasury and that of the ground surface at the nearby St. James's Park greenfield control site during the passage of the west – bound tunnel. It can be seen that over the sagging portion of the subsidence trough the façade shows very small relative deflections in comparison with the greenfield site trough. However, over the hogging portion of the subsidence trough the relative deflections of the façade are similar to those from the greenfield site measurements. There is thus further evidence the load bearing walls in hogging can be more flexible than in sagging.

(a)

(b)
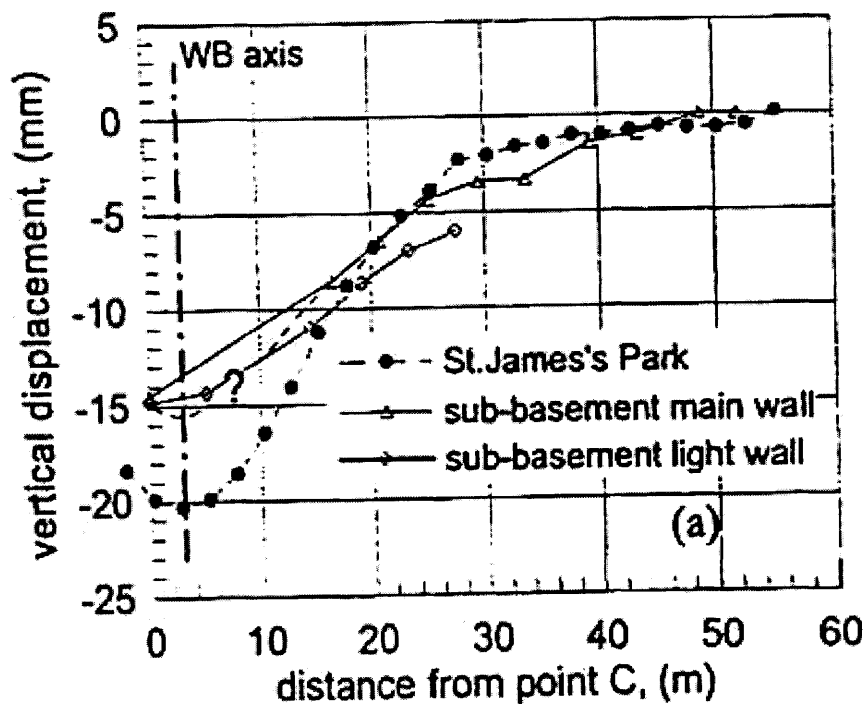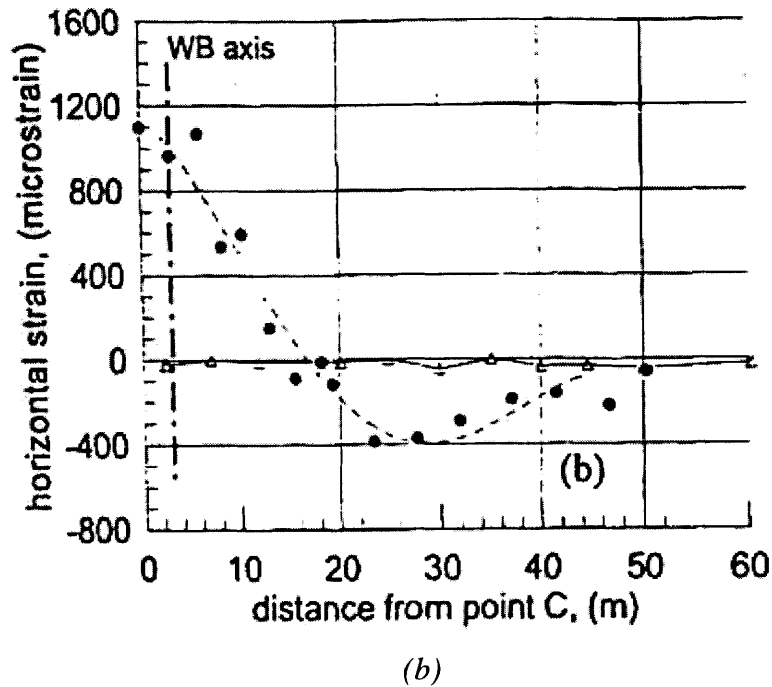
Figure 2.18. Comparison of the Treasury Building and "greenfield" response during westbound tunnel excavation. (a) Vertical displacements, (b) Horizontal strains (after Burland, Standing, and Jardine, 2002)

Figure 2.18(b) shows a comparison between the horizontal strains measured in the sub – basement of the Treasury beneath the west façade and the surface horizontal strains measured at the St. James's Park "greenfield" control site. It can be seen that the horizontal strains measured close to the foundation level on the building are negligible in comparison with the "greenfield" site values.

In the above, just three out of many examples have been given over the measured influence of the building stiffness. It would be inappropriate to draw general conclusions as it is hoped that each of these case records will be treated on its own merits. It is clear however that building stiffness can substantially reduce the greenfield site relative deflections although care is needed for load – bearing walls undergoing hogging. There is also overwhelming evidence that, for buildings founded on rafts and strip footings, little or no transfer of the "greenfield" horizontal strains takes place up into the building. Further measurements are required on pad footings and piled foundations. The presented examples can difficultly work as evidence of the validity of the conclusions derived by Potts and Addenbrooke. For that many more case studies are required and such a validation is out of the scope of this thesis. However, they can serve as representative examples of how the developed methodology is meant to be implemented in real projects.

CHAPTER 3
PRELIMINARY CALCULATIONS – SET UP OF THE MODEL

3.1 INTRODUCTION

The purpose of this chapter is to present some initial calculations that were judged necessary before the main bulk of the calculations would be performed. Since the main bulk of the calculations was referenced to a model set up by some other researchers (Potts and Addenbrooke, 1997), it would be beneficial if some of the results presented by them could be reproduced. Even more, it would lead to a better understanding of some parameters of the problem that have been considered throughout prior analyses.

In terms of a methodological investigation, the sequential steps in the analysis and the way the excavation of the tunnel was modeled, were given special attention. Could such factors affect the final results? Is the simulation of the tunnel excavation a significant factor in the shape of the settlement trough as derived from numerical analysis?

Apart from these separate small-scale parametric analyses and investigations it was thought that a result in Potts' and Addenbrooke's work could be reproduced here in order to get the sense that the model is "working". This was a small but necessary test and if a satisfactory result would be obtained, this could serve as a passage into performing and organizing the main bulk of the calculations.

This third chapter is organized as follows: Initially the pilot is presented for validation purposes. This is based on an interesting result presented by Potts and Addenbrooke. They show via the results from their parametric study that the relationship between the volume loss in soil occurring during the excavation of the tunnel cross – section and an arbitrary displacement within the model is linear. For example if a volume loss of 1.5% during the excavation of the tunnel gives rise to a specific vertical settlement above the centerline then a volume loss of 3% in the same tunnel and soil conditions will give double the previously observed vertical displacement above the centerline.

In the second part of chapter 3, a limited parametric analysis considers how the coefficient of earth pressure at rest K_0 affects the predicted ground deformations. The coefficient of earth pressure at rest is important in defining the initial stress condition in the model. Several aspects are examined such as the settlement trough at the surface of the ground or the response of the tunnel lining as the coefficient of earth pressure at rest is varied.

3.2 BASE CASE ANALYSIS

The derivation of the relationship between the volume loss occurring during the excavation of the tunnel and any deformation within the numerical model was selected to serve as validation test in the beginning of performing the calculations for this thesis. This was motivated by the interesting result presented in Potts and Addenbrooke (1997) research study where it is shown that this relationship is linear. The most important observation on this result is that linearity is valid for all displacements within the model. Potts and Addenbrooke tested the validity of this observation for the specific case of the vertical surface displacement above the centerline, which is also the maximum vertical displacement in the settlement trough. Since, the main topic of their paper concerned the effect of an existing structure on the settlement trough generated by a tunneling operation, the validity of this result was not only tested for the "greenfield" scenario, but also for the scenario at which a surface structure is positioned centrally above the centerline of the tunnel. The same displacement was plotted vs. volume loss, in the tunnel and linearity was again found to hold. Apparently, in this second scenario (i.e. with a building existing at the ground surface, the slope of the linear relationship was different (actually it was smaller, as expected, since the overall rigidity was increased). This proved a quick way to demonstrate that the above is true not only for the simple and conventional scenario of the greenfield conditions but also for the most advanced scenario, where tunnel, soil and structure are all included in one model.

In order to understand the significance of this result it is useful to recall the key assumptions of their analyses. The first pivotal point is that the response is assumed to be undrained. This means that, since volume change is zero, the volume of the settlement trough is equal to the volume loss in the tunnel cross – section. This is how linearity arises naturally. The second pivotal point is that the two researchers are really looking into the effect of an existing surface structure on the settlement profiles. Thus, if they want to isolate the effect of an overlying structure they have to make sure that the volume loss parameter in the tunnel will be the same. Otherwise, the effect of the surface structure cannot be assessed since it is coupled with the effect of the volume loss. The third point is the way the excavation is simulated. Initially the geostatic pressures are defined. These are evaluated along the perimeter of the tunnel. Then the soil elements, within the tunnel cross – section, are removed from the finite element mesh and they are replaced by the initially calculated pressure along the perimeter of the tunnel. Up to this point no excavation of the tunnel has been implemented. Simply a transition between two equilibrium situations is being performed. After the soil elements within the tunnel have been replaced with the pressure along the tunnel that satisfies equilibrium (apparently no displacements occur in this transition), the gradual release of this pressure is implemented. As the pressure along the perimeter of the cross – section of the tunnel is gradually reduced, the cross – section shrinks. This is what generates the volume loss and eventually the settlement trough. The reduction proceeds until a volume loss equal to 1.5% is achieved. When this value is obtained by the reduction of stress, the reduction stops and the settlement trough is assessed.

The above process makes it clear that a quick transition from a value of the volume loss parameter to another is beneficial in the sense that the degree of stress release can be loosely defined. In all cases, the removal of stress is incremental and unless offered by the finite element code automatically, the researcher has to calculate the volume loss manually. The availability of a linear relationship between the volume loss and the deformations allow the researchers to establish a reference constant value of stress release percent[1] and apply this stress release percent to all analyses. Then evaluate the observed volume loss for each analysis and correct the deformation profiles by linearly interpolating to the reference volume loss. It is interesting to note that this methodology led to the observation that for a fixed stress release among different scenarios of structures lying above the tunnel, the volume loss did not differ significantly. For example, the stress release that generated a volume loss of 1.5% in the greenfield scenario led to a volume loss of 1.37% in the extreme case of a 5 story structure (exhibiting extreme values of axial and flexural rigidity when represented as a linear elastic beam). This is a result, which is also reproduced in the context of this thesis.

A very similar approach to the aforementioned calculations is performed within the framework of this thesis. There are, however, some changes and modifications, which add a special interest to this approach. A model is established in the finite element code PLAXIS (Vermeer, Brinkgreve, 1998). In the following the main characteristics of the model will be defined and its similarities or differences compared to the Potts and Addenbrooke approach will be discussed.

Establishment of the numerical model

The first task when establishing a numerical model is the definition of the geometry. The geometric characteristics that could define the problem according to Potts and Addenbrooke are the depth of the tunnel axis, the shape and diameter of the tunnel cross – section, the width of the structure represented by an elastic beam, and the eccentricity in the positioning of the beam relative to the tunnel central axis. This is equal with the horizontal distance between the centerline of the tunnel and the midpoint of the beam.

It was decided to establish a fixed value for the geometrical characteristics of the model. The eccentricity was chosen to be zero. This was beneficial in the sense that allowed only half the model to be analyzed, since having eccentricity equal to zero implies that the geometry is symmetrical. As far as the tunnel is concerned, a circular tunnel with its centerline at a depth of 20m and a diameter of 4.146m was selected. This is a typical dimension and depth for the London Subway system and it is the scenario that was mostly investigated in the Potts and Addenbrooke study. The structure was chosen to have a width of 60m or, if considered only in half the model, a width of 30m and a moment fixity at its midpoint. This geometry was not only implemented in this preliminary analysis but also in all the analyses performed in this thesis. It was not on the

---

[1] For the greenfield case Potts and Addenbrooke (1997) quote β = 0.44, where $\beta = \dfrac{\sigma_i - \sigma_f}{\sigma_i}$, where σ_i is the initial normal pressure and σ is the final normal pressure at the tunnel cavity.

geometry that was put emphasis on, but rather on the behavior of the system of interaction so, after a simple geometry was selected, no other geometry scenarios were examined.

Concerning the dimensions of the mesh and the level of mesh coarseness, there was not any serious investigation performed. As far as the dimensions of the mesh, the dimension in the horizontal direction was taken to be 100m with the beam spanning 30m. This was considered to be sufficiently large so that no geometrical effects would appear in the results. In the vertical direction, the mesh dimension was taken equal to 70m with the tunnel being at a depth of 20m. These dimensions were kept constant for all the analyses. The same was done for the mesh coarseness. Since computational time was still negligible, a very fine mesh was implemented with local refinements on the areas of the beam and the tunnel cross – section. Figure 3.1 presents a typical finite element mesh used in the analyses. It comprises of 6 – node triangular elements. The model mesh typically comprises of 1000 elements. This number also includes the linear three node elements used for modeling the structure and the tunnel lining. Approximately 50 linear elements are generated in the model mesh.
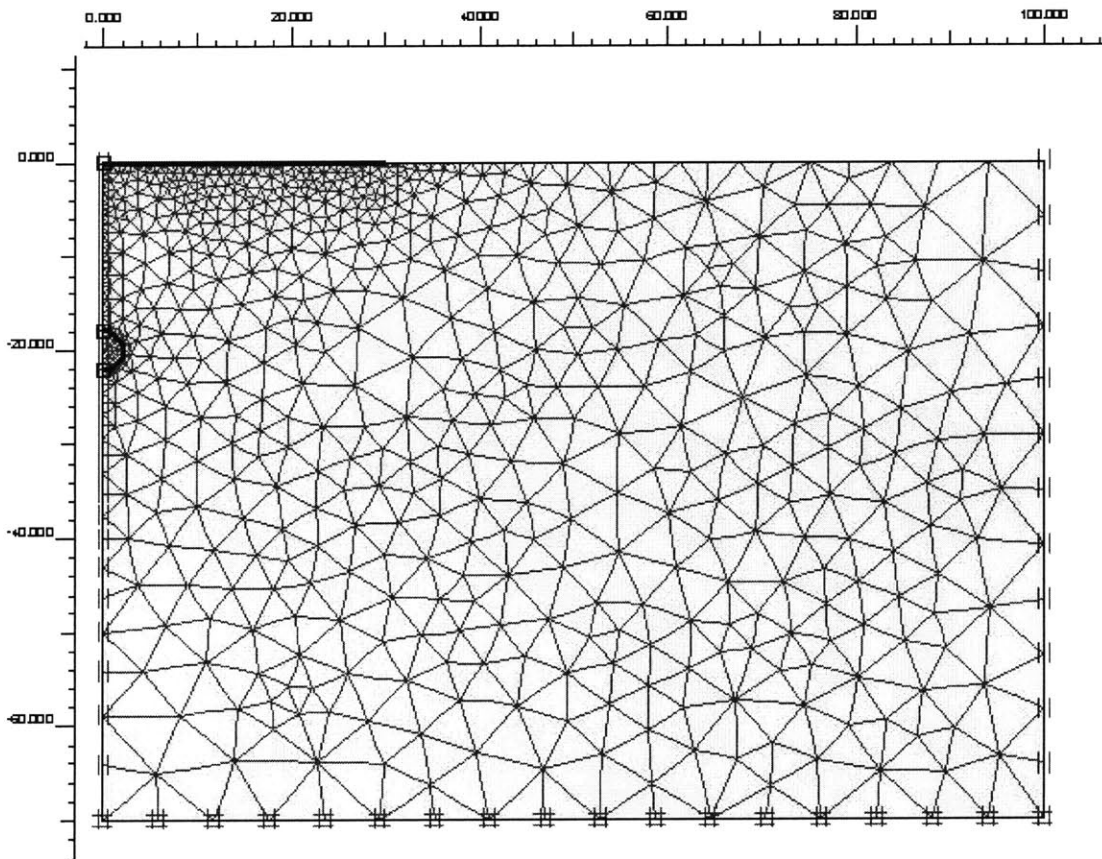
Figure 3.1. A typical finite element mesh

The second task concerned the selection of the soil profile. A major difference was applied here in comparison with the Potts and Addenbrooke approach. Instead of a saturated and undrained scenario for the soil profile and the excavation of the tunnel as

implemented in the Potts and Addenbrooke approach, a dry soil profile and drained conditions are selected. In general, these will be the two scenarios in terms of effect of the water pressures on the examined phenomenon. No cases of consolidation were examined. This is by itself a wide topic with several interesting aspects and it is out of the scope of this thesis. The major difference between the undrained and drained scenario is that in the undrained scenario due to the constrained volume change, the volume of the settlement trough is equal to the volume loss in the tunnel cross – section. This is not the case in a dry (drained) scenario. The volume loss in the tunnel can be the same as in the undrained scenario but there is no condition to imply that the Volume of the settlement trough is equal to the volume loss in the tunnel cross – section. This is of course not devoid of practical implications. For example, it is usual in conventional practice to express the Volume of the Settlement trough as a function of some important parameters of the trough such as the maximum settlement of the trough or the coordinate of the point of inflection of the trough. This is especially the case when the settlement trough is described by a Gaussian normal curve (Chapter 1). It is evident that in undrained conditions the knowledge of the volume loss in the tunnel, the equality of volume loss with the settlement trough volume and the use of empirical correlations for the description of the settlement trough can be a sufficient set of equations for the determination of all the necessary parameters that need to be identified (maximum settlement, inflection point and shape of the trough – Chapter 1). However, in drained conditions this is not valid because no equality holds in general between the volume loss in the tunnel is not equal with the volume of the settlement trough.

It becomes interesting to check whether the linear relationship between the value of volume loss in the tunnel and a displacement in the model also holds in case of a dry scenario. In a dry scenario it is more difficult to claim that the linear relationship arises naturally because now the zero volume change condition is not valid.

The soil was described by the Mohr – Coulomb soil model offered in PLAXIS. This model is presented in detail in Appendix A. It constitutes a linearly elastic – perfectly plastic soil model with soil stiffness varying linearly with depth. This is a practical way to mimic the stress – dependency of soil stiffness at least in terms of geostatic pressures; the deeper the soil element, the larger the geostatic pressure and the larger the soil stiffness. Despite of the fact that soil stiffness varies linearly with depth, it remains constant at a given depth and does not vary with the reduction of the confining pressure in the tunnel. However, when the tunnel is excavated, a change in the stress state of the soil is caused as well as in the soil stiffness state, which the model cannot describe. When the Hardening soil model (Schanz, 1998) is applied in the analysis, this feature of the soil behavior can be captured. In the model implemented by Potts and Addenbrooke, the stress dependency of soil stiffness is taken into account with a linear law. The simplicity of the Mohr – Coulomb soil model and the reduced number of parameters used to define it, make it the most attractive choice in preliminary calculations even though some features of soil behavior cannot be accurately described.

Selection of Mohr – Coulomb soil model parameters.

In the following, the selection of the values of the parameters for the definition of the Mohr – Coulomb soil model is being discussed.

The parameters that needed to be identified are:

- *The self weight of the soil γ [KN/m^3] and the coefficient of earth pressure at rest K_0*

The unit weight of the soil is chosen to be equal to $\gamma = 20$KN/m^3 and the coefficient of earth pressure at rest $K_0 = 1$. This is a point where the approach presented here differs from the approach presented by Potts and Addenbrooke (1997) as the two researchers used a value of $K_0 = 1.5$ in their analyses.

- *E: Young's modulus of elasticity [KN/m^2]*

For the selection of the Young's modulus of elasticity the option of a linearly varying profile vs. depth was selected. This could be defined with 3 parameters:

1. E_{ref}: being the soil stiffness at a reference depth in the model
2. y_{ref}: being the reference depth for which the reference soil stiffness is defined and
3. E_{incr}: being the change in stiffness within one unit of depth or more simply, the slope of the linear relationship of soil stiffness vs. depth.

The selected values are:

1. E_{ref}: 103MN/m^2
2. y_{ref}: 10m
3. E_{incr}: 10MN/m^2

Figure 3.2. Linear Variation of Soil Stiffness with depth
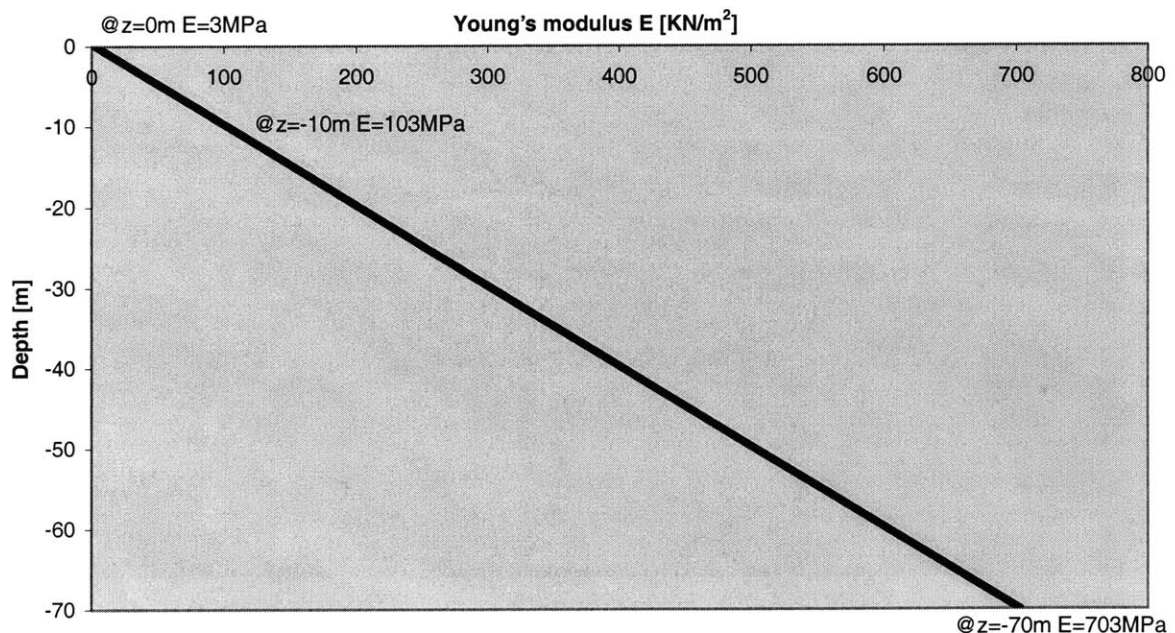
The selection of the first two parameters was driven by the definition of the relative axial and flexural rigidity parameters for the combined system soil – structure, ρ^* and α^*. In the definition of these parameters the soil stiffness is defined as the secant stiffness modulus obtained in a triaxial compression test performed on a sample taken from a depth equal to half the depth of the centerline of the tunnel. In Potts and Addenbrooke approach and for a depth of tunnel equal to 20m, this quantity is equal to 103MPa. This is the value that is also chosen for this analysis. The values for these two parameters were extracted from the Potts and Addenbrooke methodology and they were kept the same, since this would facilitate, the desired comparisons with respect to the relative flexural rigidity parameters. The value of the third parameter was chosen more loosely. The value of E_{incr} being equal to 10MN/m^2 gives rise to a ratio of $E/\sigma'_v = 500$, which is a common average value for clayey materials. It was not considered necessary to keep the calculation consistent with the Potts and Addenbrooke methodology here and despite of the fact that it would be easy to back – calculate the ratio E/σ'_v that Potts and Addenbrooke used, this was not implemented. In all cases, the aimed relationship should hold for all realistic cases of this ratio.

- *v: Poisson's ratio*

Poisson's ratio was back - calculated from the parameters of the soil model used by Potts and Addenbrooke. Similarly to the value of the ratio E/σ'_v, the value of Poisson's ratio was not that significant in this calculation but since it would be needed for the main bulk of the calculations presented later, it was implemented here too. The value of Poisson's ratio considered is $v = 0.2$.

Strength parameters

The strength parameters of the Mohr – Coulomb soil model were the same as the ones in the soil model presented by Potts and Addenbrooke with the exception of the dilatancy angle:

- $c = 10KPa$
- $\phi' = 25°$
- $\psi = 0°$ [2]

This concludes the definition of the Mohr – Coulomb soil model parameters.

The points at which there is a difference between the Potts and Addenbrooke approach and the approach presented here are summarized below:

1. The soil model. A simpler soil model was implemented in this analysis.

---

[2] Potts and Addenbrooke (1997) considered $\psi = 12.5°$. An assumption for $\psi = 0°$ is more realistic in the sense that it implies zero volumetric increase at failure. This can be very important for points that reach yield.

2. The undrained vs. drained conditions. In this model dry conditions were applied in contrast with the approach of undrained conditions of Potts and Addenbrooke that assumed a water table and undrained conditions.

3. The ratio E/σ'_v for this approach was chosen independently of Potts and Addenbrooke's soil model.

4. The coefficient of earth pressure at rest was taken equal to 1 in contrast with Potts and Addenbrooke assumption for $K_0 = 1.5$.

5. The dilatancy angle was considered $\psi = 0°$ instead of $\psi = 12.5°$.

Process of analysis

This paragraph discusses the process of analysis that was followed. The displacement within the model that was chosen to be investigated was the maximum vertical settlement at the ground surface occurring above the centerline of the tunnel. The method the tunnel was excavated was according to the methodology presented by Potts and Addenbrooke. In the input model, no lining for the tunnel was considered. As a first stage, the initial stresses were evaluated in the model. In the Calculations Module of PLAXIS simply one stage is defined, in which the soil within the tunnel cross – section is removed. This is done via the "Staged Construction" feature. The removal of the soil elements is controlled by the so - called ΣM stage factor, which denotes the percentage of the removal that has been performed in an incremental iteration towards convergence. This means that within the program, a nonlinear analysis involving an incremental increase of stress removal is performed until convergence is achieved when all the soil within the tunnel cross – section has been removed. If ΣM stage = 1, then the removal of the soil is performed totally. On the other hand, for a specified value of ΣM stage, for example 0.9, this corresponds to a 90% removal of the normal stress at the soil cavity. Different values of the ΣM stage give rise to different volume losses within the tunnel. The volume loss of the tunnel is calculated according to the following. Since, the parameter of volume loss is defined as the ratio of the change in volume of the tunnel cross section over the initial volume (or more simply the ratio of the change of the tunnel cross sectional area over the initial cross sectional area), the initial and final cross sectional area of the tunnel need to be calculated. The initial cross sectional area is known from the input geometry. It is essential here that the initial cross sectional area considered is the area of the model and not the area of the ideal circular cross section. The cross sectional area of the model is the area of a polygon inscribed in the circle defining the real cross section. For the calculation of the final cross sectional area, after the removal of the soil, the deformed shape had to be assessed. The output of the program offered the displacements of each node of the polygon defining the cross sectional area. From the displacements (both in horizontal and vertical directions) the coordinates of the nodes in the deformed geometry were defined. The calculation of the area of the deformed cross sectional area was performed via Green's theorem, which gives the area defined by a set of points joined with straight lines in a Cartesian coordinate system:

$$A = 0.5 \sum_{i=1}^{n} (x_i y_{i+1} - y_i x_{i+1}) \tag{3.1}$$

where x_i and y_i are the coordinates of a point i, and n is the number of points.

The analysis proceeded as follows: A number of values for the ΣM stage factor were selected and the model was solved. For each analysis, the maximum displacement above the centerline was obtained as well as the volume loss in the tunnel cross sectional area.

The procedure was performed for two scenarios; the "greenfield" one and a scenario at which a 5 – story building is positioned at the surface of the ground. The bending and axial stiffness for the structure are calculated according to the methodology suggested by Potts and Addenbrooke as presented in earlier sections of this study. The applied values are:

- EA = 20.7 GN/m
- EI = 1707 GPa /m

The following pages present the results of the analyses. Three figures are given. Figure 3.3 presents the variation of the volume loss with respect to the stress release factor, ΣM stage. Figure 3.4 shows the variation of the vertical displacement at the center of the structure relative to the ΣM stage factor and finally Figure 3.5 presents the variation of the centerline surface settlement versus the ground loss around the tunnel cavity.

The results for both scenarios are plotted together. Tabulated are given in Table 3.1.

EXISTING STRUCTURE SCENARIO			GREENFIELD SCENARIO		
ΣM stage	Volume Loss [%]	Vertical Displacement [m]	ΣM stage	Volume Loss [%]	Vertical Displacement [m]
0.00	0	0	0.00	0	0
0.45	0.235	0.0005	0.45	0.235	0.0005
0.60	0.323	0.0007	0.60	0.323	0.0008
0.75	0.672	0.0015	0.75	0.676	0.0017
0.80	0.923	0.0022	0.80	0.930	0.0028
0.85	1.385	0.0035	0.85	1.401	0.0039
0.90	2.337	0.0061	0.90	2.369	0.0068

Table 3.1. Results from the analysis for the assessment of the relationship between the vertical displacement at the center of the structure (above the centerline of the tunnel) and the volume loss at the tunnel cross - section

Figure 3.3. Relationship between volume loss and stress release factor at tunnel cavity. Base case Analysis
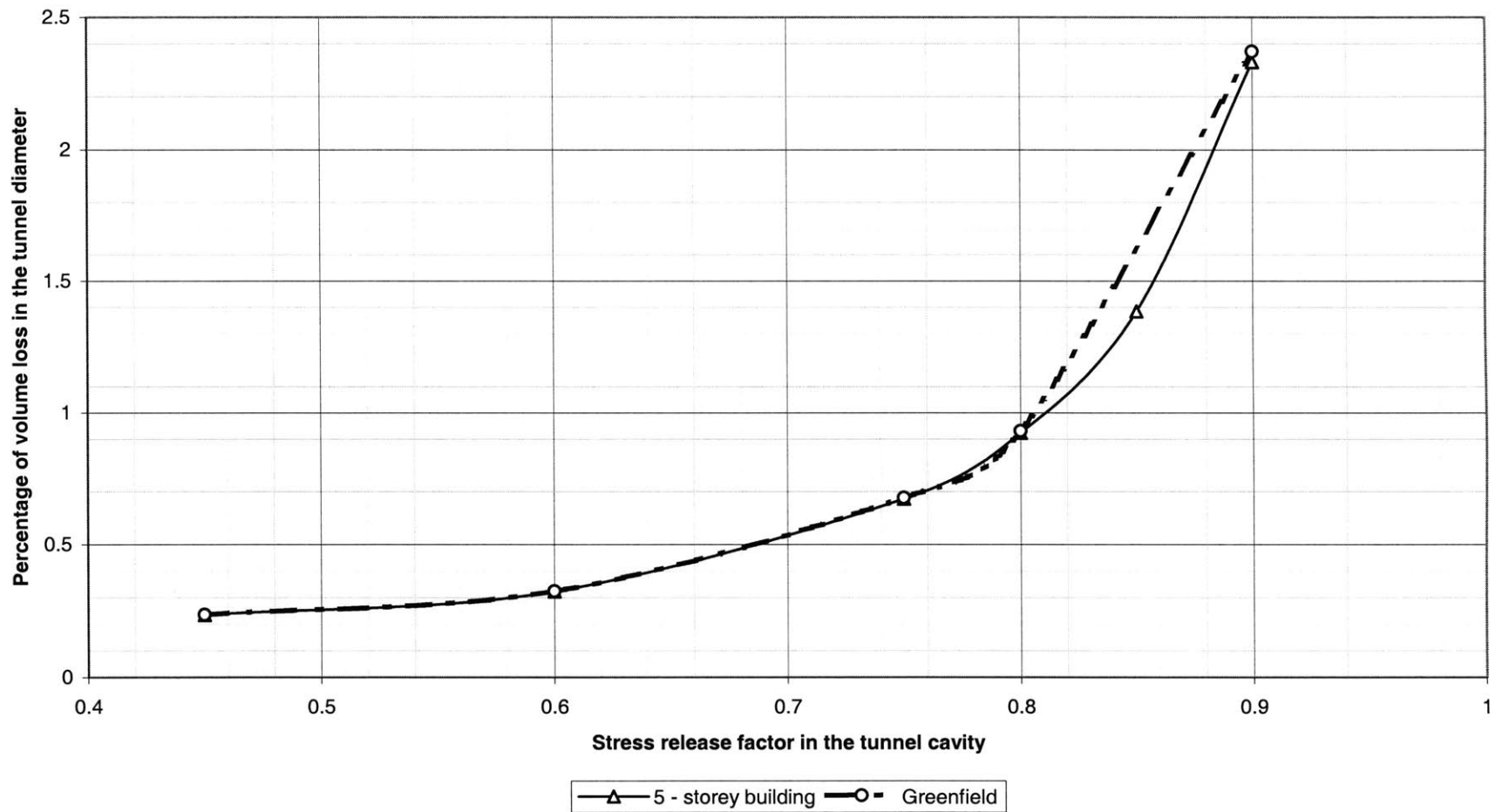
Figure 3.4. Relationship between centerline surface settlement and stress release factor at tunnel cavity. Base case analysis.
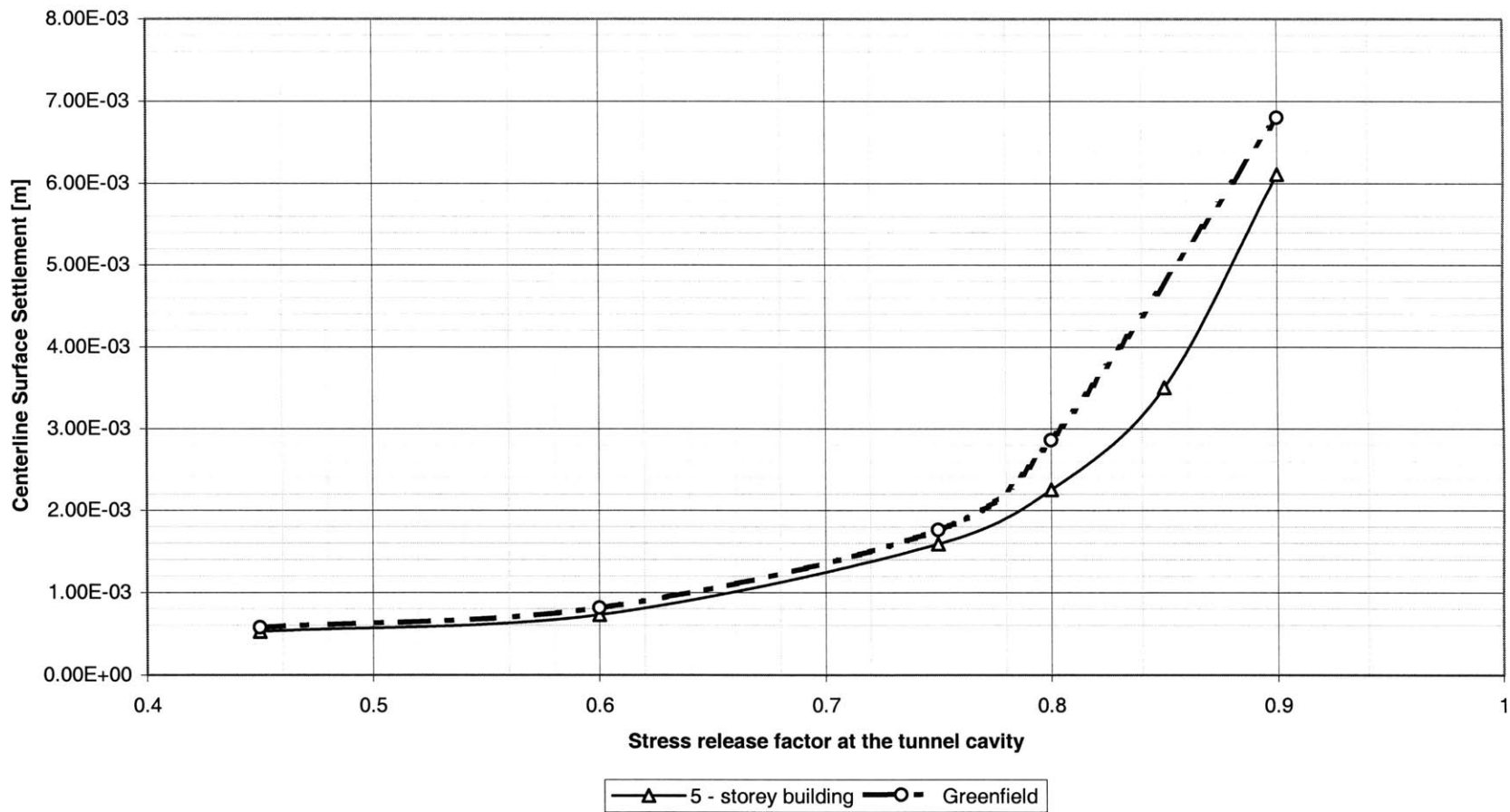
Figure 3.5. Relationship between centerline surface settlement and volume loss in the tunnel cavity. Base case analysis.
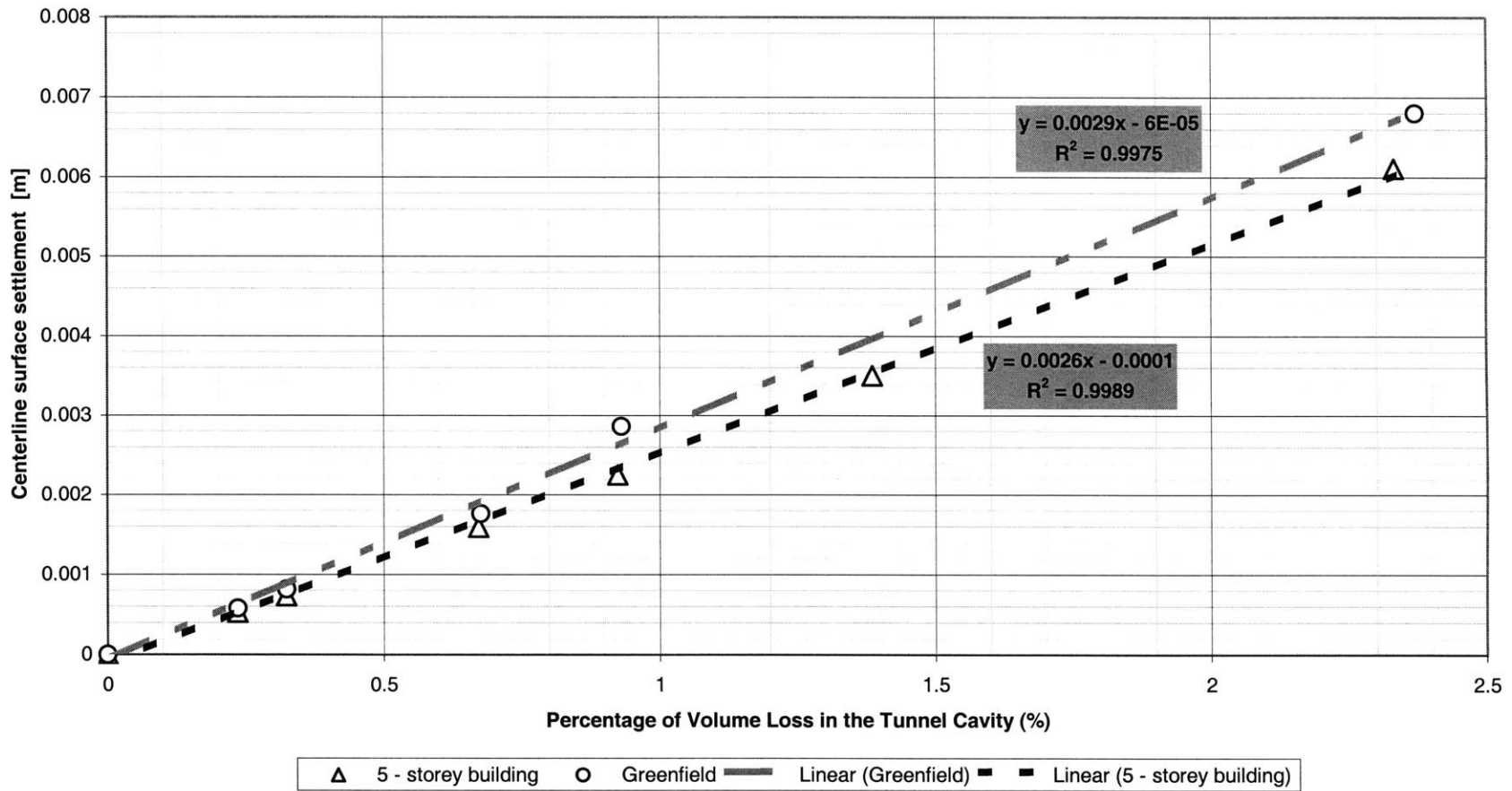
Comments

- Figure 3.5 is proving that the linear relationship between the volume loss percentage and the maximum vertical displacement holds not only for undrained scenarios but also for drained conditions as well. The correlation coefficients R^2 for both scenarios are very close 1 and in the relationship $y = ax + b$, with $b = 0$ is within tolerated limits of error (i.e. no displacement occurs for zero volume loss).

- In the proven linear relationship, the slope for the case of a 5-story building is less than the slope recorded for the "greenfield" scenario. It is true that the difference is not very large, but for axially or flexurally beams it is expected that the difference is more revealing.

- From figure 3.3, it is concluded that the presence of the structure causes a negligible difference in the calculated volume loss for a specific ΣM stage factor. This comes as a verification of the result as reported by Potts and Addenbrooke.

3.3 COEFFICIENT OF EARTH PRESSURE AT REST

This section presents a pilot level study of the influence of the coefficient of earth pressure at rest K_0 on the predicted ground deformations status of the model after tunnel excavation.

The coefficient of earth pressure at rest is the parameter, which defines the relative magnitudes of the initial geostatic stresses, namely those acting at the horizontal direction. The stresses at the vertical direction are controlled by the unit weight of soil. As it turns out, the significance of the coefficient of earth pressure at rest becomes larger since it also controls to a considerable extent the shape of the settlement trough. The analyses are organized as follows: The factors that need to be investigated are the value of the coefficient of earth pressure at rest, the dry or wet scenario and the transition from the simplistic Mohr – Coulomb model to the more advanced Hardening Soil Model.

Thus the analyses that have been performed are tabulated in the following table:

Vertical Displacements				
	Drained Conditions		Undrained Conditions	
	Mohr - Coulomb Soil Model	Hardening Soil model	Mohr - Coulomb Soil Model	Hardening Soil model
K_0	0.5	0.5	0.5	0.5
	1.0	1.0	1.0	1.0
	1.5	1.5	1.5	1.5

Horizontal Displacements				
	Drained Conditions		Undrained Conditions	
	Mohr - Coulomb Soil Model	Hardening Soil model	Mohr - Coulomb Soil Model	Hardening Soil model
K_0	0.5	0.5	0.5	0.5
	1.0	1.0	1.0	1.0
	1.5	1.5	1.5	1.5

Table 3.2 Analyses for the effects of K_0 on the predicted "greenfield" ground movements

Some important details should be noted:

1. **Method of excavating the tunnel.** In this study over the coefficient of earth pressure at rest, we are departing from the stress release method of simulating the excavation of the tunnel. Instead a new approach is applied, which takes advantage a feature offered in the finite element code PLAXIS. Until now, what was being implemented was that the tunnel remained unsupported and the stress along the tunnel perimeter was being reduced until a volume loss equal to a reference number (namely 1.5%) was being recorded. Exploiting the contraction feature offered in PLAXIS what is being performed is the following. A lining of certain stiffness is applied to the tunnel cross section. As an initial stage of calculation, the soil within

the tunnel is removed. In a second step, a specific contraction is applied to the tunnel. If, for example, a contraction of 1.5% is applied, this is equivalent to a volume loss of 1.5%. The only difference is that the contraction in the tunnel is applied uniformly, or in other words, the cross section changes in size, but it does not change in shape and this holds for all cases of K_0. In other words, if a contraction of 1.5% is applied and the K_0 is changed, the deformations of the tunnel cross – section will still be the same. This is not the case when the tunnel is unsupported and a stress release is being implemented. Then, the change in the value of K_0 will have an effect on the deformed shape of the tunnel cross section. One might expect that if the deformations in the tunnel cross section are kept fixed, then the settlement trough may be the same no matter what the value of K_0 is. This may come about especially when considering the link of the volume loss and the volume of the settlement trough in greenfield conditions. They are equal! The analyses presented below aim to show that such a thought is wrong. This is also why the method of applying a uniform contraction to the tunnel cross – section, instead of applying the stress release methodology. It was aimed to isolate the effect of K_0 on the settlement trough. The effect of the deformed tunnel cross – section on the shape of the settlement trough was thus extinguished.

2.   **Stiffness of the tunnel lining.** As stated above, a certain realistically stiff tunnel lining should be applied, for the contraction technique to be applied. The values selected are for an elastic beam describing the tunnel lining are EA = 1.4E7 KN/m and EI = 1.43E5 KNm^2/m. These values are quite common values for tunnels with a shotcrete lining.

3.   **Calibration of the Hardening Soil model.** In the above it is mentioned that the Hardening Soil model will be implemented in an attempt to give a better description of the anticipated soil behavior due to the excavation of the tunnel. More specifically, it is the stress dependent soil stiffness as obtained by the equations of the Hardening soil model, that offers an improvement in describing the soil behavior. What should the parameters of the Hardening soil model be so that there is a certain degree of consistency with the Potts and Addenbrooke model and the MC soil model that can make the results of the analyses comparable? Although the Hardening soil model is applied in this chapter as well, for an investigation of the effects of the coefficient of earth pressure at rest, the calibration of the values of the model parameters is presented in section 4.2.

The results are presented in the diagrams of the following pages.

- Figures 3.6 and 3.7 present the vertical and horizontal displacements respectively when the Hardening Soil model is implemented.

- Figures 3.8 and 3.9 present the vertical and horizontal displacements respectively when the Mohr – Coulomb soil model is implemented.

- The same results are replotted in Figures 3.10 to 3.13. In figures 3.10 and 3.11 the vertical and horizontal displacements for both soil models are plotted for the dry scenario and drained conditions.

- In Figures 3.12 and 3.13 the vertical and horizontal displacements respectively are plotted for the wet undrained scenario. Both soil models are included.

Figure 3.6. Hardening soil model - Vertical surface displacements - Comparison of different scenarios with drainage conditions and K_0

Distance from the tunnel centerline [m]

Legend:
- Wet scenario - K0 = 1
- Wet scenario - K0 = 1.5
- Wet scenario - K0 = 0.5
- Dry scenario - K0 = 1
- Dry scenario - K0 = 1.5
- Dry scenario - K0 = 0.5
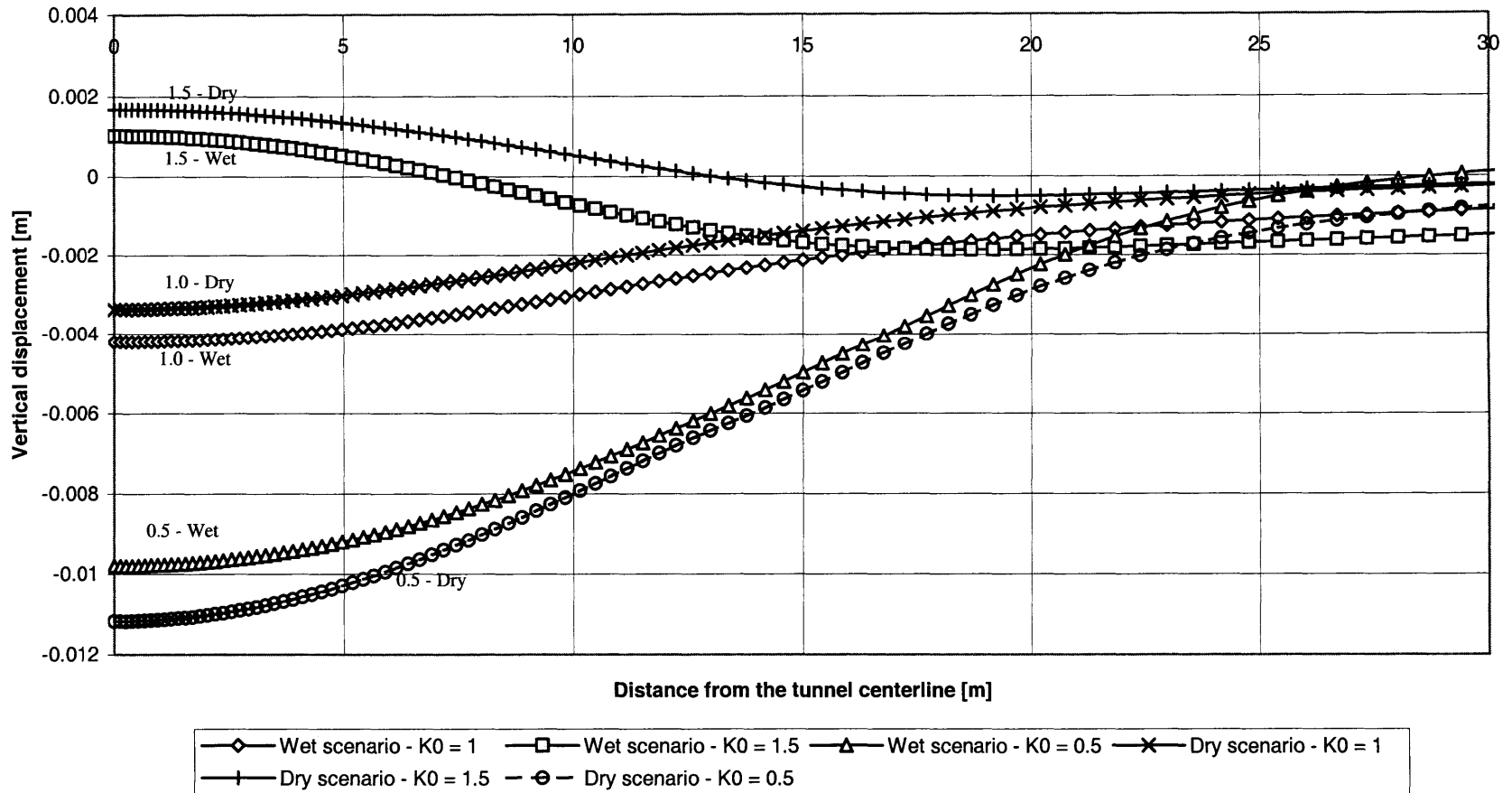
Figure 3.7. Hardening soil model - Horizontal surface displacements - Comparison of different scenarios with drainage conditions and K_0

Distance from the tunnel centerline [m]

◆ Wet scenario - K0 = 1   □ Wet scenario - K0 = 1.5   ▲ Wet scenario - K0 = 0.5   × Dry scenario - K0 = 1   + Dry scenario - K0 = 1.5   ○ Dry scenario - K0 = 0.5
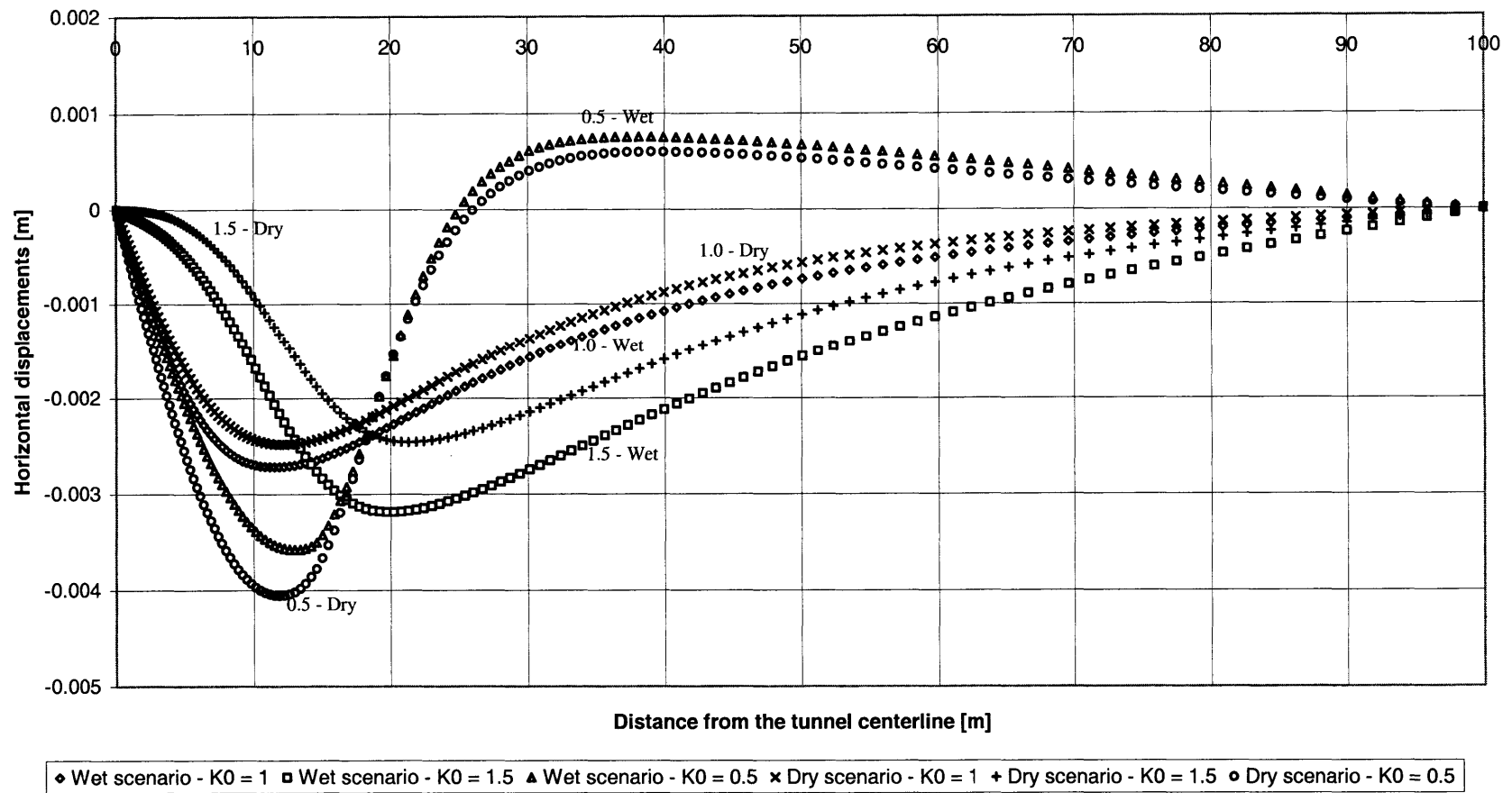
Figure 3.8. Mohr - Coulomb soil model - Vertical surface displacements - Comparison of different scenarios with drainage conditions and K_0

Distance from the tunnel centerline [m]

—◇— Wet scenario - K0 = 1	—□— Wet scenario - K0 = 1.5 —△— Wet scenario - K0 = 0.5 —✕— Dry scenario - K0 = 1
—+— Dry scenario - K0 = 1.5	—⊖— Dry scenario - K0 = 0.5
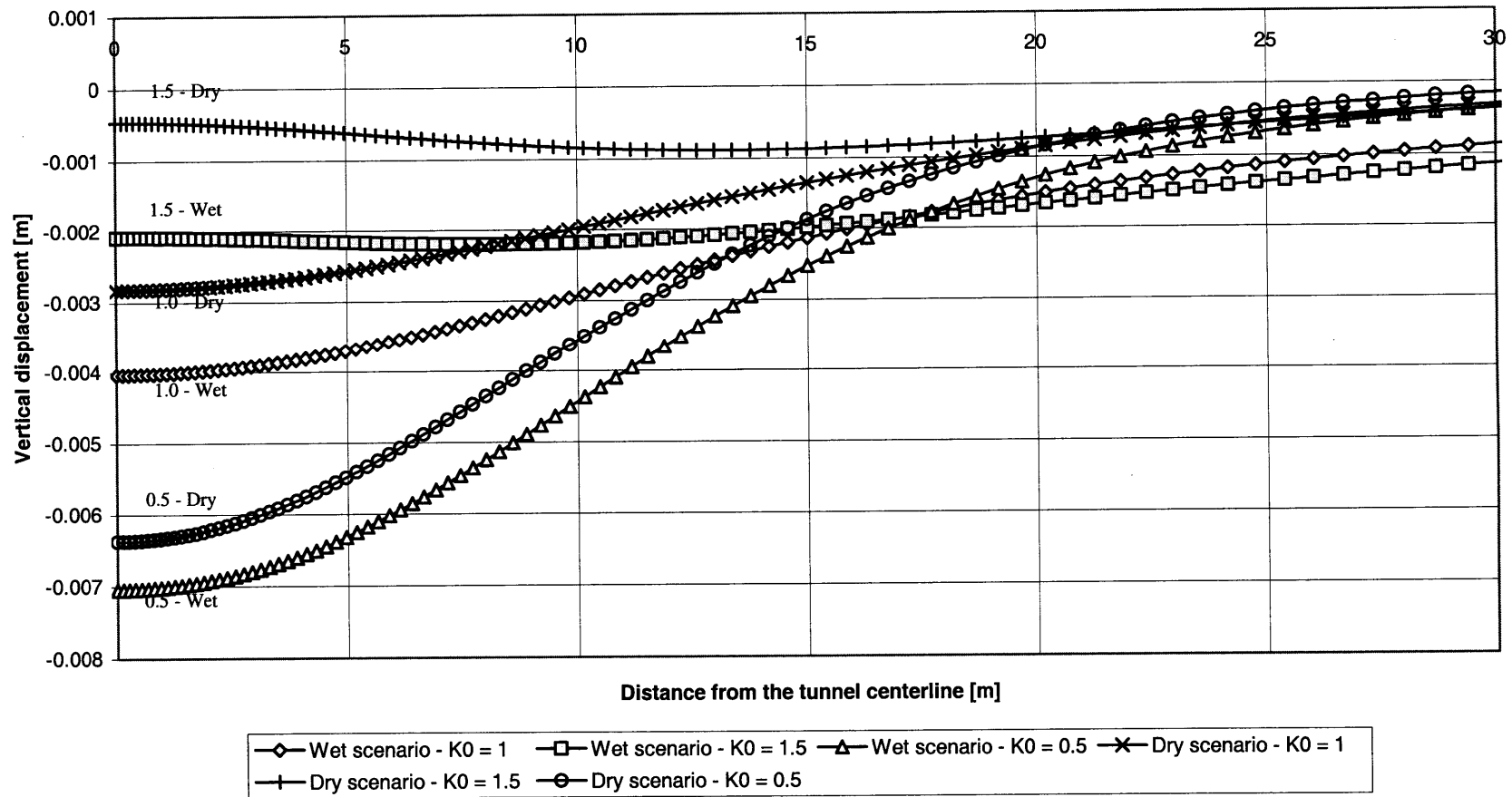
Figure 3.9. Mohr - Coulomb soil model - Horizontal surface displacements - Comparison of different scenarios with drainage conditions and K_0
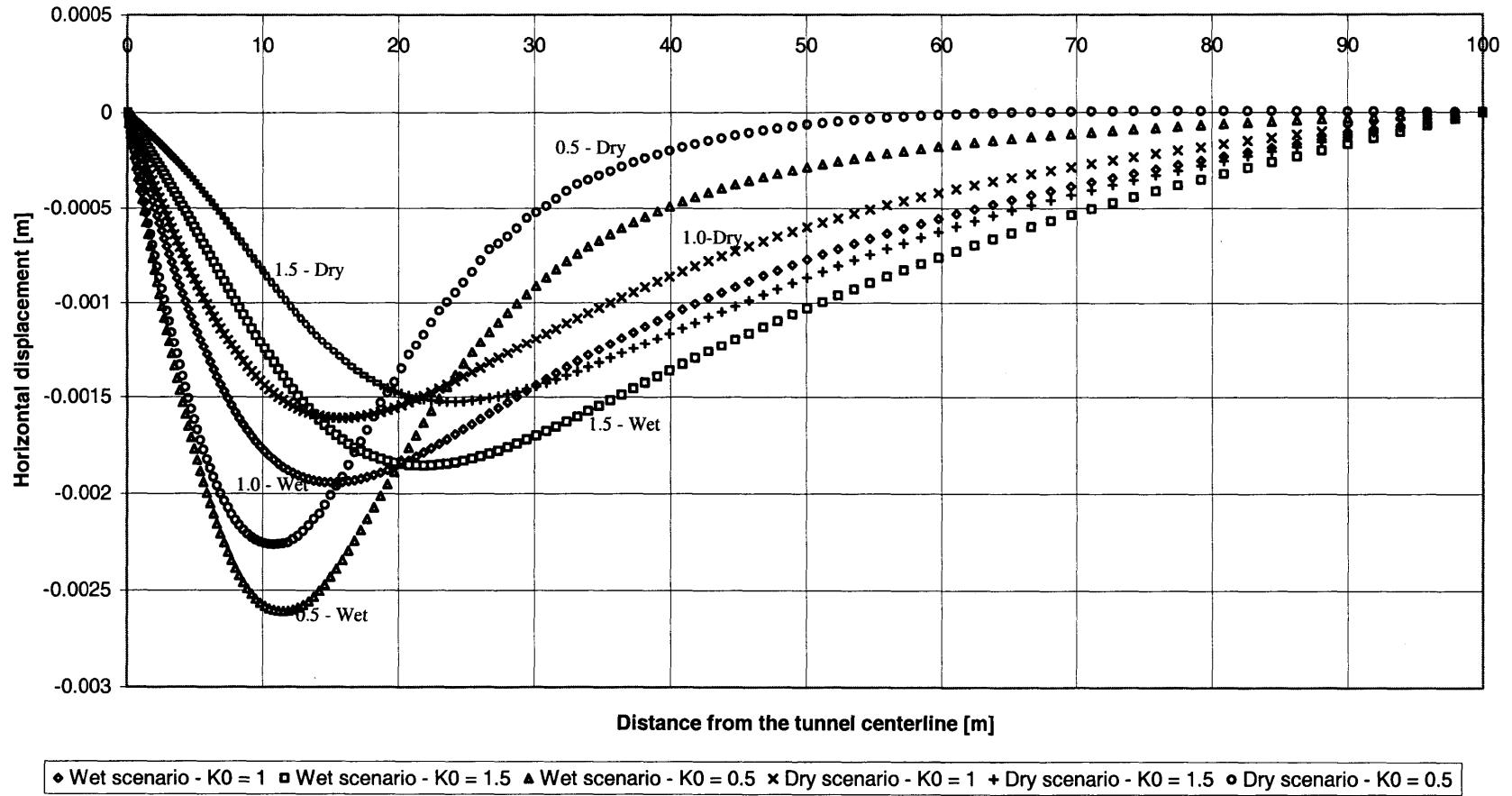
Figures 3.6 to 3.9 show the variation of vertical and horizontal displacements with respect to drainage conditions and the value of the Coefficient of earth Pressure at rest K_0. The results from the soil models (Hardening soil model and Mohr – Coulomb soil model) are presented separately.

Concerning the vertical displacements the following can be stated:

- Recalling that the depth of the tunnel is $Z = 20m$, the effect of K_0 seems to be minimized at a distance from the centerline of the tunnel equal to the depth of the tunnel.
- For both drained and undrained conditions, a normal Gaussian curve seems to be able to describe the settlement trough for values of K_0 less or equal to 1.
- In case where $K_0 = 1.5$, a heave is taking place above the centerline. This cannot be captured by a normal Gaussian curve.
- The smaller the value of K_0, the larger the vertical settlement.
- According to the definitions of sagging and hogging deflections, for $K_0 = 1.5$ there is a hogging above the centerline and a sagging area away from the centerline. The opposite is true when $K_0 \leq 1.0$. For this case, the inflection point moves away from the centerline as K_0 decreases.
- Between the two models and among the different values of K_0 there in not a specific pattern on whether drained or undrained conditions give rise to larger ground movements.

Concerning the horizontal displacements the following can be stated:
- The effect of the change in K_0 is significant even far away from the centerline in contrast with what is being observed for the vertical settlements.
- The point of maximum horizontal displacement moves closer to the centerline as the coefficient of earth pressure decreases. This point also divides the trough in two areas: the area of compressive strain (close to the centerline) and the area of tensile strain away from the centerline.
- The value of maximum horizontal displacement is increasing as K_0 is decreasing.
- No general patterns were observed concerning the differentiation between drained and undrained conditions. The difference between horizontal displacements for drained and undrained conditions seems to be larger in the Mohr – Coulomb soil model than in the Hardening Soil model.

Figures 3.10 to 3.13 compare the results as obtained for the Hardening Soil model and the Mohr – Coulomb soil model.

67

Figure 3.10. Dry scenario, drained conditions - Vertical surface displacements - Comparison of different scenarios with drainage conditions and K_0

Distance from the tunnel centerline [m]

| —◇— Hardening - K0 = 1 | —□— Hardening - K0 = 1.5 | —△— Hardening - K0 = 0.5 | —✕— MC - K0 = 1 | —+— MC - K0 = 1.5 | —⊖— MC - K0 = 0.5 |
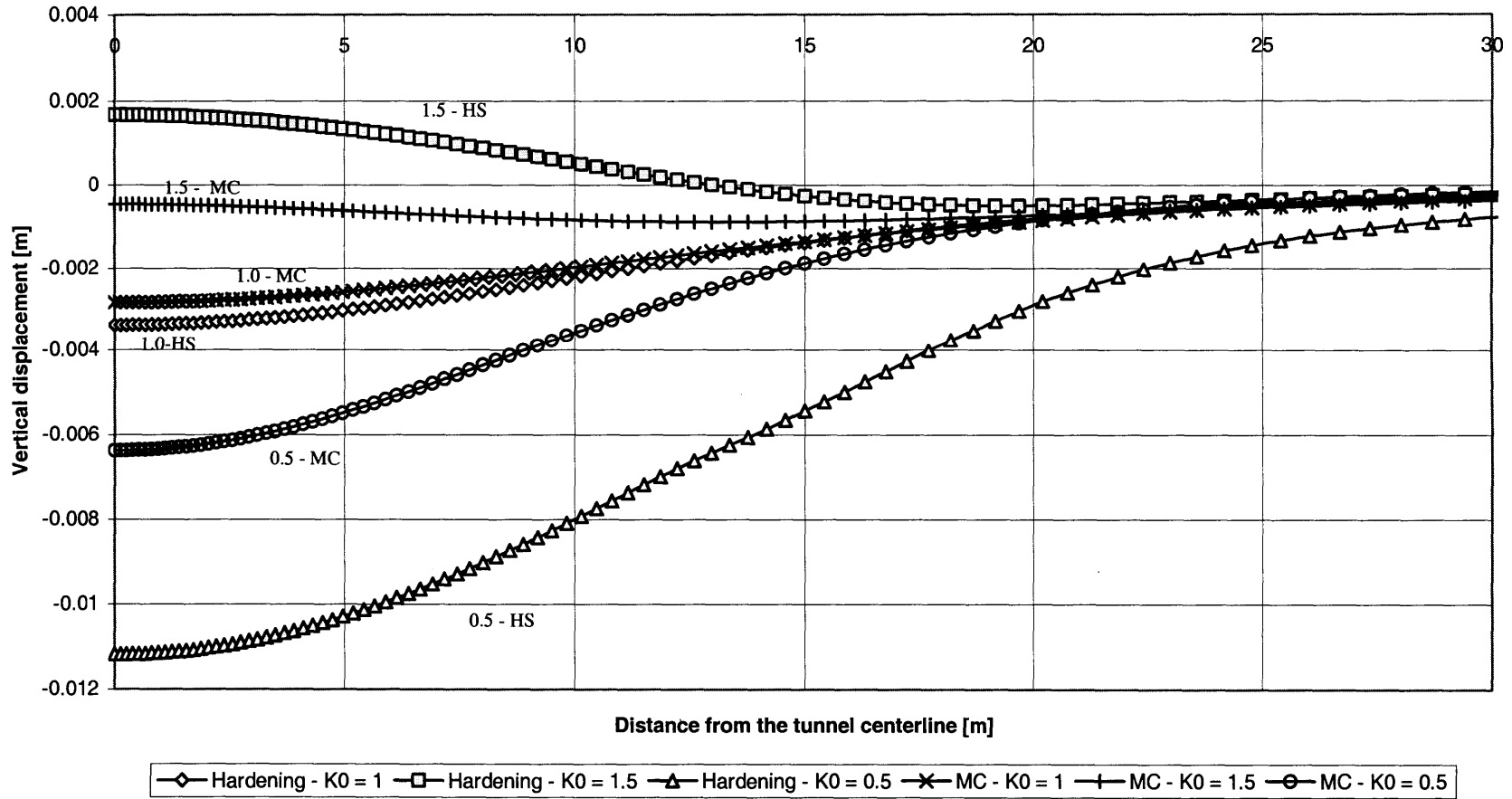
Figure 3.11. Dry scenario, drained conditions - Horizontal surface displacements - Comparison of different scenarios with drainage conditions and K_0

Distance from the tunnel centerline [m]

◆ Hardening - K0 = 1   □ Hardening - K0 = 1.5   ▲ Hardening - K0 = 0.5   × MC - K0 = 1   + MC - K0 = 1.5   ○ MC - K0 = 0.5

69
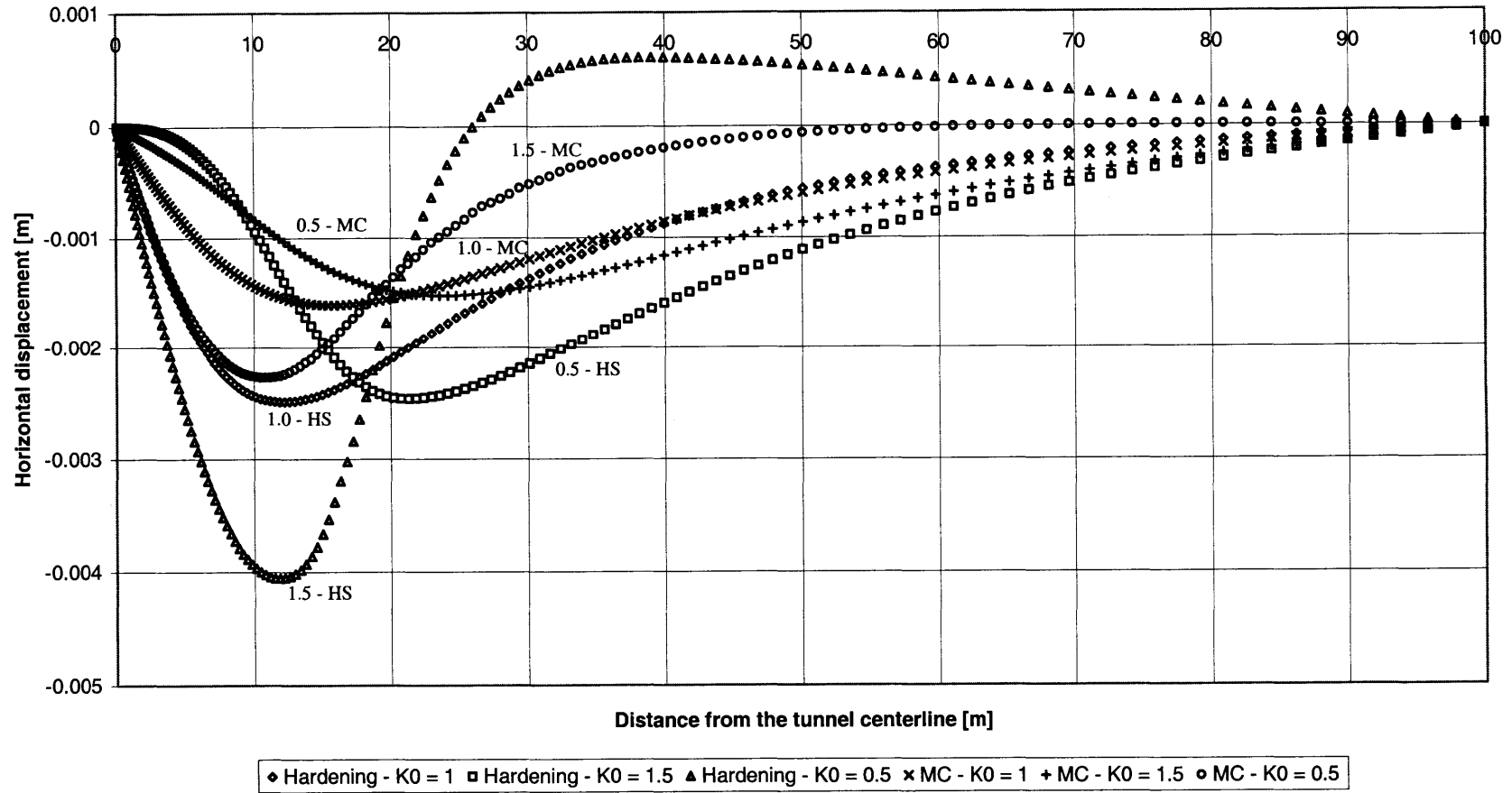
Figure 3.12. Wet scenario, undrained conditions - Vertical surface displacements - Comparison of different scenarios with drainage conditions and K_0

Distance from the tunnel centerline [m]

—◇—Hardening - K0 = 1   —☐—Hardening - K0 = 1.5   —△—Hardening - K0 = 0.5   —✕—MC - K0 = 1   —+—MC - K0 = 1.5   —⊖—MC - K0 = 0.5
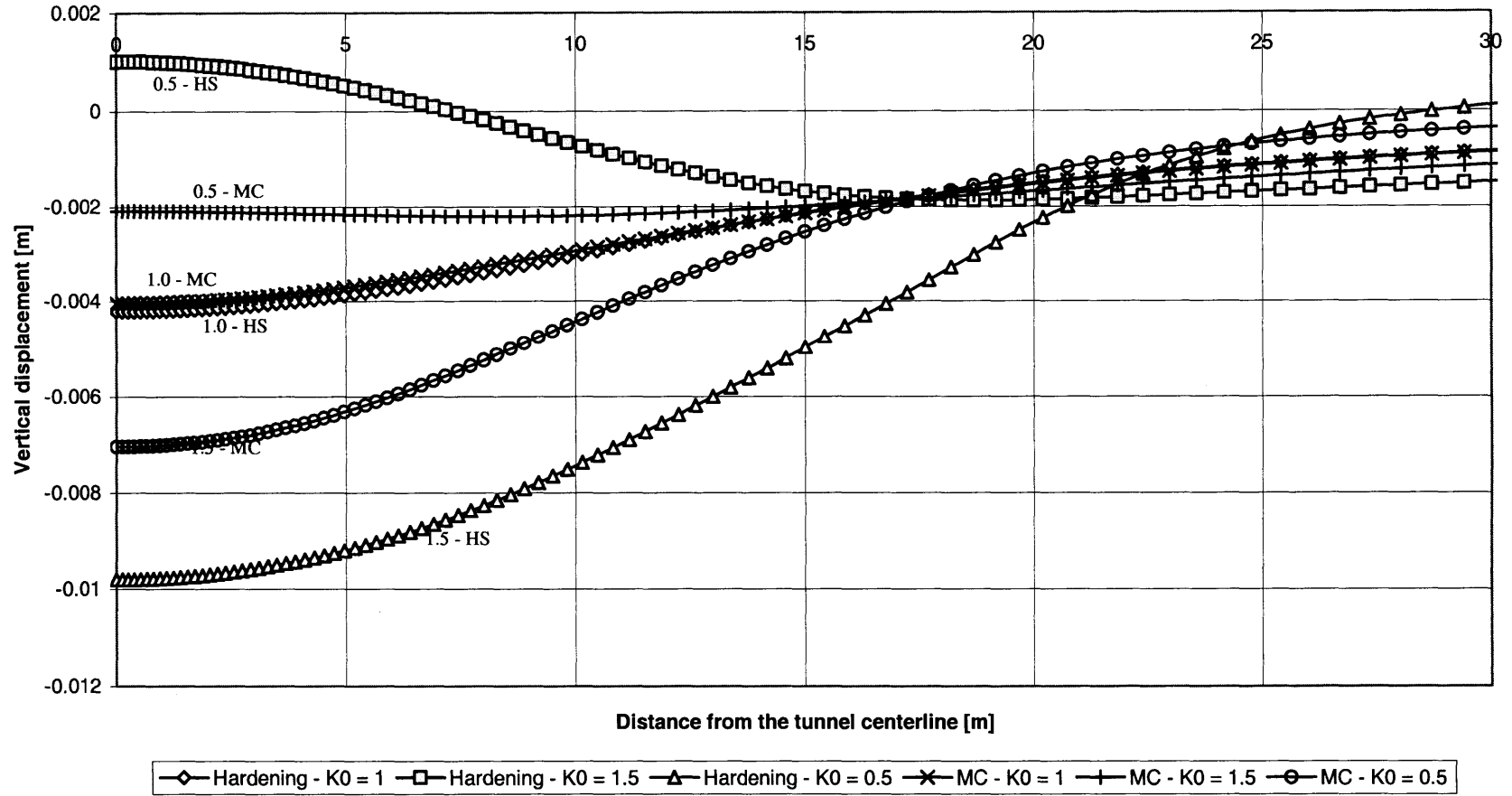
Figure 3.13. Wet scenario, undrained conditions - Horizontal surface displacements - Comparison of different scenarios with drainage conditions and K_0

Distance from the tunnel centerline [m]

◆ Hardening - K0 = 1   □ Hardening - K0 = 1.5   ▲ Hardening - K0 = 0.5   × MC - K0 = 1   + MC - K0 = 1.5   ○ MC - K0 = 0.5
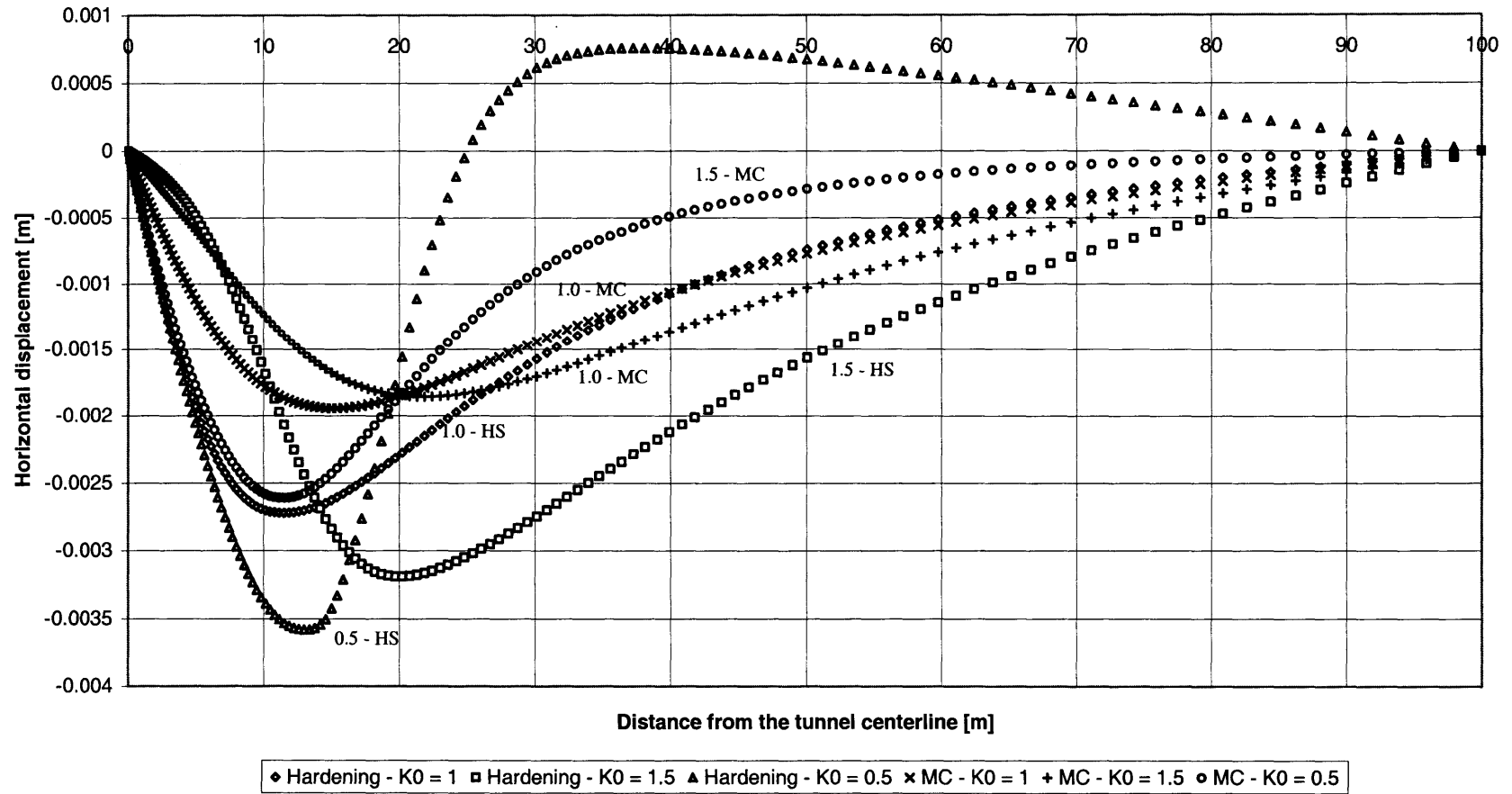
The figures presented in the previous pages show the profiles of the vertical and horizontal displacements for the two examined soil models, for drained and undrained conditions and for three distinct values of the coefficient of earth pressure at rest. Some general remarks can be made.

- It is obvious that the value of the coefficient of earth pressure at rest K_0 is very strongly related not only with the magnitude but also with the shape of the settlement trough or even the profile of the horizontal displacements. A normal Gaussian curve - trough is the obtained result when $K_0 = 1.0$. When $K_0 = 0.5$ the trough is radically extended to much larger settlements but the shape basically remains the normal Gaussian curve type trough. However, in the case where $K_0 = 1.5$ the trough changes shape. In the region directly above the tunnel, there is a heave instead of a settlement. This phenomenon obtains a physical interpretation when one considers that K_0 being equal to 1.5 means that the deformed shape of the excavated tunnel may look like an ellipse with the major axis in the vertical direction. It should be noted that in the analyses, the shape of the deformed cross section remains circular due to the imposed contraction. But, the effect of a K_0 larger than one is still expressed in the formation of the settlement trough and eventually a trough with a shape very different from a normal Gaussian type curve is obtained. The differentiation between drained and undrained conditions does not seem to affect this result. However, the magnitudes of the displacements are slightly affected.
- In terms of horizontal displacements, the effect of the coefficient of earth pressure at rest is also significant. Originating with a value of $K_0 = 1.0$, if the value is increased, the horizontal displacement trough moves away from the tunnel getting wider and wider. If the value of K_0 is decreased, the trough of horizontal displacements becomes narrower and develops closer to the tunnel. The difference between drained and undrained conditions again does not influence the shape of the trough that much but rather the magnitude of the horizontal displacements but not to a very important extent.
- The above remarks are true for both the Hardening Soil Model and the Mohr – Coulomb soil model. When results from these two models are compared (figures 3.10 to 3.13) it can be said that the Hardening soil model gives significantly larger displacements (according to the K_0 value) compared to the Mohr – Coulomb model. The vertical settlement troughs are deeper and narrower. For example, the heave in both drained and undrained conditions is much more spectacular when the Hardening soil model is being implemented. In general, this is true for both drained and undrained scenarios and for both horizontal and vertical displacements as it can be proven by Figures 3.10 to 3.13.
- It is expected that if the self – weight of the building was taken into account, the settlement troughs would be significantly affected. For example, it is doubtful if in case of $K_0 = 1.5$, heave would be obtained above the centerline.
- While for the vertical displacements the effects of the differences in examined scenarios vanish at around a distance from the centerline of the tunnel equal to the depth of the tunnel axis (approximately 20m in this example), this is not the case

for the horizontal displacements. In this case, the value of K_0 is very important in determining the practical width of the trough.

- The hogging and sagging areas as well as the areas of compressive or tensile strain can be defined in all cases of soil model, drainage conditions and values of the coefficient of earth pressure at rest. It is obvious, however that if they control the damage of an overlying structure, this will be very different among the different cases of values for K_0. For example, let us compare the troughs in undrained conditions and using the Hardening Soil model. Let us also assume that the building undergoes the greenfield troughs as presented in Figure 3.11. The building is centrally positioned relative to the tunnel and has a half width equal to 30m. If $K_0 = 1.5$ then the center of the building will undergo hogging and the edges of the building will undergo sagging. On the contrary, if $K_0 = 0.5$ then the center of the building will undergo sagging and the edges will undergo hogging. An interesting observation can be made. The damage assessment entails two damage parameters; the deflection ratio in hogging and sagging and the horizontal strain either compressive or tensile. Now, from the two aforementioned scenarios for $K_0 = 1.5$ and $K_0 = 0.5$ it is very unlikely that the same deflection ratios and horizontal strains will arise, which means that the value of K_0 directly influences the damage assessment procedure. But even if the same deflection ratios arise, will the damage be the same? The available methodology would say that yes, the damage would be the same. However, the answer in not at all obvious. Within the framework of this thesis such a question was not administered but it might be an interesting topic for further research. Of course, similar comments hold for the horizontal strain parameters but in this case, the issue is not that striking since the shape of the horizontal displacement trough does not change that radically (at least in terms of the first derivative which expresses the horizontal strain) as the value of K_0 varies from 0.5 to 1.5.

In the last part of chapter 3, the results obtained from the analysis of a slightly modified scenario will be discussed. This scenario concerns the examination of Hardening soil Model and Mohr – Coulomb model for three values of K_0 in drained conditions. The difference here is that neither a contraction (i.e. a fixed deformation in the tunnel cross – section) is applied nor a constant volume loss. On the contrary, what is being implemented is fixed stress release in an unsupported opening. The geometrical data are not changed. The Stress release is fixed via the ΣM – stage factor to a value = 0.85. The results are presented in the following two pages.

As far as the settlement troughs are concerned Figure 3.13 presents the same trends as in figures 3.5 – 3.12. The value of K_0 has a strong effect on the shape of the settlement trough and the hardening soil model predicts larger displacements than the Mohr – Coulomb soil model.

In figure 3.14, the deformation of the tunnel - cross section is presented. For every case, the deformation does not obey a prescribed uniform pattern.

Either stress release or uniform contraction is applied to the tunnel, it seems that the conclusions presented above concerning the surface displacements are in general, true.

Figure 3.14. Drained Conditions-Comparison of settlement troughs for different values of K0
Fixed Stress release = 0.85
Hardening Soil Model in comparison with the Mohr Coulomb Soil Model
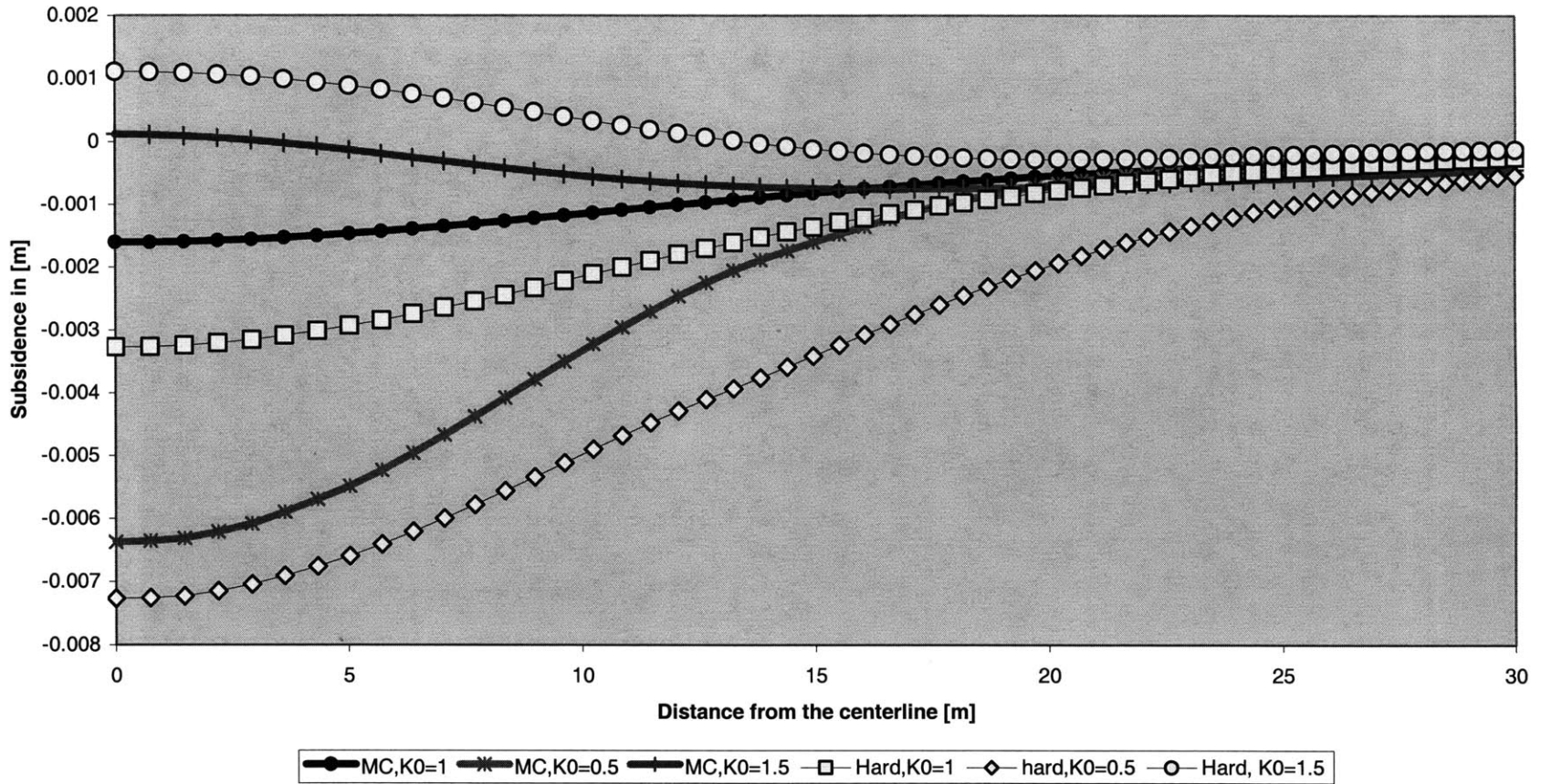
Figure 3.14. Deformation of the tunnel for different values of K0
Hardening Soil Model in comparison with the Mohr Coulomb Soil Model
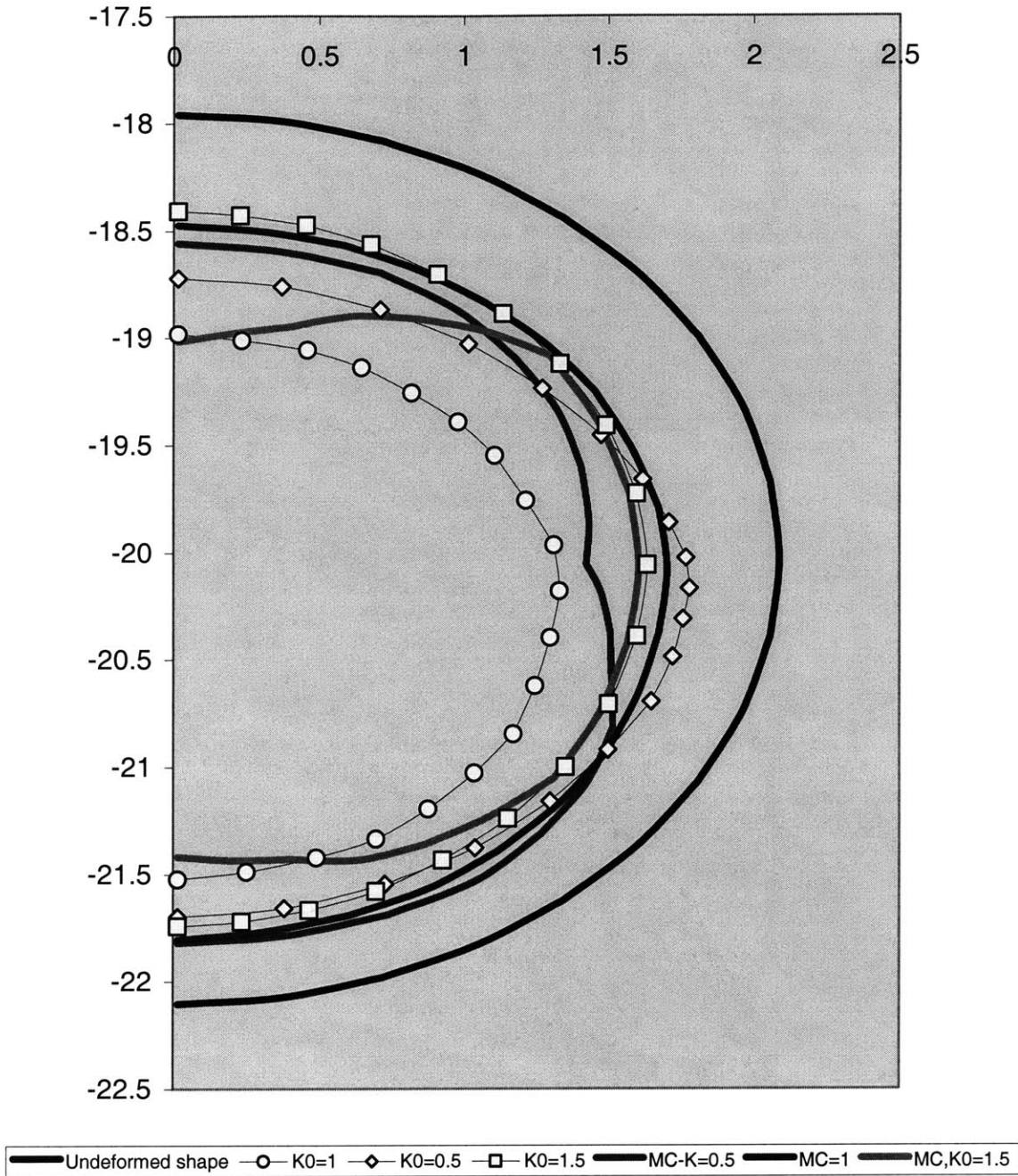
CHAPTER 4

PREDICTIONS OF THE EFFECTS OF STRUCTURE ON SURFACE DEFLECTIONS AND LATERAL STRAIN

4.1 INTRODUCTION

So far, an extensive presentation of many aspects concerning the phenomenon of interaction between a surface structure and the excavation of a tunnel has been made, mainly from the point of view of how the settlement trough above the tunnel is modified because of the existence of the structure. The goal is of course a more refined and realistic assessment of the potential of damage to existing surface structures when a tunneling project is undertaken in an urban area. In this effort, the focus lies on the evaluation of some parameters defined by the settlement trough that will develop below the foundation of a structure. These parameters are the deflection ratio both in hogging and in sagging and the horizontal strain either tensile or compressive. Their definition is given in Chapter 1. The selection of these parameters is not of course arbitrary. They are the parameters that are used as input in the currently used methodologies for the assessment of potential damage to surface structures because of underground construction in general or tunneling in specific. The work by Burland (1995) is a very well known example of methodology, where the damage assessment parameters are the deflection ratios (sagging – hogging) and the horizontal strain.

The introduction of the modification factors in this whole concept comes about in an attempt to depart from the conventional assumptions of greenfield settlement troughs developing below the buildings to a more realistic view of the world, where the existing surface structure is also considered. The idea behind the definition of the modification factors is simple. What the engineer is interested at the end of the day is nothing more than the value of deflection ratio (hogging – sagging) and the value of horizontal strain (tensile – compressive) that will develop in the trough below the foundation of the building, so that he can apply the well-established damage assessment methodologies. A cheap and presumably conservative assessment considers the deflection ratios and the horizontal strains of the greenfield scenario – no building is present during the development of the settlement trough. In an improved, more realistic assessment, the building damage parameters will not be the same as those in greenfield conditions. In other words, if the greenfield damage parameters are known, they need to be *modified* to yield the improved parameters. In Chapter 2, where the work by Potts and Addenbrooke has been presented, it was made clear how numerical analysis could be used to provide with such modification factors. In the following, the basic principles of the work presented by Potts and Addenbrooke will be more or less implemented in an attempt to provide with such modification factors for different scenarios of soil conditions (distinction mainly between drained and undrained conditions) and different ways of modeling the soil behavior.

4.2 DIFFERENT SCENARIOS AND SOIL MODEL PARAMETERS

The modification factors for the building damage parameters (deflection ratio and horizontal strain) are calculated for different scenarios of soil drainage conditions and two separate soil models in PLAXIS. The first model is the simpler Mohr – Coulomb soil model and the second is the more advanced Hardening soil model. More specifically, the modification factors are calculated for the following scenarios:

- In drained conditions, the modification factors for sagging and hogging deflection ratios as well as for compressive and tensile horizontal strains, are calculated for both the Mohr – Coulomb soil model and the Hardening soil model. It is reminded that when considering drained conditions in this problem, we assume a dry soil. The excavation in the tunnel is simulated in terms of the stress release method and a volume loss of 1.5% is obtained. By presenting the results obtained from this analysis, a comparison between the Mohr – Coulomb and the Hardening Soil model can be achieved.

- In undrained conditions, the modification factors are calculated for the case of the Hardening soil model, being the more realistic and the one capturing most features of soil behavior. The scenario is very similar to the one studied by Potts and Addenbrooke and an immediate comparison of the results is feasible. After such a calculation has been completed, a comparison between the results from drained and undrained conditions can be performed. Of course, in this scenario as well, both the deflection ratio and the horizontal strains are examined.

It is interesting to note that in the above analyses, not the same range of parameters is examined as in the work performed by Potts and Addenbrooke. For instance, the effect of eccentricity is not studied in this work. In all cases, the structure is centrally positioned in terms of the tunnel (above the tunnel centerline) and a predefined width of the tunnel is considered. This width is taken to be 60m. The half - width of the structure is 30m. Also the depth of the tunnel is kept constant. The tunnel axis is positioned at a depth of 20m below the ground surface. The diameter of the tunnel is also fixed. A value of 4.146m, typical for the models implemented for the London Underground Projects, is assigned to the tunnel diameter. The geotechnical profile is another "fixed" variable in this problem, although the models that describe this profile or the drainage conditions in the soil profile are changed. The stiffness parameters of the underlying structure, being represented by a linear elastic surface beam are varied within a wide range from very stiff beams (axially or flexurally) to very flexible beams. In the analyses presented below, a decoupling of the stiffness parameters of the beam with respect to the building damage parameters is considered. In other words, it is considered that the deflection ratio in the developing settlement trough is a function of the flexural rigidity of the beam (EI) and the horizontal strain a function of the axial rigidity of the beam (EA). This leads in the following practice for the determination of the modification factors. For the modification factors of the deflection ratio in sagging or hogging, the axial rigidity of the beam is kept constant and the flexural rigidity of the beam varies within the range of several orders of magnitude. Similarly, the determination of the modification factors for the horizontal strains is performed by changing the axial rigidity of the beam while the flexural rigidity

of the beam is kept constant. It is understandable that this provides a limited assessment of the modification factors in the 2D space of axial and flexural rigidities. This means that the modification factors for deflection ratio or horizontal strain can be viewed as a surface in the 3D space. The axes of this Cartesian system can be defined as follows: the x-axis and y-axis can correspond to the axial and flexural rigidity of the beam respectively, and the z-axis can correspond to the modification factor of deflection ratio or horizontal strain. Of course, in order to define sufficiently the four desired surfaces (deflection ratio in sagging and hogging and horizontal strain compressive and tensile), a large number of analyses would be demanded. In this thesis, what is actually being performed is the evaluation of two representative cross – sections of these surfaces, one parallel to the axis of the axial rigidity and one parallel to the axis of the flexural rigidity of the beam. These "cross –sections" are chosen according to typical values as presented by Potts and Addenbrooke and hopefully can capture the basic characteristics of these 3D surfaces.

The variation of the beam axial and flexural rigidity is depicted through the variation of the relative rigidity parameters ρ^* and α^*. In the definition of these parameters other quantities are also included:

- The soil stiffness E_s, which is kept constant even though the soil model is varied. (Actually, this serves as the criterion for the transition between the soil models, since there cannot be a unique correspondence between soil models with different input parameters and different view of the soil behavior. In the soil model implemented by Potts and Addenbrooke, the parameter E_s is equal to 103MPa for a tunnel at a depth of 20m. The parameters of the Mohr-Coulomb and Hardening Soil model are obtained so that they preserve this property; the parameter E_s is in all cases equal to 103MPa.
- The dimensions of the structure. These are kept fixed as presented above.

Since in the definitions of the relative rigidity parameters ρ^* and α^*, all other parameters besides the rigidity of the beam are kept constant, then apparently the variation on ρ^* and α^* is nothing more than a variation on the value of the rigidity (axial and flexural) of the beam.

It is deemed that the above remarks will make clearer the presentation of the results in the following parts of Chapter 4.

Soil Model Parameters. In earlier chapters, a presentation of the different soil models has been given. These are the soil model applied by Potts and Addenbrooke, which is actually an elastoplastic model presented earlier by Jardine et al. (1986), the Mohr–Coulomb soil model as offered in the finite element code PLAXIS and the Hardening Soil model also offered in PLAXIS. The question which now arises is what parameters should be implemented so that there is a certain degree of consistency between the models?

In general, this is not a trivial question. Actually, for two separate problems in geotechnical engineering, for which comparison of soil models is desired, the

implemented parameters may be totally different. The most rational methodology is assuming the transition occurring from the more complicated model to the simpler. Then, it is not possible to include all the features of soil behavior as given by the more complicated model, but having understood the principles of a more complicated model, it is possible to identify the prevailing stress paths or characteristics of the examined phenomenon and "shrink" the model by optimizing its behavior for the examined phenomenon. It is also possible to move in the opposite direction from the simpler to the more complicated model and actually this is how things are being developed in engineering. But, an improved understanding of the problem has to be acquired. In most cases, this is obtained through experimental schemes or observations in real engineering projects. In the problem examined here, there are very few experimental results (for example, Taylor and Grant, 1998) and the database from real projects is still being extended. It is not within the scope of this thesis to move towards such directions. But such an orientation would definitely be of interest for further research.

In the problem examined here, the point of tangency between the different models is determined by the parameter E_s, the one that is used to define the soil participation in the assessment of the relative rigidity parameters α^* and ρ^*. According to Potts and Addenbrooke (1997), this parameter is the secant stiffness modulus in a drained triaxial compression test performed at a sample extracted from a depth equal to $Z/2 = 10m$ and corresponding to a value of axial strain equal to 0.01%. From the exhaustive catalog of parameters used for the elastoplastic model of Jardine et al. (1986), they evaluated $E_s = 103MPa$.

Mohr-Coulomb Soil Model. The parameters used to define the implemented Mohr-Coulomb soil model have been presented on Chapter 3. They are summarized briefly below:

- $E_{ref} = 103MPa$
- $\nu = 0.2$
- $y_{ref} = -10m$ (this is determined by the definition of coordinates in PLAXIS. We assume $y = 0$ at the ground surface)
- $E_{incr} = 950*20 = 19000KPa/m$
- $c' = 10KPa$
- $\phi' = 25°$
- $\psi = 0°$
- $K_0 = 1.0$

The selection of the above values is justified in Chapter 3. The Poisson' ratio ν and the value of E_{incr} are evaluated from the parameters that define the elastoplastic model of Jardine as follows:

It is known from the definitions of the model presented by Jardine et al. that the following equations hold:

$$\frac{3G}{p'} = A + B\cos\left[\left(\alpha\left(\log_{10}\left(\frac{E}{\sqrt{3}C}\right)\right)\right)^{\gamma}\right] \qquad (4.1a)$$

$$\frac{K}{p'} = R + S\cos\left[\left(\delta\left(\log_{10}\left(\frac{\varepsilon_v}{T}\right)\right)\right)^{\gamma}\right] \qquad (4.1b)$$

If in the above equations we neglect the sinusoidal and logarithmic terms and simply consider the values for A and R, we get:

$$\frac{3G}{p'} = 1120 \qquad (4.2a)$$

$$\frac{K}{p'} = 549 \qquad (4.2b)$$

We also know from the theory of elasticity the following:

$$G = \frac{E}{2(1+v)} \qquad (4.3a)$$

$$K = \frac{E}{3(1-2v)} \qquad (4.3b)$$

Hence,

$v = 0.22$

On the contrary if we consider, instead of the constants A and R, the values G_{min} = 2333KPa and K_{min} = 3000KPa are obtained by the same procedure leading to:

$v = 0.19$

Hence, an average value of $v = 0.2$ is finally adopted.

For the determination of the slope in the linear variation of the Young's modulus with depth, the following is obtained:

$$\frac{E'}{\sigma'_{v0}} = \frac{1}{3}\frac{3G}{\sigma'_{v0}}2(1+v) = \frac{1}{3}\frac{3G}{p}2(1+v) = 0.333*1120*2*(1+0.2) = 895$$

or

$$\frac{E'}{\sigma'_{v0}} = \frac{K}{\sigma'_{v0}}3(1-2v) = \frac{K}{p'}3(1-2v) = 549*3*(1-2*0.2) = 990$$

In the above relationships $\sigma'_{v0} = p'$, and this is true because $K_0 = 1.0$. Hence, the current analyses consider an average value $E/\sigma'_{v0} = 950$.

Parameters of the Hardening Soil Model – Dry scenario. The assessment of the parameters for the Hardening soil model for the dry scenario in PLAXIS begins by assessing the strength parameters of the applied Mohr – Coulomb failure surface. These will be, in accordance with the model presented by Jardine et al. the following:

- $c' = 10$KPa
- $\phi = 25°$

For the dilatancy angle, it is preferred to use the exact value as suggested by Potts and Addenbrooke. Thus:

- $\psi = 12.5°$

Next, the ultimate deviatoric stress is calculated:

$$q_f = (c\cot\phi - \sigma'_3)\frac{2\sin\phi}{1-\sin\phi} = (10\cot 25° + 200)\frac{2\sin 25°}{1-\sin 25°} = 325 KPa \qquad (4.4)$$

The pressure σ'_3 is $10*20 = 200$KPa being equal to the vertical effective stress at a depth of 10m. This is because the K_0 remains equal to 1.0.

The asymptotic value for the hyperbolic relationship between q and ε_1, q_a is calculated via the reduction factor R_f, the value of which is retained as default and equal to 0.9.

Thus $q_a = q_f / R_f = 325 / 0.9 = 361$ KPa.

The next step entails the calculation of the parameter E_{50}. This will be done with aid of the equation:

$$-\varepsilon_1 = \frac{1}{2E_{50}}\frac{q}{1-\dfrac{q}{q_a}} \qquad (4.5)$$

Solving the above equation 4.5 for E_{50} we obtain:

$$E_{50} = \frac{1}{2\varepsilon_1}\frac{q}{1-\dfrac{q}{q_a}} \qquad (4.6)$$

In the above expression describing the stress – strain law in a drained triaxial compression test, it is known from the model by Jardine et al. (1986) that for an axial strain of $\varepsilon_1 = 0.01\%$ the secant stiffness modulus is 103MPa. Thus, the corresponding deviatoric stress $q = 103 \times 10^3 * 0.0001 = 10.3$ KPa.

This gives rise to an E_{50}, which is:

$$E_{50} = \frac{1}{2\varepsilon_1}\frac{q}{1 - \dfrac{q}{q_a}} = \frac{1}{2 * 0.0001}\frac{10.3}{1 - \dfrac{10.3}{361}} = 53\text{MPa}$$

In PLAXIS, E_{50} is defined indirectly via E_{50}^{ref}, p^{ref} and m.
The default values for p^{ref} and m are set as following:

- m = 1(for soft clays)
- p^{ref} = 100KPa (default value).

The value for E_{50}^{ref} is back - calculated according to the following relationship:

$$E_{50} = E_{50}^{ref}\left(\frac{c\cot\phi - \sigma_3'}{c\cot\phi + p^{ref}}\right)^m = E_{50}^{ref}\left(\frac{10\cot 25^o + 200}{10\cot 25^o + 100}\right)^1 = E_{50}^{ref} * 1.823$$

$$\Rightarrow E_{50}^{ref} = 53/1.823 = 29MPa$$

The pressure σ'_3 is 200KPa as before.
The parameter E_{oed}^{ref} is approximated using the relationship from the theory of 1D loading:

$$E_{oed}^{ref} = \frac{E_{50}^{ref}(1 - v)}{(1 + v)(1 - 2v)}, v = 0.2 \tag{4.7}$$

This gives $E_{oed}^{ref} = 32$MPa

The rest of the parameters are kept as default as proposed by Schanz (1998).

Parameters of the Hardening Soil Model – Wet scenario. The assessment of the parameters for the Hardening soil model for the wet scenario in PLAXIS is similar to the one for the dry case. The equations and the parameters are presented below.

- c' = 10KPa
- $\phi = 25°$
- $\psi = 12.5°$

Next, the ultimate deviatoric stress is calculated:

$$q_f = (c\cot\phi - \sigma_3')\frac{2\sin\phi}{1-\sin\phi} = (10\cot25° + 120)\frac{2\sin25°}{1-\sin25°} = 210KPa$$

The pressure σ'_3 is 10*20 – 8*10 = 120 KPa being equal to the vertical effective stress at a depth of 10m. This is because the K_0 remains equal to 1.0 and the water table is 2 meters below the surface of the ground.

- $q_a = q_f / R_f = 210 / 0.9 = 233$ KPa.

- $$E_{50} = \frac{1}{2\varepsilon_1}\frac{q}{1-\dfrac{q}{q_a}} = \frac{1}{2*0.0001}\frac{10.3}{1-\dfrac{10.3}{233}} = 54000KPa = 54MPa$$

- $$E_{50} = E_{50}^{ref}\left(\frac{c\cot\phi - \sigma_3'}{c\cot\phi + p^{ref}}\right)^m = E_{50}^{ref}\left(\frac{10\cot25° + 120}{10\cot25° + 100}\right)^1 = E_{50}^{ref}*1.165$$

  $$\Rightarrow E_{50}^{ref} = 54/1.165 = 46MPa$$

The pressure σ'_3 is 120KPa as before.
The parameter E_{oed}^{ref} is approximated using the relationship from the theory of 1D loading:

- $$E_{oed}^{ref} = \frac{E_{50}^{ref}(1-v)}{(1+v)(1-2v)}, v = 0.2$$

This gives $E_{oed}^{ref} = 51MPa$

The rest of the parameters are kept as default.

Table 4.1 tabulates the strength and stiffness soil parameters for the dry and wet scenario in the implementation of the Hardening soil model.

Parameter	Units	Dry Scenario	Wet Scenario
c	[KPa]	10	10
ϕ'	[°]	25	25
ψ	[°]	12.5	12.5
q_f	[KPa]	325	210
q_a	[KPa]	361	233
E_{50}	[MPa]	53	54
E_{50}^{ref}	[MPa]	29	46
E_{oed}^{ref}	[MPa]	32	51

Table 4.1 Strength and stiffness Hardening soil parameters for dry and wet scenarios

4.3 PRESENTATION OF THE RESULTS

In this paragraph the results of the main bulk of the numerical analyses are presented. They concern the calculation of the modification factors of the deflection ratio in sagging and hogging and of the horizontal strain either compressive or tensile that develop in the settlement trough of a surface beam when a tunnel is excavated. As it has been stated, different scenarios of the rigidity of the beam (axial and flexural) have been studied and two different cases of drainage conditions in the soil. First, the dry scenario is presented, which is established so that a comparison between the Mohr – Coulomb model and the Hardening Soil Model can be achieved.

> a. *Dry Scenario – Comparison between the Mohr – Coulomb model and the Hardening Soil model*

In this first examined scenario a dry soil profile is examined and the model is assigned a drained behavior condition. The geometric characteristics of the model as well as the properties of the soil models have been presented in previous chapters and paragraphs.

The following four pages present the results.

Figures 4.1 and 4.2 summarize the modification factors for the deflection ratios in both sagging and hogging. For this purpose the flexural rigidity parameter $\rho*$ varies from 5×10^{-8} m^{-1} to 5×10^{-1}m^{-1} with constant $\alpha* = 50$. This is a relatively high value but is considered to be realistic in describing the real relative axial rigidity parameter of a structure. The second figure (Fig. 4.2) presents similar results but for the horizontal strain (compressive and tensile) with constant $\rho* = 0.005$m^{-1} and $\alpha*$ varying from 5×10^{-5} to a value $5 \times 10^{+3}$. Theses same results have been tabulated in tables 4.2 and 4.3.

Figure 4.1. Modification factors in sagging and hogging for analyses using the Hardening soil model and the Mohr - Coulomb soil model for constant α^*=50
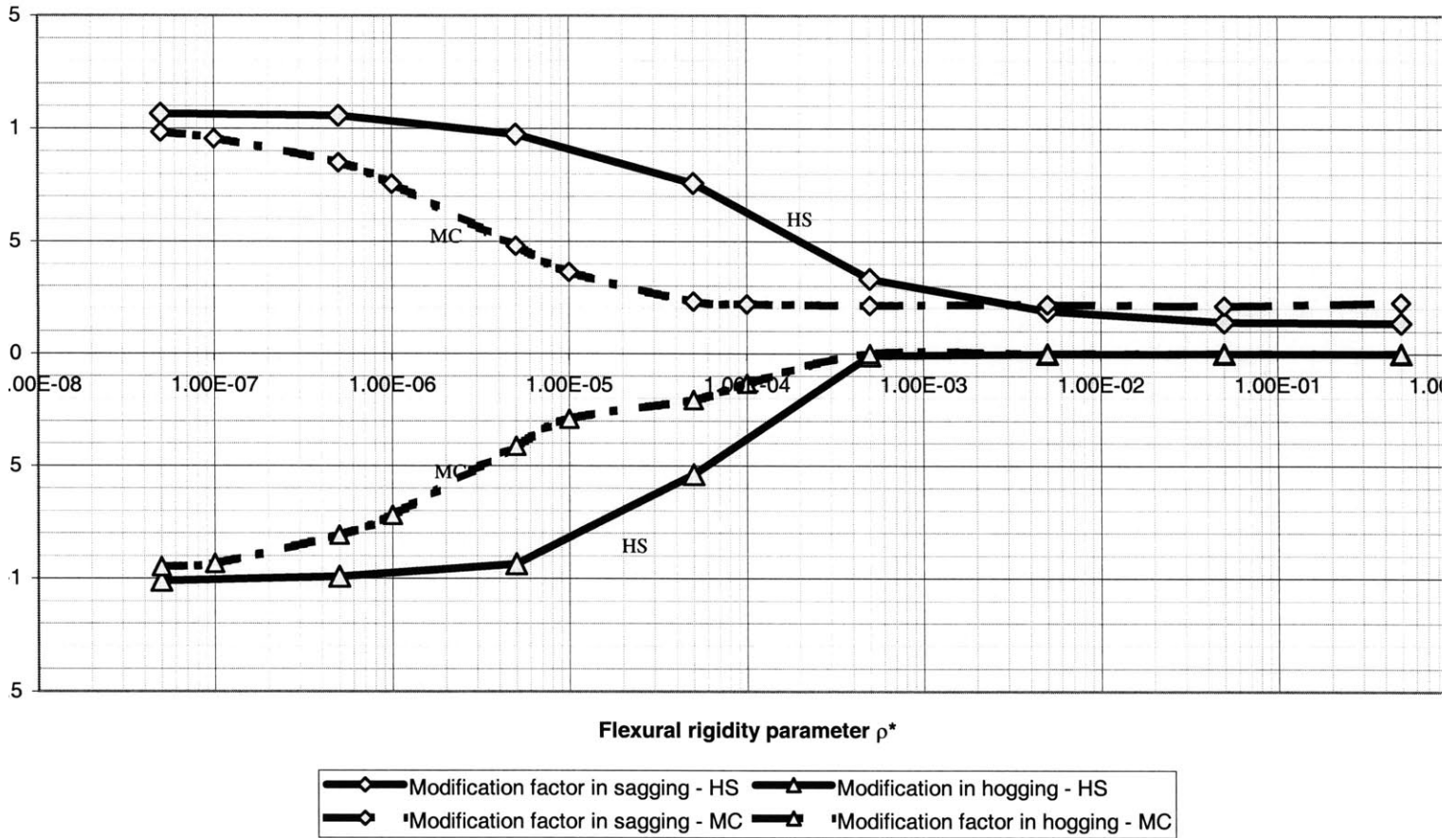
Flexural rigidity parameter ρ^*

Modification factor in sagging - HS   Modification in hogging - HS
Modification factor in sagging - MC   Modification factor in hogging - MC

Mohr Coulomb Soil model

ρ*	α*	Es	H	H⁴	EI	EA	V. loss	MDR^{sag}	MDR^{hog}
[m^{-1}]		[KPa]	[m]	[m⁴]	[KNm²]	[KN]	[%]	-	-
greenfield	greenfield	103000	30	810000	0.1	1	1.466	1.000	1.000
5.00E-08	50	103000	30	810000	4.05E+03	150000000	1.499	0.984	0.949
1.00E-07	50	103000	30	810000	8.10E+03	150000000	1.499	0.955	0.934
5.00E-07	50	103000	30	810000	4.05E+04	150000000	1.496	0.850	0.808
1.00E-06	50	103000	30	810000	8.10E+04	150000000	1.494	0.754	0.719
5.00E-06	50	103000	30	810000	4.05E+05	150000000	1.488	0.479	0.412
1.00E-05	50	103000	30	810000	8.10E+05	150000000	1.486	0.363	0.291
5.00E-05	50	103000	30	810000	4.05E+06	150000000	1.482	0.231	0.207
1.00E-04	50	103000	30	810000	8.10E+06	150000000	1.482	0.219	0.133
5.00E-04	50	103000	30	810000	4.05E+07	150000000	1.481	0.213	0.000
5.00E-03	50	103000	30	810000	4.05E+08	150000000	1.481	0.217	0.000
5.00E-02	50	103000	30	810000	4.05E+09	150000000	1.481	0.212	0.000
5.00E-01	50	103000	30	810000	4.05E+10	150000000	1.481	0.227	0.000

Hardening Soil model

ρ*	ΣM-Stage	V. loss	MDR^{sag}	MDR^{hog}
[m^{-1}]		[%]	-	-
5.00E-08	0.851	1.523	1.065	1.014
5.00E-07	0.851	1.523	1.056	0.991
5.00E-06	0.851	1.523	0.974	0.936
5.00E-05	0.851	1.520	0.758	0.539
5.00E-04	0.851	1.518	0.331	0.009
5.00E-03	0.851	1.502	0.184	0.001
5.00E-02	0.851	1.494	0.142	0
5.00E-01	0.851	1.496	0.137	0

Table 4.2. Computed correction factors using Mohr Coulomb and Hardening Soil models at constant α = 50*

Figure 4.2. Modification factors for the compressive and tensile strain using the Hardening soil model and the Mohr - Coulomb soil model for constant ρ*=0.005

Axial rigidity parameter α*

◇ Modification factor in compressive strain-HS	△ Modification in tensile strain-HS	
◇ 'Modification factor in compressive strain - MC	△ 'Modification factor in tensile strain - MC	
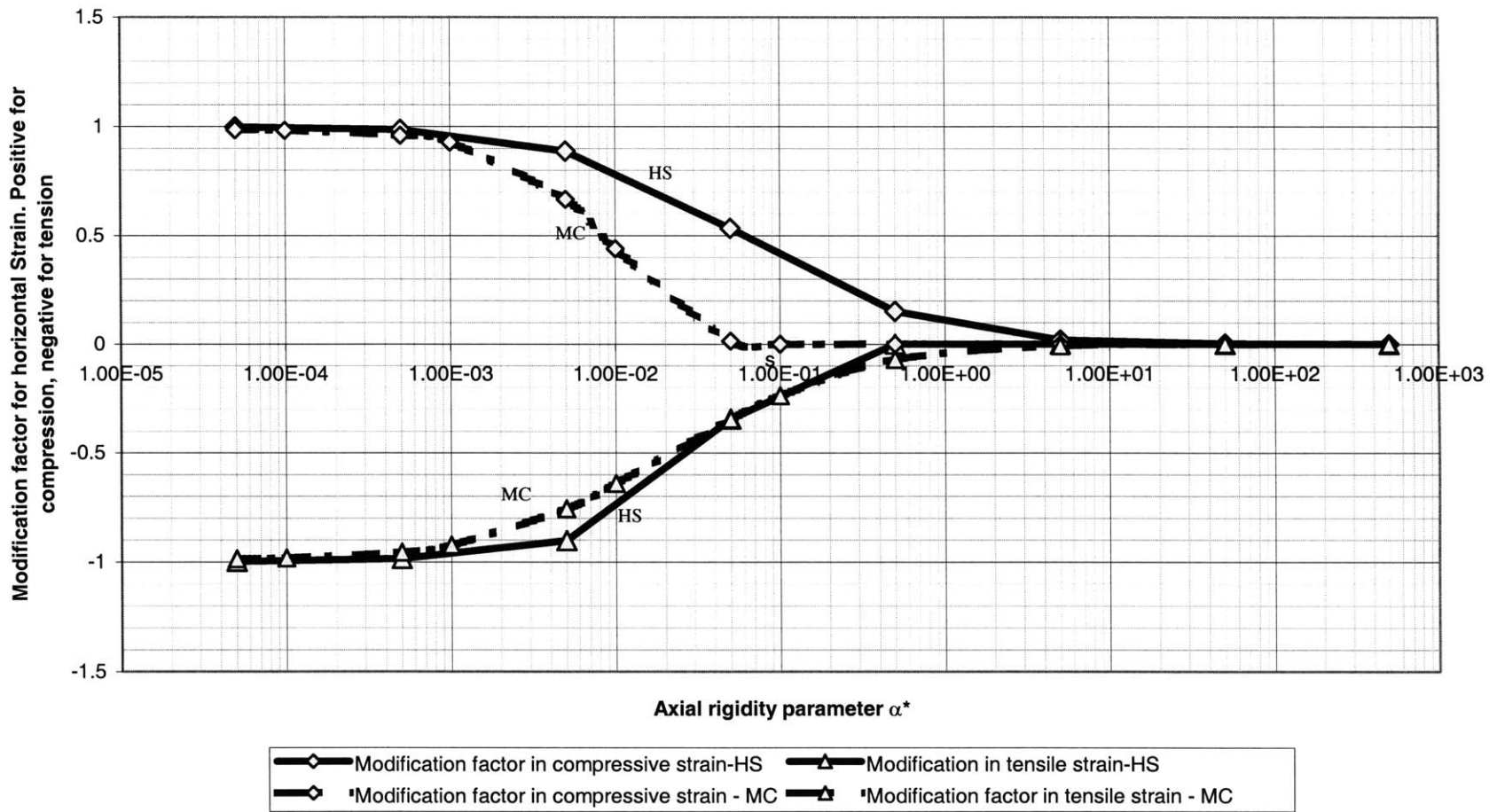
Mohr-Coulomb soil model

ρ*	α*	Es	H	H⁴	EI	EA	V.loss	Mε^{comp}	Mε^{tens}
[m^{-1}]	-	[KPa]	[m]	[M⁴]	[KNm²]	[KN]	[%]	-	-
greenfield	greenfield	103000	30	810000	0.1	1	1.466	1.0000	1.0000
0.005	5.00E-05	103000	30	810000	4.17E+08	1.55E+02	1.499	0.9849	0.9860
0.005	1.00E-04	103000	30	810000	4.17E+08	3.09E+02	1.499	0.9821	0.9824
0.005	5.00E-04	103000	30	810000	4.17E+08	1.55E+03	1.496	0.9593	0.9554
0.005	1.00E-03	103000	30	810000	4.17E+08	3.09E+03	1.494	0.9284	0.9236
0.005	5.00E-03	103000	30	810000	4.17E+08	1.55E+04	1.488	0.6673	0.7574
0.005	1.00E-02	103000	30	810000	4.17E+08	3.09E+04	1.486	0.4392	0.6411
0.005	5.00E-02	103000	30	810000	4.17E+08	1.55E+05	1.482	0.0149	0.3454
0.005	1.00E-01	103000	30	810000	4.17E+08	3.09E+05	1.482	0.0000	0.2363
0.005	5.00E-01	103000	30	810000	4.17E+08	1.55E+06	1.481	0.0000	0.0712
0.005	5.00E+00	103000	30	810000	4.17E+08	1.55E+07	1.481	0.0000	0.0085
0.005	5.00E+01	103000	30	810000	4.17E+08	1.55E+08	1.481	0.0000	0.0008
0.005	5.00E+02	103000	30	810000	4.17E+08	1.55E+09	1.481	0.0000	0.0000

Hardening Soil Model

ρ*	ΣM-Stage	V. loss	Mε^{comp}	Mε^{tens}
[m^{-1}]	-	[%]	-	-
5.00E-05	0.851	1.4939	0.998	-0.998
5.00E-04	0.851	1.4937	0.986	-0.984
5.00E-03	0.851	1.4918	0.888	-0.902
5.00E-02	0.851	1.4845	0.534	-0.344
5.00E-01	0.852	1.5	0.152	0.000
5.00E+00	0.852	1.5063	0.019	0.000
5.00E+01	0.852	1.5102	0.001	0.000
5.00E+02	-	-	0.000	0.000

Table 4.3. Computed correction factors using the Mohr Coulomb and the Hardening Soil Model at constant r* = 0.005m^{-1}

Comments and remarks

- From figures of both the deflection ratio and the horizontal strain one can observe that the Mohr – Coulomb model gives more conservative modification factors. This tendency can be more clearly observed in the curves of the modification factors for the deflection ratios (Figure 4.1). The curve of the Mohr – Coulomb model seems to be displaced to lower values of modification factors of deflection ratio for a distance of one to two orders of magnitude for ρ*. This tendency is milder for the modification factors for horizontal strains. It is interesting to note that in the case of the horizontal tensile strength the two models give very similar results.

- A very important step in the calculation of the modification factors for the deflection ratios is the determination of the inflection point in the settlement trough. If we consider that the settlement trough can be described as a function of the distance from the centerline of the tunnel line or the mid – point of the structure, then the inflection point is the point for which the second derivative of this function becomes zero. Numerically this point can be established by interrogating the data obtained as output of the numerical analysis. This was done as follows: The output file of the finite element analysis provided with a number of points at the surface of the ground for which, the initial coordinates and the vertical displacements are given. Then, it was feasible to calculate discretely the second derivative of the variation of the vertical settlement (i.e. the settlement trough) by considering three consecutive points x-a, x and x+b and applying the formula for a central difference:

$$f''(x) = \frac{2f(x) - f(x-a) - f(x+b)}{ab} \qquad (4.8)$$

When this technique is applied to an analysis in which the Mohr – Coulomb soil model has been implemented, the variation of the second derivative is smooth and it is very easy to find with accuracy in the level of the finite element discretization, the point of inflection. An example is represented in Figure 4.3, for which the vertical displacement and the second derivative of its variation are plotted. The range covers the width of the structure (30m). The same holds for either "greenfield" analyses or coupled analyses. Unfortunately this smooth behavior is not retained when the model is changed to the Hardening Soil Model. When the formula of central difference is applied to the output data in this case, the second derivative fluctuates significantly from point to point and the determination of a root for the second derivative is not possible. An example of such behavior is represented in Figure 4.4. To overcome this problem a high – order polynomial equation is fitted in the settlement trough, the equation of which is known. Then the inflection point is calculated analytically from the equation of the fitted polynomial. When half the trough is examined (due to symmetry), a fourth – degree polynomial can give very satisfactory correlation factors (on the order of $R^2 = 0.99$).

Figure 4.3. Calculation of the inflection point from surface settlements, using the Mohr - Coulomb Soil Model

Distance from the centerline [m]

◇   second derivative   —○— vertical displacement
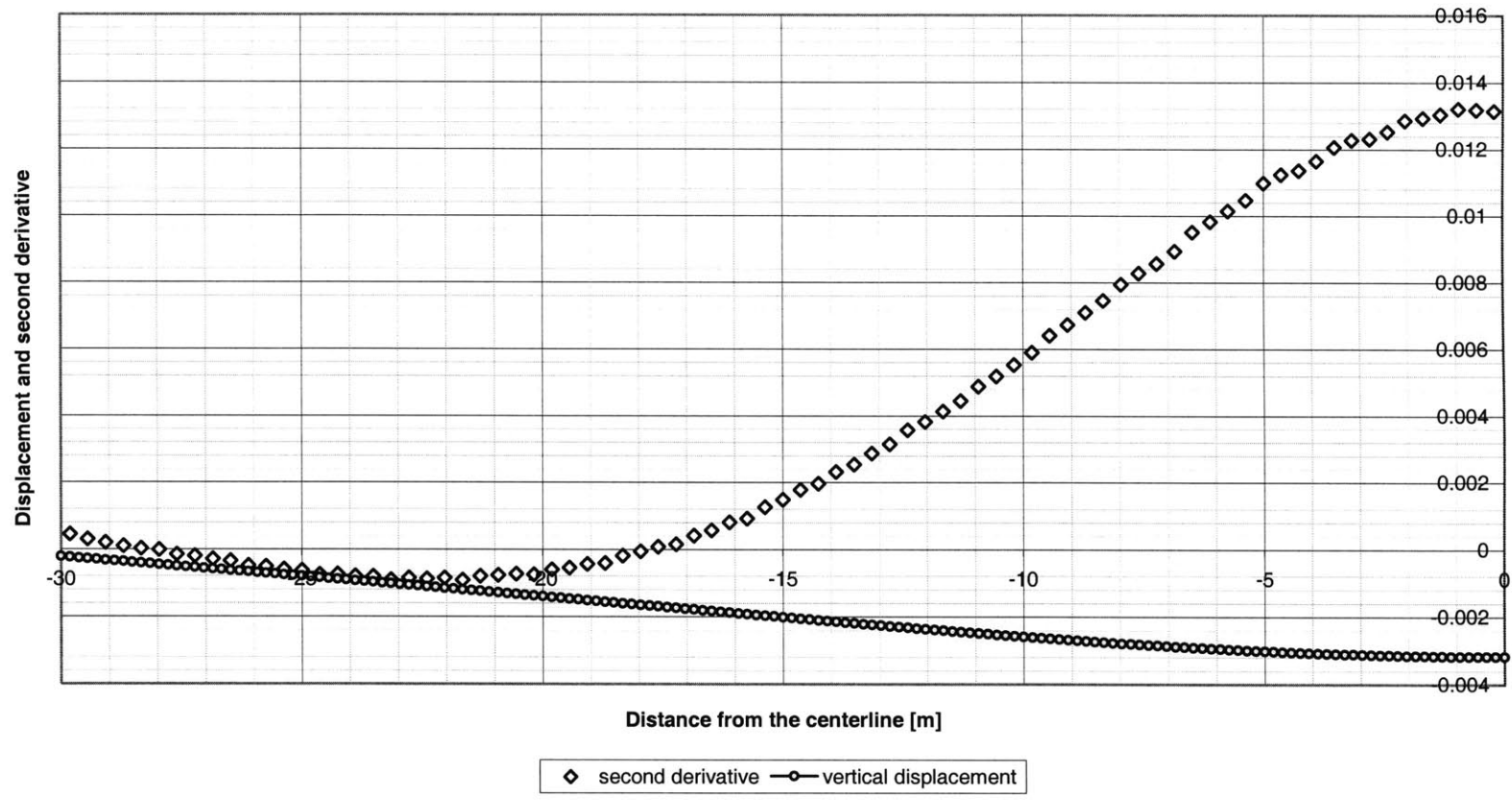
Figure 4.4. Problems in estimating the inflection point from Hardening Soil surface settlements. The settlement trough is approximated by a 4th - degree polynomial

$$y = 1.260\text{E-}08x^4 - 9.283\text{E-}07x^3 + 2.027\text{E-}05x^2 - 1.434\text{E-}05x - 3.165\text{E-}03$$
$$R^2 = 9.999\text{E-}01$$

Distance from the Centerline [m]

Settlement   □ Second Derivative ——— Poly. (Settlement)
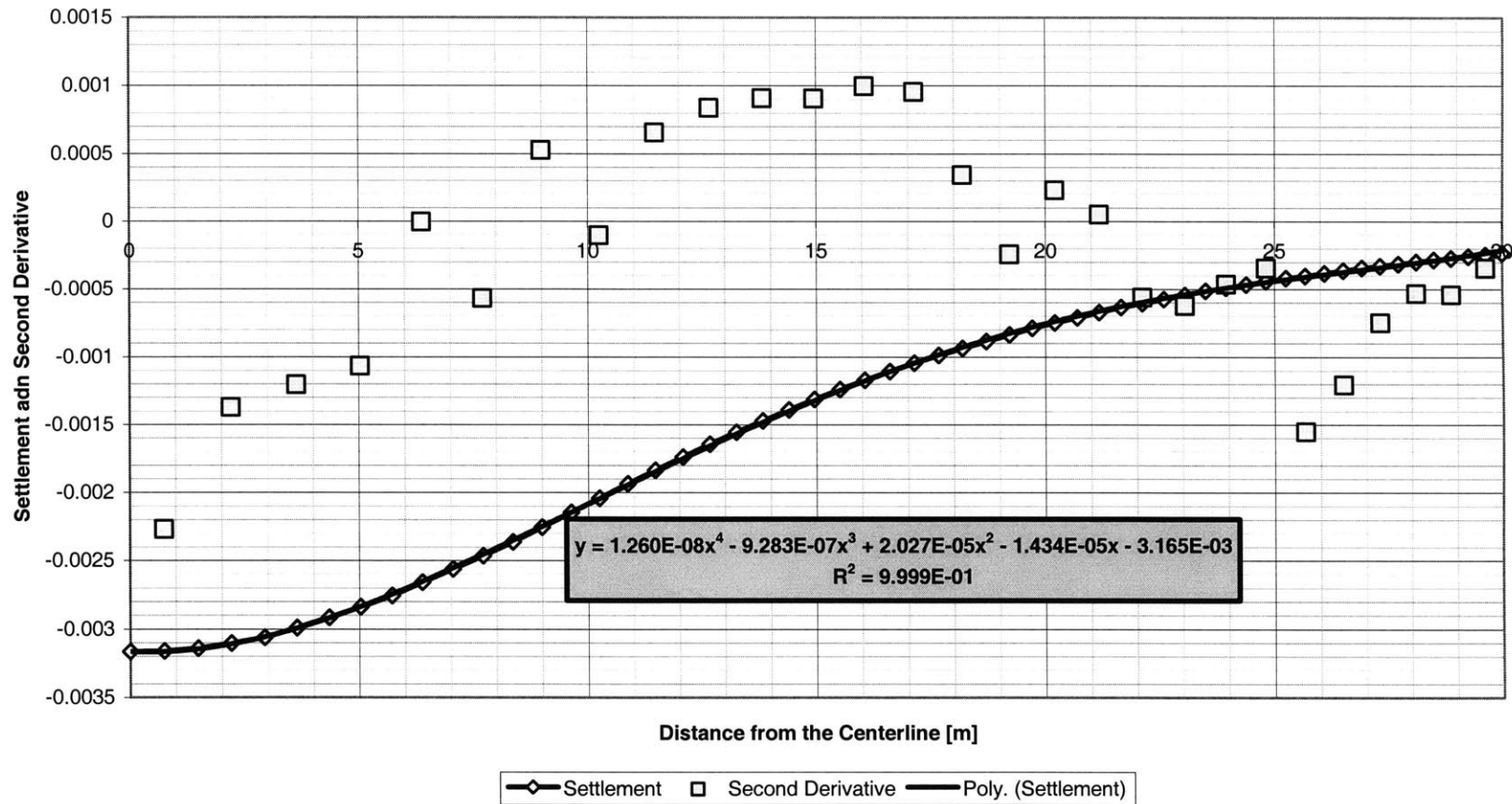
It is interesting to note on the issue of the second derivative that for the Hardening Soil model, a smooth variation is not obtained even when the 15 – node element is implemented. In this study, sixth – degree polynomials where applied to fit the settlement troughs (the symmetric parts). This gave very accurate results. A question may arise: Why were not the settlement troughs fitted with a Gaussian curve, in which the determination of the inflection point would be trivial? It was noticed in this study and it is also commonly accepted that the Gaussian curve does not fit satisfactorily the results from the numerical analyses. It was thus decided to proceed in the selection of a polynomial in the curve fitting process. In such a curve fitting function, the determination of the inflection point is a little bit more complicated, but it is still quite straightforward.

- An interesting observation can be made concerning the Volume Loss. Figures 4.5 and 4.6 plot the variation of the volume loss with respect to $\alpha*$ and $\rho*$ for a fixed ΣM – stage. These figures present that the volume loss does not depend on the variation of either $\alpha*$ or $\rho*$, as suggested in chapter 3, and this is true for both implemented soil models.

Volume Loss varying with $\alpha*$ - Mohr - Coulomb and Hardening Soil Model
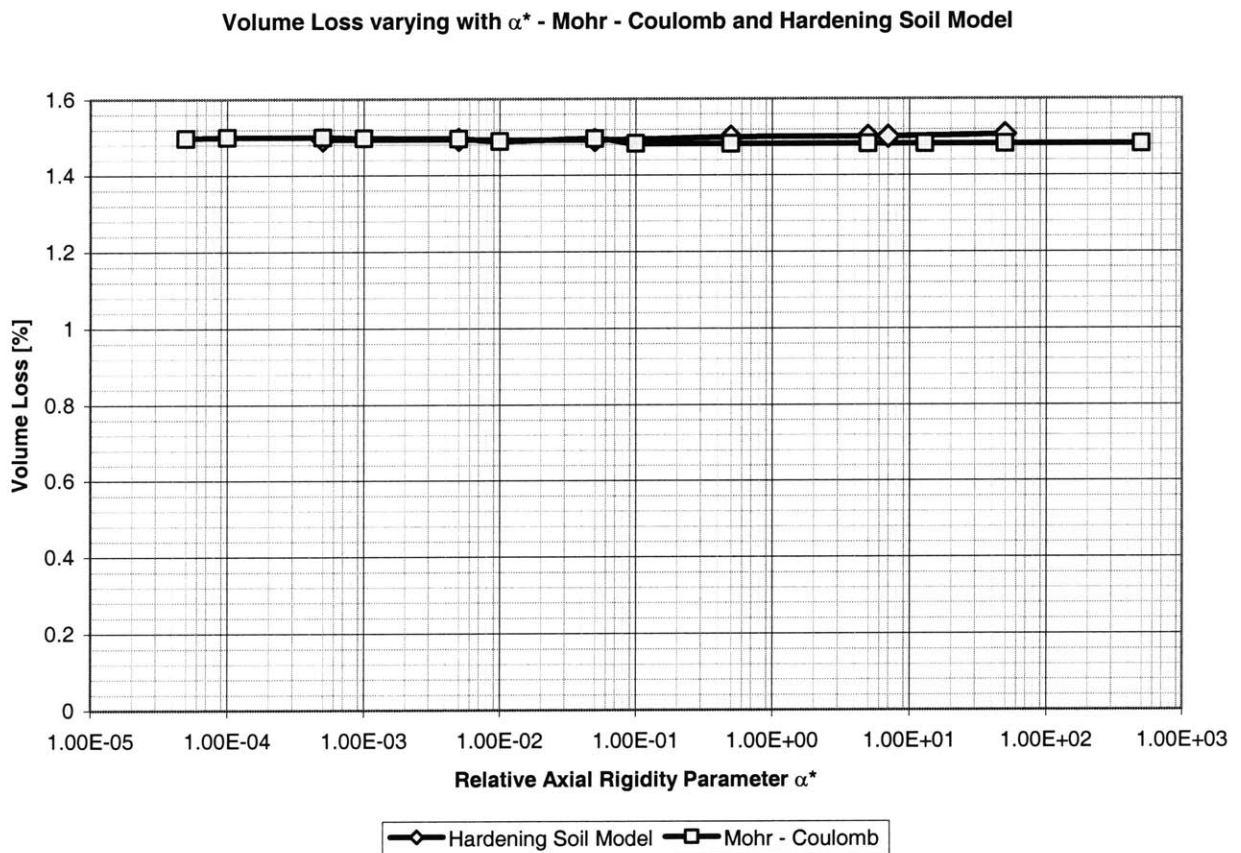
Figure 4.5 Volume loss as a function of $\alpha*$

Volume Loss varying with ρ* - Mohr - Coulomb and Hardening Soil Model
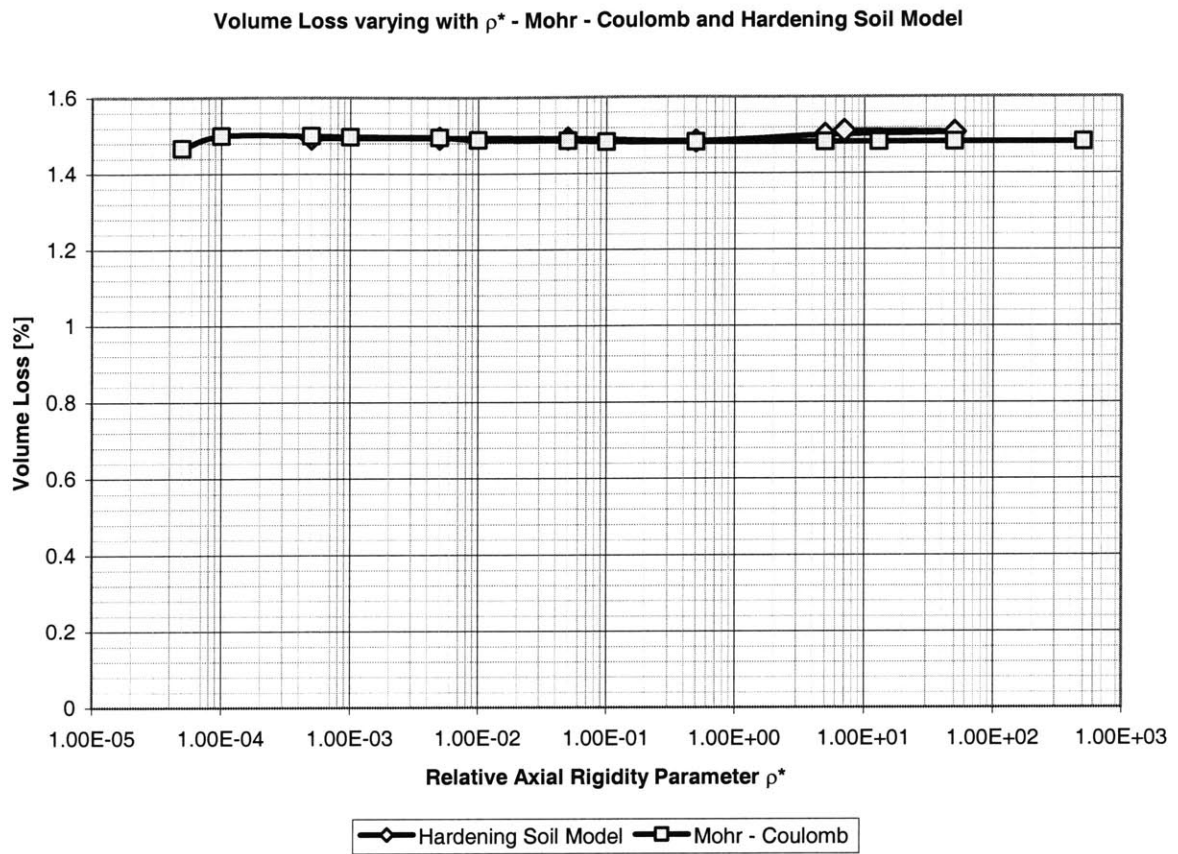
Figure 4.6 Volume loss as a function of ρ*

This result is very useful, in the sense that the ΣM – stage parameter need not be changed for each analysis.

b. Wet Scenario – Undrained Conditions. Comparison with the results of Potts and Addenbrooke

The second scenario that is being examined is a soil profile in which there is a water table two meters below the ground level. The soil is assumed to respond in an undrained fashion during the excavation of the tunnel. In this scenario, only the Hardening soil model is implemented. The Mohr – Coulomb cannot capture in an undrained analysis a realistic settlement trough and therefore there is no meaning in trying to obtain modification factors. It comes as a recommendation that for undrained analyses of settlements due to tunneling, the Mohr – Coulomb model should be avoided.

Figures 4.7 and 4.8 compare the modification factors directly with solutions published by Potts and Addenbrooke (1997).

Modification Factors for Deflection Ratios

					Potts and Addenbrooke	
ρ^*	ΣM-Stage	V. Loss	MDR^{sag}	MDR^{hog}	MDR^{sag}	MDR^{hog}
$[m^{-1}]$	-	[%]	-	-	-	-
5.00E-08	0.851	1.523	1.482	1.268	*1.26*	*1.39*
5.00E-07	0.851	1.523	1.469	1.244		
5.00E-06	0.851	1.523	1.333	1.1986	*1.15*	*1.28*
5.00E-05	0.851	1.520	1.001	0.8856	*0.78*	*1.75*
5.00E-04	0.851	1.518	0.557	0.0942	*0.46*	*0*
5.00E-03	0.851	1.502	0.273	0	*0.22*	*0*
5.00E-02	0.851	1.494	0.279	0		
5.00E-01	0.851	1.496	0.268	0	*0.01*	*0*

Modification Factors for Horizontal Strains

					Potts and Addenbrooke	
α^*	ΣM-Stage	V. loss	$M\varepsilon^{comp}$	$M\varepsilon^{tens}$	$M\varepsilon^{comp}$	$M\varepsilon^{tens}$
-	-	[%]	-	-	-	-
5.00E-05	0.851	1.493	0.9979	-0.9969	*1.0306*	*-0.9851*
5.00E-04	0.851	1.493	0.9837	-0.9816	*0.9987*	*-0.9578*
5.00E-03	0.851	1.491	0.877	-0.92	*0.8029*	*-0.7632*
5.00E-02	0.851	1.484	0.517	-0.4303	*0.3676*	*-0.2346*
5.00E-01	0.852	1.5	0.1241	-0.0057	*0.0934*	*-0.0061*
5.00E+00	0.852	1.506	0.015	-0.0035	*0.0123*	*-0.0006*
5.00E+01	0.852	1.510	0.0015	-0.0004	*0.0013*	*-0.0001*
5.00E+02	-	-	0.0001	-4.60E-05	*0.0001*	*0.00E+00*

Table 4.4 Comparison of results with results presented by Potts and Addenbrooke (1997)

Finally Figures 4.9 and 4.10 present a comparison between the undrained and the drained scenario for the implementation of the Hardening Soil Model.

Figure 4.7. Modification factors in sagging and hogging compared with the analyses presented by Potts and Addenbrooke (1996) for constant $\alpha^*=50$ (=48.6 in the analyses of Potts and Addenbrooke)
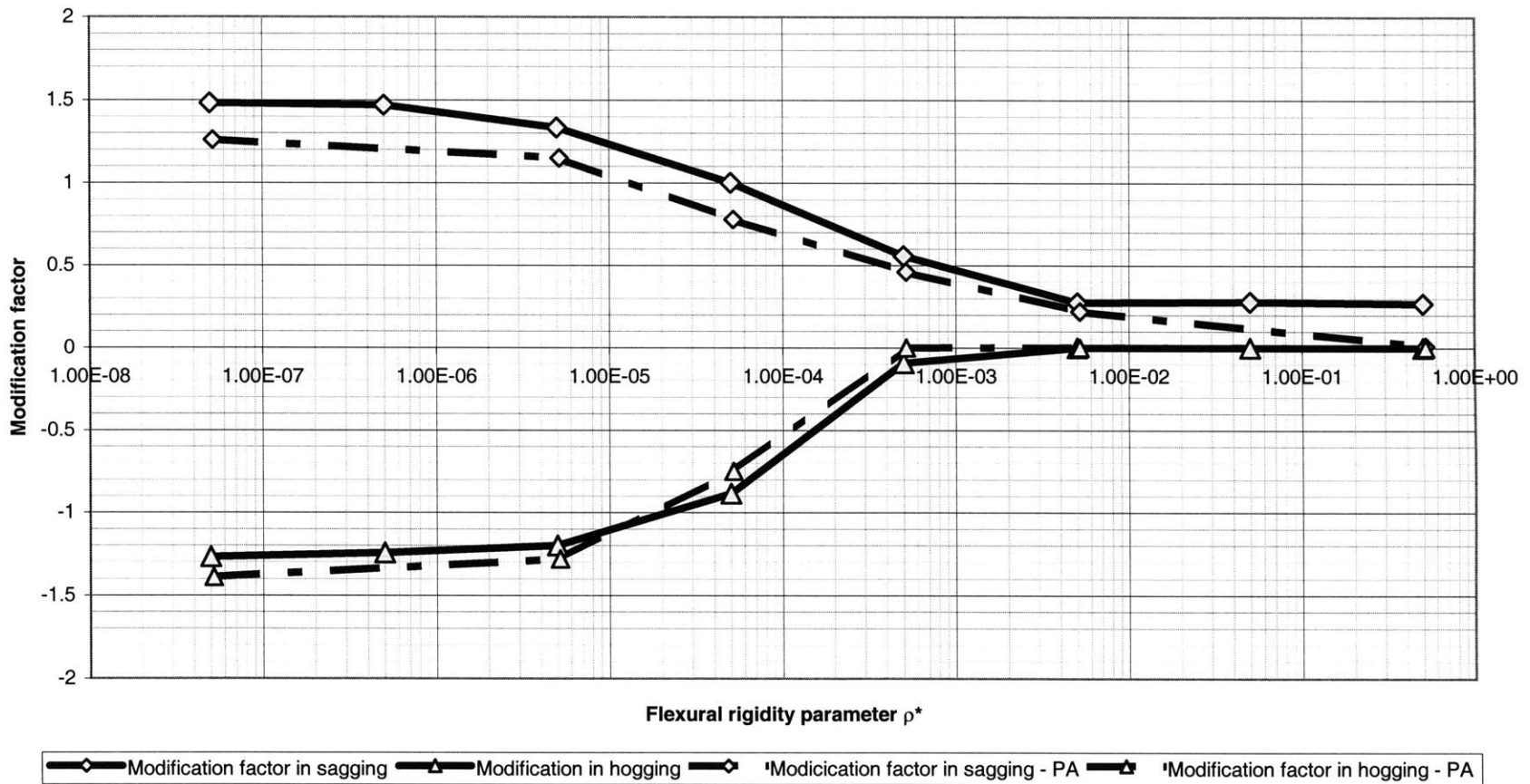
Figure 4.8. Modification factors for the compressive and tensile strain compared with the results presented by Potts and Addenbrooke (1996) for constant $\rho^*=0.005$ (=0.00518 in the analyses of P&A
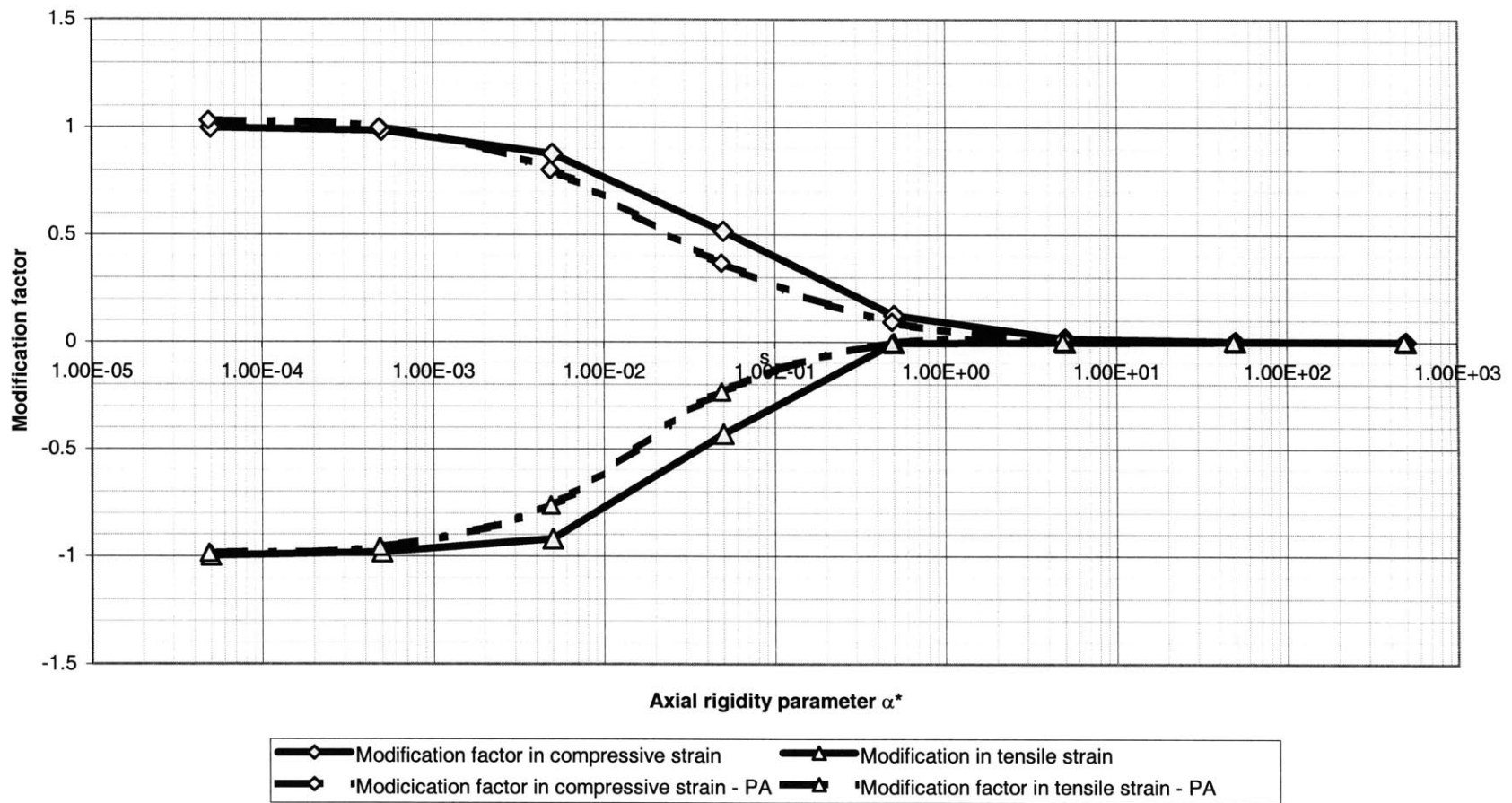
Figure 4.9. Modification factors for the compressive and tensile strain for drained and undrained scenario

Axial rigidity parameter α^*

Compressive horizontal strain - undrained ◆ Tensile horizontal strain - Undrained
◇ Compressive horizontal strain - Drained △ Tensile horizontal strain - Drained

Figure 4.10. Modification factors in sagging and hogging deflection ratios for drained and undrained conditions
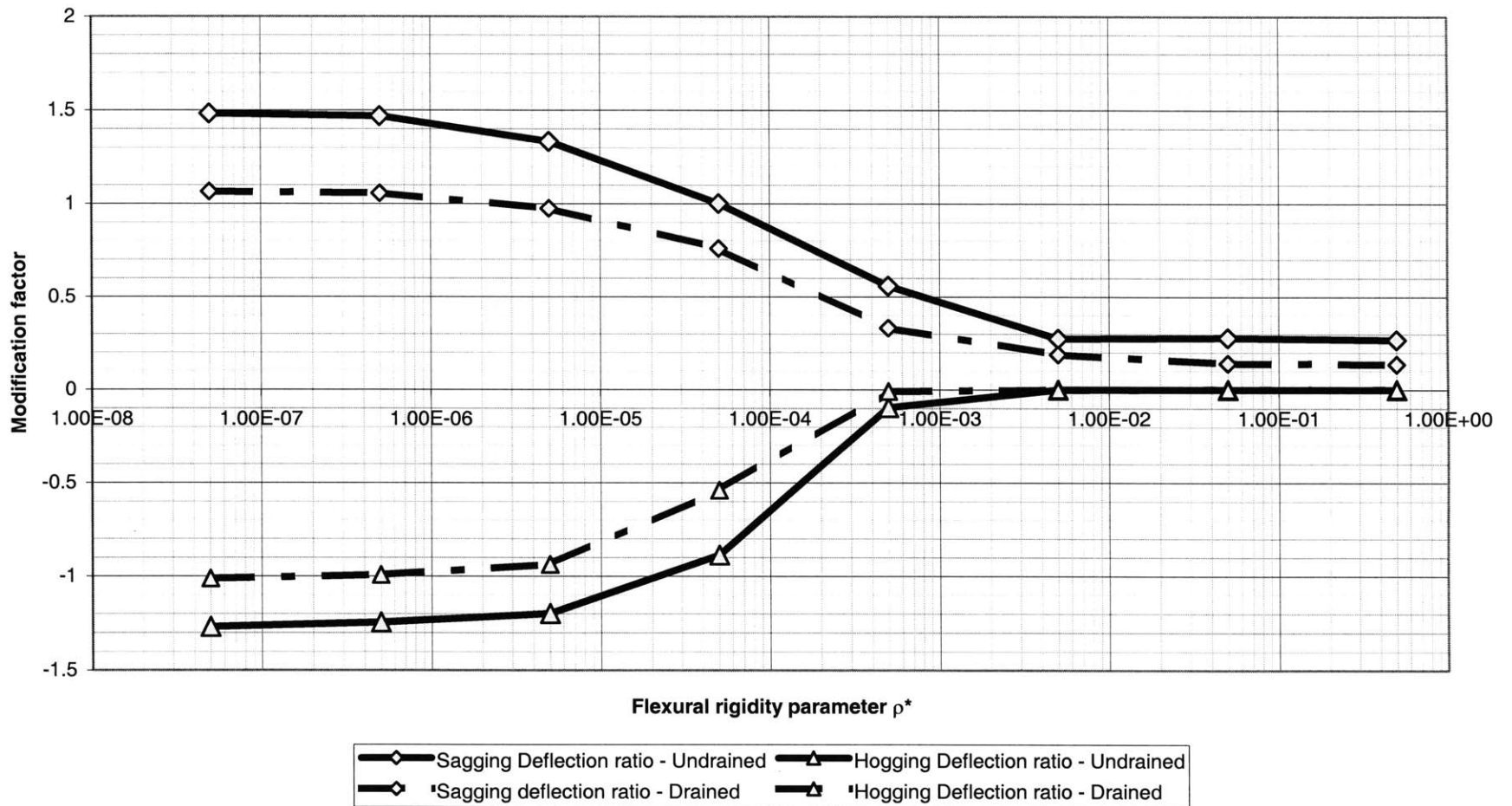
Discussion on the results

In the previous diagrams similar to those presented by Potts and Addenbrooke (1997) (see also Chapter 2) are given. These diagrams depict the variation of the modification factors with respect to the relative stiffness parameters (ρ^*, α^*). The definition of the relative stiffness parameters is given by Potts and Addenbrooke and can also be found in Chapter 2. The modification factors are derived through a series of numerical analyses. Parameters of the model that are fixed are the tunnel depth and diameter, the eccentricity and width of the linear elastic beam, which is used to represent the structure, and the soil profile. The stiffness of the beam is varied and several scenarios concerning the drainage response of the soil and the model describing the soil behavior are implemented. The diagrams that provide with the modification factors are constructed in the following way: For the variation of the modification factor for the deflection ratio (in either sagging or hogging) only a variation in the relative bending stiffness parameter ρ^* is considered whereas the relative axial stiffness parameter α^* is kept constant. In the analyses for this thesis only one value for α^* was considered whereas ρ^* was varied within a range from 5.18×10^{-8} to 5.18×10^{-1} m^{-1}. This range was set from an academic point of view to include extreme values of ρ^* and it contains the range that may arise for real structures. This can be identified as varying from 5.0×10^{-4} to 5.0×10^{-1} m^{-1}. The value of α^* for the analyses where ρ^* was varied, was set equal to $\alpha^* = 50$. Similar approach was applied in dealing with the modification factors for the maximum horizontal compressive and tensile strain. The relative axial stiffness parameter α^* is varied within a range from 5×10^{-5} to 500 whereas ρ^* is being kept constant and equal to $\rho^* = 0.005$. Again the range of values examined for α^* is extended to extreme values. Likely values for α^* that can occur for real structures are $\alpha^* > 0.5$.

The first scenario presented concerns a dry soil profile and a drained response of the soil. In this case, two soil models are being compared: the Mohr – Coulomb soil model and the Hardening soil model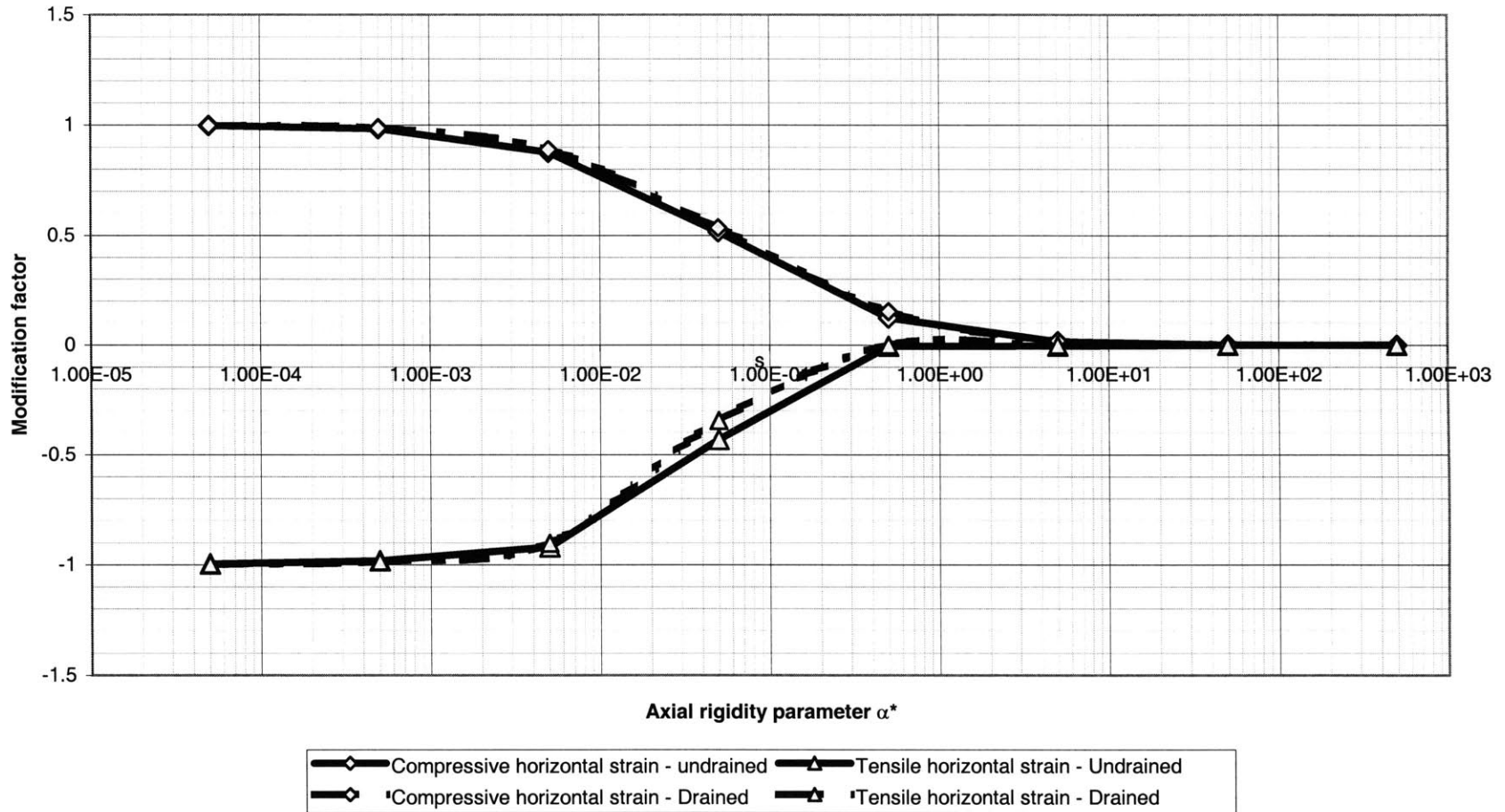. They are both offered in the finite element code PLAXIS and have been presented in the supplement to Chapters 1 and 2. Both models are calibrated with respect to the reference soil stiffness E_s as defined by Potts and Addenbrooke (1997) (see also Chapter 2).

Initially, the diagram presenting the variation of the sagging and hogging deflection ratio with the relative flexural rigidity parameter ρ^* is examined (Figure 4.1):

- The values for the modification factors obtained from the Mohr – Coulomb soil model are smaller (i.e. less conservative) than those obtained for the Hardening Soil model for $\rho^* < 10^{-3}$ m^{-1}. For $\rho^* > 10^{-3}$ m^{-1} the values are results are almost the same. This fact can be qualitatively justified by the fact that in the Hardening soil model the stiffness of the soil is stress – dependent whereas in the Mohr – Coulomb model it is not. The process of excavating a tunnel causes unloading of the soil so the in the Hardening soil model the soil stiffness is bound to decrease in contrast to soil stiffness in a Mohr – Coulomb soil, which will remain fixed. Reduced stiffness will give rise to larger displacements and eventually steeper settlement troughs. This observation underlies the fact that the two models are

calibrated with respect to E_s but this match is satisfied only before the excavation of the tunnel.

- When the relative flexural rigidity parameter is taking large values ($\rho^* > 10^{-3} \, \text{m}^{-1}$), the modification factor for the hogging deflection ratio converges to zero whereas the modification factor for the sagging deflection ratio to a small positive value around 0.15-0.2. This is in accordance with the results presented by Potts and Addenbrooke (1997) that are presented in Figure 2.7b.

- The modification factors for sagging and hogging deflection ratios in drained conditions are never larger than 1. In the case of very flexible beams ($\rho^* = 5 \times 10^{-8}$ m^{-1}) the value fluctuates around 1, and it can be considered that this extreme condition is equivalent to the "greenfield" condition and certainly not more crucial than the "greenfield" scenario. This means, that when drained response of the soil is considered the effect of a structure on the settlement trough gives rise to smoother troughs. In the damage assessment procedure, a "greenfield trough" will always give rise to larger damage than a modified trough for drained conditions. It is also interesting that the values of ρ^* that give a modification factor very close to 1 are outside the range of likely values for ρ^*.

By examining Figure 4.2, depicting the variation of the modification factor for compressive and tensile horizontal strain, similar observations can be made:

- The values obtained by application of the Mohr – Coulomb model are still smaller than those obtained for the Hardening Soil model. However, it seems that the modification factor for horizontal strain is less sensitive to a transition from a stress – independent soil stiffness model to a stress – dependent one. Especially, for the modification factor of the tensile horizontal strain, the results are almost identical.

- Similarly to the modification factor for the deflection ratio, the modification factor for horizontal strain is always less or equal to 1. It is interesting that for the likely values of α^* ($\alpha^* > 0.5$) the modification factors are very close to zero. This is means that the presence of the foundation of a real structure annihilates the development of horizontal strains in the ground. This result has been predicted by Potts and Addenbrooke (1997) and has been verified for some study cases (see for example in Chapter 2, the case study of the Treasury (after Burland, Standing and Jardine (2002)).

The second scenario that is being studied concerns "undrained" soil response. In this scenario, it is only the Hardening Soil model that is implemented and comparison is performed with the results presented by Potts and Addenbrooke (1997). Figure 4.7 presents the diagram for the modification factor for deflection ratio with respect to ρ^*. The following can be observed:

- There seems to be a satisfactory agreement with the results presented by Potts and Addenbrooke (1997). More interesting is the fact that for low relative flexural stiffness parameters, modification factors larger than unity are obtained. This is true for modification factors of deflection ratio for both hogging and sagging. In

100

specific, the modification factor is larger than one when $\rho*$ is in the range of 10^{-5} to 10^{-4} m^{-1}. It is true that these values are in the edge of the range for likely $\rho*$ values in buildings and maybe they can be obtained for sensitive buildings. A modification factor larger than one means that the "greenfield" scenario is not conservative but rather unsafe! This result of modification factors larger than one is encountered for large values of $\alpha*$ as verified by the study here (for which $\alpha* = 50$) but also from the results presented by Potts and Addenbrooke (1997).

In order to understand why a modification factor larger than one is obtained for a beam with large axial stiffness and small flexural stiffness in undrained conditions, the following Figures are presented.
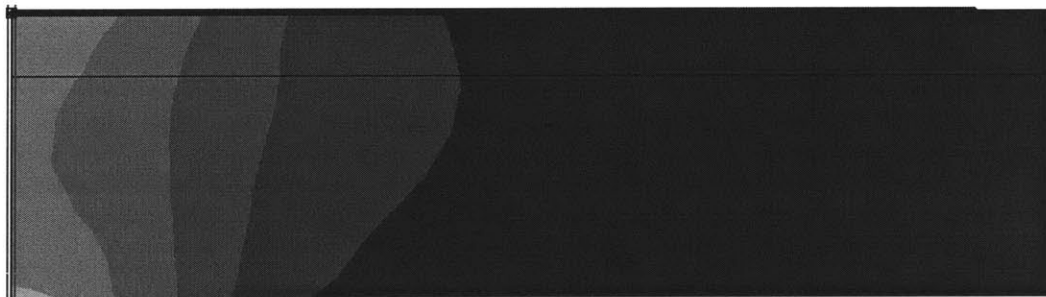
Figure 4.11. Horizontal Strains in the "greenfield scenario – Undrained response
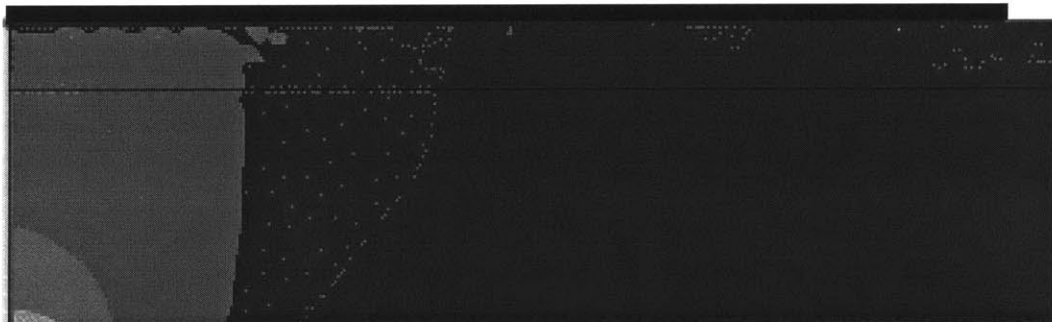
Figure 4.12. Horizontal Strains beneath a beam with high axial and low flexural stiffness parameters – Undrained response

Figure 4.11 presents the contours of horizontal strains at the upper part of the model for the "greenfield" scenario in undrained conditions. Figure 4.12 presents the same contours in the case where a beam with high axial and low bending stiffness. As it can be observed, the high axial stiffness of the beam reduces significantly the horizontal strains at the ground level. Since the soil response is undrained, the condition of zero volume change in the model is applied. This means that the volume of the settlement trough is equal to the volume loss at the tunnel. For both analyses the same volume loss in the tunnel is considered. Physically, one can sense that the vertical strain in the case of the

building has to be larger than the "greenfield" case so that the difference in the horizontal strains can be counterbalanced and the volumetric strain to remain zero. Mathematically, the above can be expressed as follows:

$$\varepsilon_{vol} = \varepsilon_v + \varepsilon_h = V_L \qquad \textbf{(4.9)}$$

According to equation 4.9, if the horizontal strain ε_h decreases the vertical ε_v has to increase so that the volumetric strain remains constant and equal to the volume loss parameter V_L. Indeed, this is verified by the vertical settlement troughs that correspond to these cases. Figure 4.13 presents the obtained settlement troughs. The change is not dramatic but captures the increase of the vertical settlement under a beam, which exhibits low flexural rigidity $\rho*$ and high axial rigidity $\alpha*$.

The justification of this result is further emphasized by Figure 4.10, which compares the results obtained by implementation of the Hardening Soil Model for drained and undrained response of the soil. The drained modification factors are always smaller than one. It is the condition expressed by equation 4.9 that generates modification factors larger than one, in the case of the undrained response.

Finally, from Figure 4.9, which compares the modification factors for horizontal strains in drained and undrained conditions, it is assessed that the modification factor for horizontal strain is not sensitive to the drainage behavior of the soil. The two cases seem to match exactly. In all cases, the remarks stated above for the modification factor of horizontal strain in drained conditions also hold for undrained conditions as well.

Figure 4.8 shows a satisfactory agreement with the results obtained by Potts and Addenbrooke for the modification factor of horizontal strain in either compression or tension.

Figure 4.13. Comparison of settlement troughs for "greenfield" condition and a scenario with a structure that exhibits large α^* and low ρ^* in undrained conditions

CHAPTER 5

SUMMARY, CONCLUSIONS AND RECOMMENDATIONS

5.1 SUMMARY

The effect of an existing surface structure on the settlements, which will arise because of a tunneling project, is certainly a complicated phenomenon of interaction, and many different paths or approaches can be chosen to confront the problem. In this thesis, an approach originating from conventional methodologies for assessing the risk of potential damage to buildings (for example Burland, 1995) due to tunneling was presented. The modification factors for deflection ratio and maximum horizontal strain as defined in previous chapters, can be viewed as the core of this methodology. The idea behind the introduction of the modification factors is that the effect of an existing surface structure can be taken into account by modifying the "greenfield" settlement trough with respect to these two unique elements of the settlement trough: the maximum deflection ratio in sagging and hogging mode and the maximum horizontal strain in compression and tension. It is noted that the modification factors do not allow a full transition from the "greenfield" settlement trough to the real trough developing beneath an existing structure. In other words, knowing the "greenfield" settlement trough and the modification factors for deflection ratio and horizontal strains is not sufficient to define the real trough in full detail. For example, the modification factors do not contain any information on the magnitude of vertical displacements, even though the deflection ratio contains information on the shape of the trough. This procedure is useful from a damage assessment point of view, since in assessing the risk of potential damage to a structure the necessary input parameters are the deflection ratio in sagging and hogging and the maximum tensile and compressive horizontal strain. So the effect of existing surface structures on tunneling induced settlement, as the title of this thesis suggests, is captured only from the point of view of damage assessment to buildings with respect to current damage assessment methodologies.

In Chapter 1, the main principles of these methodologies were presented, while, in Chapter 2, a summary of the work by Potts and Addenbrooke (1997), who were those that introduced the notion of modification factors, was given. Chapter 3 presented some results from numerical analyses aiming in a better understanding of the problem. These concerned the effect of the coefficient of earth pressure at rest K_0 in the shape of a "greenfield" settlement trough, as well as the relationship between the volume loss parameter in the tunnel with the deformations developing in the soil model. Chapter 4 presented the results that were obtained from analyses concerning the modification factors for deflection ratio and horizontal strain.

5.2 CONCLUSIONS AND RECOMMENDATIONS

The 2D numerical nonlinear analyses presented in the previous chapters of this thesis revealed several interesting remarks that can be made. The overall conclusion is that the establishment of generic charts offering modification factors for the deflection ratio and the horizontal strain of the settlement trough arising from a tunneling project is very difficult. The parameters that affect the shape of the trough arise not only from the characteristics of the existing structure or the construction of the tunnel but also from the soil profile. Potts and Addenbrooke (1997) performed analyses modeling the soil profile in London and produced modification factors that can be applied for tunneling projects that have been undertaken in London under specific soil conditions and tunnel construction techniques. Replicating a similar soil profile and producing very similar results within the framework of this thesis verified the validity of their results. But it was also shown that parameters assumed fixed in their study, can influence significantly not only the values of the modification factors (as for example the drainage behavior of the soil) but even the shape of the trough itself as it was shown for the coefficient of earth pressure at rest K_0 in Chapter 3.

Hence, the application of the charts as presented by Potts and Addenbrooke (1997) would not be recommended for projects in soil conditions different than those in London. But their work can be viewed as a template that can be applied with the proper modifications in other tunneling projects. In this modification the most important part is the description of the soil profile and the simulation of the tunnel excavation. It was shown through this thesis that the implemented soil model and fundamental assumptions of the behavior of the soil (for example drained or undrained response) can be very important in defining accurately the modification factors. The engineer will have to make decisions concerning all these issues. These decisions will be guided by the particularities of each project.

The type of analysis that was presented here can also be viewed as a step of maturity in modeling problems in geotechnical engineering. It is evident that we are heading towards 3D simulations and even more accurate soil models with the expectation of capturing as precisely as possible the intricate soil behavior. In this evolution process there are always lessons to be taught from the application of models that offer a certain amount of accuracy in describing a problem. In particular, the problem of interaction between soil and an existing structure on the formation of a settlement trough in the ground because of a tunneling operation was confronted by a 2D finite element model with all the aforementioned assumptions concerning the modeling of the structure and of the soil. It was shown that the "greenfield" assumption, according to which, at the foundation of an existing structure the "greenfield" soil movements were applied, is very conservative for most cases of real structures. It was also shown how the "greenfield" assumption could be less conservative in case of undrained conditions and a structure exhibiting a certain axial to bending stiffness proportion. It was also identified how parameters such as the coefficient of lateral earth pressure at rest or the yield and failure assumptions for the soil are very important when a correct and accurate description of this complicated phenomenon of interaction is desired.

5.3 FURTHER RESEARCH

This thesis presented a series of calculations and considerations for a quantitative assessment of the effects of existing surface structures on tunneling – induced settlements. This was done from the point of view of the assessment of risk of potential damage to buildings and acquires a special interest due to the increasing number of tunneling projects undertaken in urban environment. All through this process, several simplifying assumptions were considered. By briefly describing the most important of them, motivations for further research can be given:

- The whole process was based on numerical simulations of the problem of interaction between the building and the excavation of the tunnel. Empirical schemes (as for example in Taylor and Grant, 1998) or data from real cases of buildings undergoing subsidence and damage due to tunneling would be very useful in gaining a better understanding of this complicated phenomenon of interaction.
- The problem was confronted numerically assuming 2D plane strain conditions. However, the problem of subsidence due to tunneling, especially for undrained response, is a 3D problem. In the analyses performed, only the transverse settlement trough has been considered. Similar calculations can be undertaken in the longitudinal direction of the tunnel.
- The structure was modeled as a linear elastic beam exhibiting two stiffness parameters EA and EI according to the classic deep beam theory of Burland and Wroth (1974). The plane strain assumption was retained for the beam as well. Improvements can be applied in the description of the structure by more realistic models (See for example, Dias and Kastner, 2002).
- A single soil profile was considered in the analyses. It would be interesting to check whether the principal results are true for more complicated soil profiles with more than one soil layers. Same holds for the tunnels. A large research area is open concerning the volume loss in the tunnels, a rather subtle parameter.
- The weight of the structures was not taken into account. If considered, it is not at all certain whether the same results would be obtained.

All the above remarks can motivate improvements in the evaluation of the modification factors. But, in an even more fundamental level, the damage assessment methodologies, the "greenfield" settlement predictions, the interaction with deep foundations and other types of underground construction, the analysis of the long – term settlements and the protective measures that can be applied to minimize the risk of damage constitute a set of fields to which research could be extended. It is the personal opinion of the author that the variety of different aspects of the problem of interaction between underground construction and existing infrastructure make this problem one of the most exciting research fields in geotechnical engineering.

APPENDICES

A. SOIL MODELS

The purpose of this section is to describe the soil models implemented in the different analyses presented in this thesis. The selection of the soil model is a very important factor in the examined analyses. Implementation of soil models that do not exhibit the necessary features and level of refinement in modeling the soil behavior, may lead to results that deviate significantly from the reality. Three soil models will be discussed:

1. The soil model implemented in the parametric analysis of Potts and Addenbrooke (1997). This is a non – linear elasto-plastic constitutive model. The model described by Jardine et al. (1986) was used to represent the non – linear elastic pre – yield behavior and a Mohr – Coulomb yield surface and plastic potential were used to model the plastic behavior.
2. The Mohr – Coulomb soil model as incorporated in the finite element code PLAXIS.
3. The Hardening Soil Model also as incorporated in the finite element code PLAXIS.

A.1. The soil model in the work of Potts and Addenbrooke (1997)

As mentioned above, the soil model implemented in the parametric analysis performed by Potts and Addenbrooke is a non – linear elasto – plastic constitutive model. The secant stiffness expressions that describe the variation of shear and bulk moduli are given by the following equations:

$$\frac{3G}{p'} = A + B\cos\left[\alpha\left(\log_{10}\left(\frac{E}{\sqrt{3}C}\right)\right)^{\gamma}\right] \qquad \text{(A.1a)}$$

$$\frac{K}{p'} = R + S\cos\left[\delta\left(\log_{10}\frac{(\varepsilon_v)}{T}\right)^{\gamma}\right] \qquad \text{(A.1b)}$$

In the above expressions:

- G is the secant shear modulus
- K is the secant bulk modulus
- p' is the mean effective stress
- E is the deviatoric strain invariant used in the Imperial College Finite Element Program (ICFEP). This quantity is given by the following expression:

$$E = \left(\frac{2}{3}\right)^{\frac{1}{2}}\left[(\varepsilon_1 - \varepsilon_2)^2 + (\varepsilon_1 - \varepsilon_3)^2 + (\varepsilon_2 - \varepsilon_3)^2\right]^{\frac{1}{2}} \qquad \text{(A.2)}$$

The parameters A, B, C, R, S, T, δ, α, γ and λ are all constants, which are specified through laboratory or in situ testing. More specifically for the soil which is used in Potts' and Addenbrooke's analyses, which is a model of the well – known London Clay, the following values are used:

- o A = 1120
- o B = 1016
- o C [%] = 0.0001
- o α = 1.335
- o γ = 0.617
- o R = 549
- o S = 506
- o T = 0.001
- o δ = 2.069
- o λ = 0.420

Besides these parameters, the extreme values for the moduli and the strains are defined. These are the following:

- o E_{min} [%] = 8.66025x10^{-4}
- o E_{max} [%] = 0.69282
- o ε_{vmin} [%] = 0.005
- o ε_{vmax} [%] = 0.15
- o G_{min} [KPa] = 2333.3
- o K_{min} [KPa] = 3000

In addition to the above stiffness parameters, another set of parameters is necessary for the definition of the strength properties of the soil model, i.e. the definition of the Yield surface. This is going to be a Mohr – Coulomb yield surface with a general equation:

$$f_1 = \frac{1}{2}\left|\sigma_2' - \sigma_3'\right| + \frac{1}{2}\left(\sigma_2' + \sigma_3'\right)\sin\varphi - c\cos\varphi \leq 0 \qquad \text{(A.3a)}$$

$$f_2 = \frac{1}{2}\left|\sigma_3' - \sigma_1'\right| + \frac{1}{2}\left(\sigma_3' + \sigma_1'\right)\sin\varphi - c\cos\varphi \leq 0 \qquad \text{(A.3b)}$$

$$f_3 = \frac{1}{2}\left|\sigma_1' - \sigma_2'\right| + \frac{1}{2}\left(\sigma_1' + \sigma_2'\right)\sin\varphi - c\cos\varphi \leq 0 \qquad \text{(A.3c)}$$

The parameters that are assigned for this case are:

- • c' = 10KPa
- • ϕ' = 25°
- • ψ' = 12.5°
- • The saturated bulk unit weight of the soil is γ = 20KN/m^3
- • The coefficient of earth pressures at rest K_0 = 1.5

A.2. The Mohr – Coulomb soil model in PLAXIS

Plasticity is associated with the development of irreversible strains. In order to evaluate whether or not plasticity occurs in a calculation, a yield function f is introduced as a function of stress and strain. A yield function can often be presented as a surface in the principal stress space. A perfectly – plastic model is a constitutive model with a fixed yield surface, i.e. a yield surface that is fully defined by model parameters and not affected by (plastic) straining. For stress states represented by points within the yield surface, the behavior is purely elastic and all strains are reversible.

2.1 Elastic perfectly – plastic behavior

The basic principle of elastoplasticity is that strains and strain rated are decomposed into an elastic part and a plastic part:

$$\underline{\varepsilon} = \underline{\varepsilon}^e + \underline{\varepsilon}^p \qquad\qquad \text{(A.4a)}$$

$$\underline{\dot{\varepsilon}} = \underline{\dot{\varepsilon}}^e + \underline{\dot{\varepsilon}}^p \qquad\qquad \text{(A.4b)}$$

Hooke's law is used to relate the stress rates to the elastic strain rates. Substitution of Equation 3 into a generalized expression for Hooke's law gives the following:

$$\underline{\dot{\sigma}}' = \underline{\underline{D}}^e \underline{\dot{\varepsilon}}^e = \underline{\underline{D}}^e (\underline{\dot{\varepsilon}} - \underline{\dot{\varepsilon}}^p) \qquad\qquad \text{(A.5)}$$

According to classical theory of plasticity (Hill, 1950) plastic strain rates are proportional to the derivative of the yield function with respect to the stress. This means that the plastic strain rates can be represented as vectors perpendicular to the yield surface. This classical form of the theory is referred to as associated plasticity. However, for Mohr – Coulomb type yield functions, the theory of associated plasticity leads to an overestimation of dilatancy. Therefore, in addition to the yield function, a plastic potential function g is introduced. The case $g \neq f$ is denoted as non – associated plasticity. In general, the plastic strain rates are written as:

$$\underline{\dot{\varepsilon}}^p = \lambda \frac{\partial g}{\partial \underline{\sigma}'} \qquad\qquad \text{(A.6)}$$

in which λ is the plastic multiplier. For purely elastic behavior λ is zero, whereas in the case of plastic behavior λ is positive.

The above equations may be used to obtain the following relationship between the effective stress rates and strain rates for elastoplasticity:

$$\underline{\dot{\sigma}}' = \left(\underline{\underline{D}}^e - \frac{\alpha}{d} \underline{\underline{D}}^e \frac{\partial g}{\partial \underline{\sigma}'} \frac{\partial f^T}{\partial \underline{\sigma}'} \underline{\underline{D}}^e \right) \underline{\dot{\varepsilon}} \qquad\qquad \text{(A.7)}$$

$$\text{where: } d = \frac{\partial f^T}{\partial \underline{\sigma}'} \underline{\underline{D}}^e \frac{\partial g}{\partial \underline{\sigma}'} \qquad\qquad \text{(A.8)}$$

The parameter α is used as a switch. If the material behavior is elastic the value of α is equal to zero, whilst for plasticity the value of α is equal to unity.

The above theory of plasticity is restricted to smooth yield surfaces and does not cover a multi surface yield contour as present in the Mohr – Coulomb model. For such a yield surface the theory of plasticity has been extended by Koiter (1960) and others to account for flow vertices involving two or more plastic potential functions:

$$\underline{\dot{\varepsilon}^p} = \lambda_1 \frac{\partial g_1}{\partial \underline{\sigma}'} + \lambda \frac{\partial g_2}{\partial \underline{\sigma}'} + \dots \qquad (A.9)$$

Similarly, several quasi independent yield functions (f_1, f_2, ...) are used to determine the magnitude of the multipliers λ_1, λ_2, ...

2.2 Formulation of the Mohr – Coulomb model

The Mohr – Coulomb yield condition is an extension of Coulomb's friction law to general states of stress. In fact, this condition ensures that Coulomb's friction law is obeyed in any plane within a material element. The full Mohr – Coulomb yield condition can be defined by three yield functions when formulated in terms of principal stresses:

$$f_1 = \frac{1}{2}\left|\sigma_2' - \sigma_3'\right| + \frac{1}{2}\left(\sigma_2' + \sigma_3'\right)\sin\varphi - c\cos\varphi \le 0 \qquad (A.10a)$$

$$f_2 = \frac{1}{2}\left|\sigma_3' - \sigma_1'\right| + \frac{1}{2}\left(\sigma_3' + \sigma_1'\right)\sin\varphi - c\cos\varphi \le 0 \qquad (A.10b)$$

$$f_3 = \frac{1}{2}\left|\sigma_1' - \sigma_2'\right| + \frac{1}{2}\left(\sigma_1' + \sigma_2'\right)\sin\varphi - c\cos\varphi \le 0 \qquad (A.10c)$$

The two plastic model parameters appearing in the yield functions are the well – known friction angle ϕ and the cohesion c. These yield functions together represent a hexagonal cone in principal stress space as shown in Figure S.1.
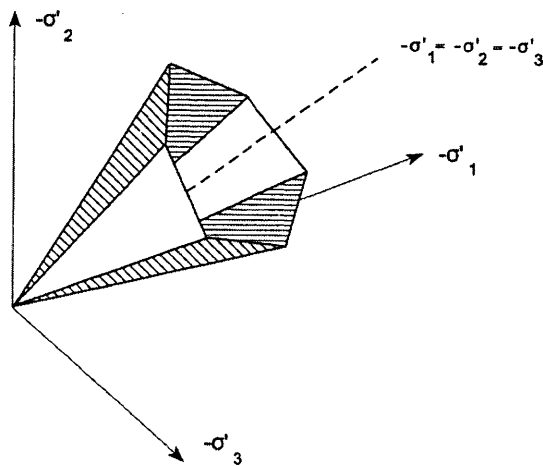

Figure A.1. Mohr – Coulomb failure surface in principal stress space

In addition to the yield functions, three plastic potential functions are defined for the Mohr – Coulomb model:

$$g_1 = \frac{1}{2}\left|\sigma_2' - \sigma_3'\right| + \frac{1}{2}\left(\sigma_2' + \sigma_3'\right)\sin\psi \qquad \text{(A.11a)}$$

$$g_2 = \frac{1}{2}\left|\sigma_3' - \sigma_1'\right| + \frac{1}{2}\left(\sigma_3' + \sigma_1'\right)\sin\psi \qquad \text{(A.11b)}$$

$$g_3 = \frac{1}{2}\left|\sigma_1' - \sigma_2'\right| + \frac{1}{2}\left(\sigma_1' + \sigma_2'\right)\sin\psi \qquad \text{(A.11c)}$$

The plastic potential functions contain a third plasticity parameter, the dilatancy angle ψ. This parameter is required to model positive plastic volumetric strain increments (dilatancy) as actually observed for dense soils. A discussion of all the model parameters used in the Mohr – Coulomb model is given at the end of this section.

When implementing the Mohr – Coulomb model for general stress states, special treatment is required for the investigation of two yield surfaces. Some programs use a smooth transition from one yield surface to another, i.e. the rounding – off of the corners. In PLAXIS, however, the exact form of the full Mohr – Coulomb model is implemented, using sharp transition from one yield surface to another. For a detailed description of the corner treatment the reader is referred to the literature.

For $c > 0$, the standard Mohr – Coulomb criterion allows for tension. In fact, allowable tensile stresses increase with cohesion. In reality, soil can sustain none or only very small tensile stresses. This behavior can be included in a PLAXIS analysis by specifying a tension cut – off. In this case, Mohr circles with negative principal stresses are not allowed. The tension cut – off introduces three additional yield functions, defined as:

$$f_4 = \left(\sigma_1' - \sigma_t\right) \le 0 \qquad \text{(A.12a)}$$
$$f_5 = \left(\sigma_2' - \sigma_t\right) \le 0 \qquad \text{(A.12b)}$$
$$f_6 = \left(\sigma_3' - \sigma_t\right) \le 0 \qquad \text{(A.12c)}$$

When the tension cut – off procedure is used, the allowable tensile stress, σ_t, is by default taken equal to zero. For these three yield functions an associated flow rule is adopted. For stress states within the yield surface, the behavior is elastic and obeys Hooke's law for isotropic linear elasticity. Hence, besides the plasticity parameters c, ϕ and ψ, input is required on the elastic shear Young's modulus E and Poisson's ratio v.

Basic Parameters of the Mohr – Coulomb model

The Mohr – Coulomb model requires a total of five parameters, which are generally familiar to most geotechnical engineers and which can be obtained from basic tests on soil samples. These parameters with their standard units are listed below:

- E → Young's modulus [KPa]
- v → Poisson's ratio [-]
- ϕ → Friction angle [°]

- c $\rightarrow$ cohesion [KPa]
- ψ $\rightarrow$ Dilatancy angle [$^{\circ}$]

1. *Young's modulus.* PLAXIS uses the Young's modulus as the basic stiffness modulus in the Mohr – Coulomb model, but some alternative stiffness moduli are displayed as well. A stiffness modulus has the dimension of stress. The values of the stiffness parameter adopted in a calculation require special attention as many geomaterials show a non – linear behavior from the very beginning of loading. In soil mechanics, the initial slope is usually indicated as E_0 and the secant modulus at 50% strength is denoted as E_{50}. Considering unloading problems, as in the case of tunneling and excavations, one needs E_{ur} instead of E_{50}.

   For soils, both the unloading modulus E_{ur}, and the first loading modulus E_{50}, tend to increase with the confining pressure. Hence, deep soil layers tend to have greater stiffness than shallow layers. Moreover, the observed stiffness depends on the stress path that is followed. The stiffness is much higher for unloading and reloading than for primary loading. Also, the observed soil stiffness in terms of a Young's modulus may be lower for drained compression than for shearing. Hence, when using a constant stiffness modulus to represent soil behavior one should choose a value that is consistent with the stress level and the stress path development. PLAXIS offers a very useful option in the Mohr – Coulomb soil model, which allows for the input of a stiffness increasing with depth.

2. *Poisson's ratio.* Standard drained triaxial tests may yield a significant rate of volume decrease at the very beginning of axial loading and consequently, a low initial value of Poisson's ratio. For some cases, such as particular unloading problems, it may be realistic to use such a low initial value, but in general when using the Mohr – Coulomb model the use of a higher value is recommended.

   The selection of a Poisson's ratio is particularly simple when the Mohr – Coulomb soil model is used for gravity loading. For this type of loading, PLAXIS should give realistic ratios of $K_0 = \sigma_h/\sigma_v$. Knowing that $\sigma_h/\sigma_v = v/(1-v)$ for one – dimensional compression it is easy to select a Poisson's ratio that gives a realistic value of K_0. In general, v is evaluated by matching K_0.

3. *Cohesion.* The cohesive strength has the dimension of stress. PLAXIS offers a special option for the input of layers in which the cohesion increases with depth.

4. *Friction angle.* The friction angle ϕ, is entered in degrees. High friction angles, as sometimes obtained for dense sands, will substantially increase plastic computational effort. The computing time increases more or less exponentially with the friction angle. Hence, high friction angles should be avoided when performing preliminary computations for a particular project. The friction angle largely determines the shear strength by means of Mohr's stress circles.

5. *Dilatancy angle ψ.* The dilatancy angle ψ, is specified in degrees. Apart from heavily overconsolidated layers, clay soils tend to show little dilatancy. This is not necessarily true for sands, however. Dense sands may exhibit a dilatancy angle

equal to $\phi - 30°$ whereas loose sands may even exhibit small negative values for the dilatancy angle.

Advanced Parameters of the Mohr – Coulomb model

The advanced features in the Mohr – Coulomb soil model comprise the increase of stiffness and cohesive strength with depth and the use of a tension cut – off. In fact, the latter option is used by default, but it may be deactivated here if desired.

- *Increase of Stiffness ($E_{increment}$).* In real soils, the stiffness depends significantly on the stress level, which means that the stiffness generally increases with depth. When using the Mohr – Coulomb model, the stiffness is a constant value. In order to account for the increase of the stiffness with depth the $E_{increment}$ value may be used, which is the increase of the Young's modulus per unit of depth (expressed in the unit of stress per unit depth). At the level given by the y_{ref} parameter, the stiffness is equal to the reference Young's modulus E_{ref}. The actual value of Young's modulus in the stress points is obtained from the reference value and $E_{increment}$. So there is a variation is stiffness applied, but still stiffness does not change as a function of the stress state.

- *Increase of cohesion.* PLAXIS offers an advanced option for the input of the clay layers in which the cohesion increases with depth. In order to account for the increase of the cohesion with depth the $c_{increment}$ – value may be used, which is the increase of cohesion per unit of depth. At the level given by the y_{ref} parameter, the cohesion is equal to the reference cohesion, c_{ref} as entered in the Parameters tab sheet. The actual value of cohesion in the stress points is obtained from the reference value and $c_{increment}$.

- *Tension cut – off.* In some practical problems an area with tensile stresses may develop. According to the Coulomb envelope this is allowed when the shear stress (or else the radius of the Mohr Circle) is sufficiently small. In some particular cases it is possible that a soil may fail in tension instead of in shear. Such behavior can be included by selecting the tension cut –off. In this case Mohr circles with positive principal stresses are not allowed. When selecting the tension cut – off allowable tensile strength may be entered.

A.3. The Hardening Soil Model (Isotropic Hardening)

In contrast to an elastic perfectly – plastic model, the yield surface of a hardening plasticity model is not fixed in the principal stress space, but it can expand due to plastic straining. Distinction can be made between two main types of hardening, namely shear hardening and compression hardening. Shear hardening is used to model irreversible strains due to primary deviatoric loading. Compression hardening is used to model irreversible plastic strains due to primary compression in oedometer loading and isotropic loading. Both types of hardening are contained in the present model.

The Hardening Soil model is an advanced soil model for the simulation of the behavior of both soft and stiff soils. When subjected to primary deviatoric loading, soil shows a decreasing stiffness and simultaneously irreversible plastic strains develop. In the special case of a drained triaxial test, the observed relationship between the axial strain and the deviatoric stress can be well approximated by a hyperbola. In the Hardening Soil Model as implemented in PLAXIS, the theory of plasticity is used rather than the theory of elasticity. Soil dilatancy and a yield cap are also included. These features make extend the Hardening Soil model greatly in comparison with a simple hyperbolic model.

The basic features of the Hardening Soil Model can be summarized below:

- Stress dependent stiffness according to a power law. This feature is essential for the problem dealt in this thesis.

- Plastic straining due to primary deviatoric loading.

- Plastic straining due to primary compression.

- Elastic unloading/reloading.

- Failure according to the Mohr – Coulomb model.

Hyperbolic relationship for standard drained triaxial test

A basic idea for the formulation of the Hardening Soil Model is the hyperbolic relationship between the vertical strain ε_1 and the deviatoric stress q, in primary triaxial loading. Here standard drained triaxial tests tend to yield curves that can be described by:

$$-\varepsilon_1 = \frac{1}{2E_{50}} \frac{q}{1-\dfrac{q}{q_a}}, q < q_f \tag{A.13}$$

In the above expression q_a is the asymptotic value of the shear strength. This relationship is plotted in figure S.2. The parameter E_{50} is the confining stress dependent stiffness modulus for primary loading and is given by the equation:

$$E_{50} = E_{50}^{ref} \left(\frac{c\cot\phi - \sigma_3'}{c\cot\phi + p^{ref}} \right)^m \tag{A.14}$$
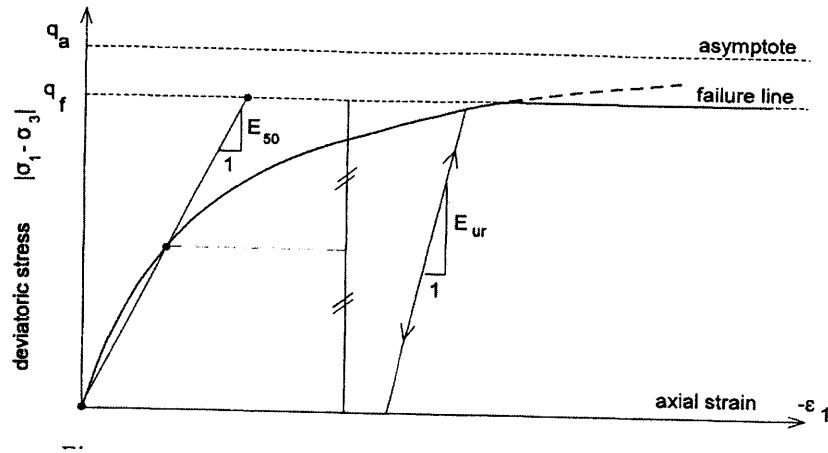
Figure A.2. Hyperbolic stress – strain relation in primary loading for a standard drained triaxial test.

E_{50}^{ref} is a reference stiffness modulus corresponding to the reference confining pressure p^{ref}. In PLAXIS, a default setting p^{ref} = 100 stress units is used. The actual stiffness depends on the minor principal stress σ'_3, which is the confining pressure in a triaxial test. The sign convention is that σ'_3 is negative for compression, contrary to conventional soil mechanics. The amount of stress dependency is given by the power m. In order to simulate a logarithmic stress dependency, as observed for soft clays, the power should be taken equal to 1.0.

The ultimate deviatoric stress q_f and the quantity q_a are defined as follows:

$$q_f = (c \cot \varphi - \sigma'_3)\frac{2\sin \phi}{1-\sin \phi}$$

$$q_a = \frac{q_f}{R_f}$$

(A.15)

Again it is remarked that σ'_3 is usually negative. The above relationship for q_f is derived from the Mohr – Coulomb failure criterion, which involves the strength parameters c and ϕ. As soon as $q = q_f$, the failure criterion is satisfied and perfectly plastic yielding occurs as described by the Mohr – Coulomb model. The ratio between q_f and q_a is given by the failure ratio R_f, which should obviously be smaller than 1. The value R_f = 0.9 is set as default.

For unloading and reloading stress paths, another stress – dependent stiffness modulus is used:

$$E_{ur} = E_{ur}^{ref}\left(\frac{c \cot \phi - \sigma'_3}{c \cot \phi + p^{ref}}\right)^m$$

(A.16)

E_{ur}^{ref} is the reference Young's modulus for unloading and reloading, corresponding to the reference pressure p^{ref}. In many practical cases, it is appropriate to set E_{ur}^{ref} equal to $3E_{50}^{ref}$; this is the default setting in PLAXIS.

Parameters of the Hardening soil model

Some parameters of the present hardening model coincide with those of the non – hardening Mohr – Coulomb model. These are the failure parameters c, ϕ and ψ.

The basic parameters for soil stiffness are:
- Secant stiffness in standard drained triaxial test $\rightarrow E_{50}^{ref}$
- Tangent stiffness for primary oedometer loading $\rightarrow E_{oed}^{ref}$
- Power for stress – level dependency of stiffness $\rightarrow$ m.

Advanced Parameters are:
- Unloading/Reloading Stiffness $\rightarrow E_{ur}^{ref}$ (default $E_{ur}^{ref} = 3E_{50}^{ref}$)
- Poisson's ratio for unloading/reloading $\rightarrow v_{ur}$ (default $v_{ur} = 0.2$)
- Reference: stress for stiffness $\rightarrow p^{ref}$ (default $p^{ref} = 100$ stress units)
- K_0 – value for normal consolidation $\rightarrow K_0^{nc}$ (default $K_0^{nc} = 1 - \sin\phi$)
- Failure ratio $\rightarrow R_f$ (default value $R_f = 0.9$)
- Tensile strength $\rightarrow \sigma_{tension}$ (default value is zero)
- The option for varying cohesion linearly with depth is also available in the Hardening Soil Model.

Stiffness moduli E_{50}^{ref}, E_{oed}^{ref} and power m

The advantage of the Hardening soil model over the Mohr – Coulomb model is not only the use of a hyperbolic stress – strain curve instead of a bilinear curve, but also the control of stress level dependency. When using the Mohr – Coulomb model, the user has to select a fixed value of Young's modulus whereas for real soils this stiffness depends on the stress level. It is therefore necessary to estimate the stress levels within the soil and use these to obtain suitable values of stiffness. With the Hardening Soil model, however, this cumbersome selection of input parameters is not required. Instead, a stiffness modulus E_{50}^{ref} is defined for a reference minor principal stress of $\sigma_3 = p^{ref}$. The default value for is $p^{ref} = 100$ stress units.

In PLAXIS, the stiffness of the soil can be input using instead of the above stiffness moduli, the shear moduli. Within classical theory of elasticity, conversion between E and G goes by the equation $E = 2(1+v)G$. As E_{ur} is a real elastic stiffness, one may thus write $E_{ur} = 2(1+v)G_{ur}$, where G_{ur} is an elastic shear modulus. In PLAXIS, G_{ur} cannot be input directly, but it can be input via E_{ur} and v_{ur}. The modulus E_{50} is not used within a concept of elasticity. As a consequence, there is no simple conversion from E_{50} to G_{50}.

In contrast to elasticity-based models, the elastoplastic Hardening Soil model does not involve a fixed relationship between the drained triaxial stiffness E_{50} and the oedometer stiffness E_{oed} for one – dimensional compression. Instead, these stiffness moduli can be input independently.

For the oedometric stiffness modulus a relationship similar to the one valid for E_{50} holds:

$$E_{oed} = E_{oed}^{ref} \left(\frac{c \cot \phi - \sigma_1'}{c \cot \phi + p^{ref}} \right)^m \qquad\qquad\text{(A.17)}$$

Figure S.3 defines E_{oed}^{ref}. Of course, the oedometric stiffness modulus is defined in terms of σ'_1 and considering primary loading.
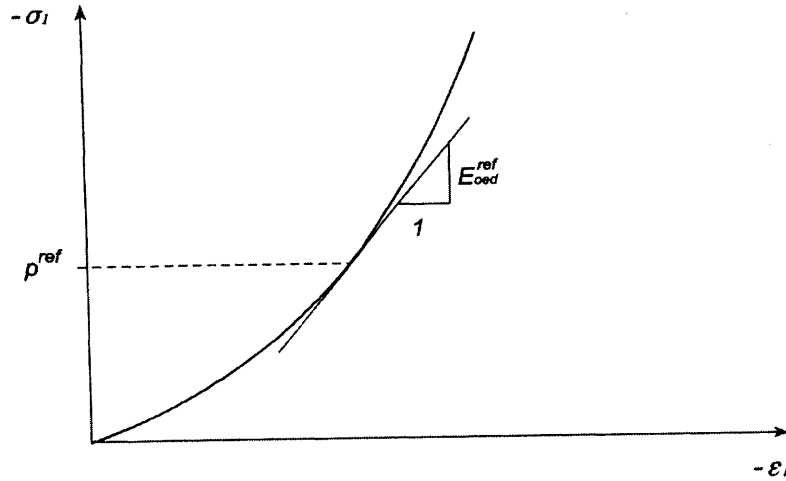

Figure A.3. Definition of E_{oed}^{ref} in oedometer test results

The details on the definition of the cap yield surface and the plastic volumetric strains will not be in focus on this thesis. The reader is referenced to the PLAXIS User Manual for further details on the Hardening Soil Model.

B. EQUIVALENT BEAM STIFFNESS, AREA, AND MOMENT OF INERTIA FOR FINITE ELEMENT MODELING OF A STRUCTURE

In the following, a rational methodology is presented for the calculation of the equivalent beam stiffness of a real structure. The problem arises in an attempt to include a structure overlying a tunnel in one model comprising of all the three components in this complicated phenomenon of interaction; tunnel lining, soil, structure. It is obvious that for the description of the structure in this case, an elegant model is desired which will reduce the complexity of the analysis. Since, in this problem emphasis is given on the influence of an existing surface structure on the shape and magnitude of the settlement trough, it is safe to reduce the geometric characteristics of the structure without losing that element, being the rigidity of the structure, which is the cause for a modification of the developed settlement trough below the structure. This can be done with the implementation of a linear elastic beam modeling the structure.

Some concerns and remarks may arise. The description of a real three – dimensional structure by a linear elastic beam constitutes a very coarse simplification. Not only in terms of the geometrical effect in the calculation of the stiffness of the equivalent beam, but also in terms of the complexity of the real structure, where columns, beams, special elements, cladding, openings, plates and foundation contribute in a special way in the structure's stiffness. Even so, what is the structure's rigidity? In a macro-scale, it may have some sense, but in reality it is the stiffness of the separate structural elements that when combined together give a total stiffness to the structure. The transition of a real structure to a beam is certainly not an easy task unless some very fundamental assumptions are considered. A second remark is that the stiffness, which is being considered, is for the description of a material that will behave as linear elastic. This may be true in reality in the range of small strains. However, this whole methodology is developed with the ultimate goal being the assessment of potential of damage in the structure. If a structure gets damaged (cracked, with large strains or large displacements or both) then the assumption of linear elastic behavior becomes a crude approximation. Later, it will be presented that the influence in the settlement trough comes about in terms of orders of magnitude of the relative stiffness of the system soil – structure or similarly in terms of orders of magnitude of the stiffness of the structure assuming that the rigidity of the soil is kept constant or that any changes in it are taken into account (actually they do, when the Hardening Soil model is implemented). Can damage reduce the stiffness of a structure one order of magnitude or more? If it does, the suggested methodology may be inaccurate in predicting the potential of damage in the structure. If the influence of damage is not that significant in evaluating the stiffness of the structure, then the suggested methodology obtains a larger validity.

Having the above remarks in mind, the method for calculating an equivalent beam stiffness, area and moment of inertia can be presented. The method considers that the structure can be viewed as a set of slabs joined with columns. An assumption is made that the columns do not contribute to the stiffness but they work as transferring the same mode of deformation to all the slabs. So, the slabs of the structure can be viewed as constituting an imaginary beam, for which the area and the moment of inertia are calculated. In the simple case in which the structure is comprised of many identical slabs and has n – stories the equivalent beam axial and flexural stiffness are given by the following expressions:

$$(E_C A)_{struct} = (n+1)(E_c A)_{slab}$$

$$(E_c I)_{struct} = E_c \sum_{1}^{n+1} (I_{slab} + A_{slab} H^2)$$

(B.1)

In the above expressions, E_c is the Young's modulus for the concrete (concrete slabs are assumed), A is the area of the cross – section of the slab or structure and I the moment of inertia. In the second equation, H denotes the distance between the neutral axis of the structure to the individual slab's neutral axis. This is the well – known Steiner's theorem.

Some representative values that can be used in analyses are:

- Elastic modulus of the concrete: $E_c = 23 \times 10^3$ MN/m^2
- Thickness of slab = 0.15m
- Area of a single slab = 0.15m^2/m
- Second moment of inertia = 2.81×10^{-4} m^4/m
- Axial Stiffness of a single slab = 3450 MN/m
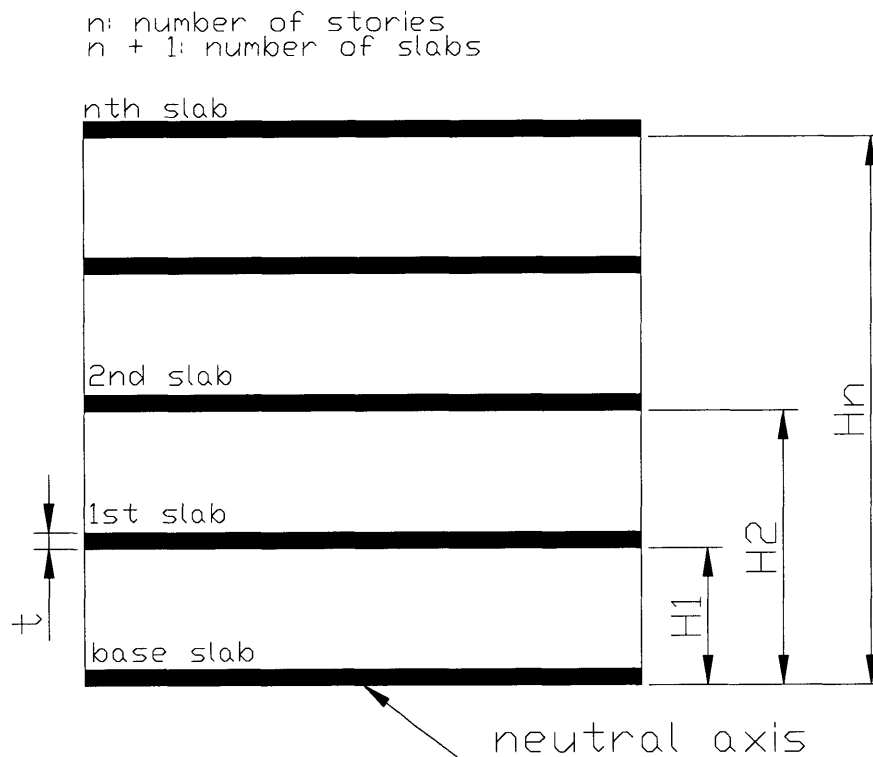- Bending Stiffness of a single slab = 6.47 MPa/m

Figure B.1 Idealization of structure by a group of slabs

119

LIST OF REFERENCES

1. Attewell, P.B., Yeates, J. and Selby, A.R., 1986. Soil movements induced by tunneling and their effects on pipelines and structures. *Blackie.*

2. Bjerrum, L., 1963. Discussion. *Proc. European Conference on Soil Mechanics and Foundation Engineering, Wiesbaden, Vol. III, 135.*

3. Boscardin, M.D. & Cording, E.J., 1989 Building response to excavated induced settlement, *Jnl. Geot. Engng., ASCE, Vol. 115, No. 1, 1-21.*

4. Breth, H. and Champosse, G., 1974. Settlement behavior of buildings above subway tunnels in Frankfurt Clay. *BGS Conference "Settlement and Structures", Cambridge, 1974, p. 329 – 336.*.

5. Burd, H.J., Houlsby, G.T., Augarde, C.E., Liu, G., 2000, Modeling tunneling – induced settlement of masonry buildings, *Proc. Instn. Civ. Engrs., Geotech. Engng., 2000, 143, Jan., 17-29.*

6. Burland, J.B & Wroth, C.P., 1974, Settlement of buildings and associated damage, *BGS conference "Settlement and Structures", Cambridge, 611-651.*

7. Burland, J.B., 1995, Assessment of risk of damage to buildings due to tunneling and excavation, *Proc. 1st Int. Conf. Earthquake Geot. Engineering IS – Tokyo, 1995.*

8. Burland, J.B. & Standing, R.J., Mair, R.J., Linney, L.F., Jardine, F.M., 1996, A collaborative research programme on subsidence damage to buildings: Prediction, Protection, Repair, *Geotechnical Aspects of Underground Construction in Soft Ground, Mair & Taylor Eds. Balkema, Rotterdam, 1996.*

9. Burland, J. B., Standing R. J., Jardine, F. M., 2002. Assessing the risk of damage due to tunneling – lessons from the Jubilee Line Extension, London. *Proc. 2nd Int. Conference on Soil Structure Interaction in Urban Civil Engineering, Zurich / March 2002.*

10. Dias, D. and Kastner, R., 2002. Tunneling in Soils – ground movements and damage to buildings. *Proc. 2nd Int. Conference on Soil Structure Interaction in Urban Civil Engineering, Zurich / March 2002.*

11. Forbes, J., Bassett, R.H. and Latham M.S., 1994. Monitoring and Interpretation of the movement of the Mansion House due to tunneling. *Proc. Instn Civ. Engrs Geotechnical Engineering 1994, 107, Apr., 89.98.*

12. Frischmann, W.W., Hellings, J.E., Gittoes, G. & Snowden, C., 1994, Protection of the Mansion House against damage caused by ground movements due to the Docklands Light Railway Extension, *Proc. Instn. Civ. Engnrs, Geotechnical Engineering, Vol. 107, 65 – 76*

13. Harris, D.I., Mair, R.J., Love, J.P., Taylor, R.N. and Henderson, T.O., 1994. Observations of ground and structure movements for compensation grouting during tunnel construction at Waterloo station. *Geotechnique, 44;4;691 – 713.*

14. Harris, D. I., Mair R. J., Burland J. B., Standing J. R., 2000. Compensation Grouting to control tilt of Big Ben Clock Tower. *Geotechnical Aspects of Underground Construction in Soft Ground, Kusakabe, Fujita & Miyazaki (eds.). Balkema, Rotterdam, 2000.*

15. Jardine, R.J., Potts, D.M., Fourie, A.B. & Burland, J.B., 1986, Studies of the influence of nonlinear stress – strain characteristics in the soil – structure interaction, Geotechnique, Vol. 36, No. 3, 377-396.

16. The Institution of Structural Engineers, 1978, 1989 and 2000. State of the Art Report – Structure – Soil Interaction. Revised and extended in 1989, 2nd edition August 2000. *The Institution of Structural Engineers, London.*

17. The Institution of Structural Engineers, 1994. Subsidence of low rise buildings. *The Institution of Structural Engineers.*

18. Jennings, J.E. and Kerrich, J. E., 1962. The heaving of buildings and the associated economic consequences, with particular reference to the Orange Free State Goldfields. *The Civil Engineers of South Africa, 5;5;122.*

19. Koiter, W. T., 1960. General theorems for Elastic – Plastic solids. In: Progress in Solid Mechanics (eds. I.N. Sneddon, R. Hill), Vol. I., North – Holland, Amsterdam, pp. 165 – 221.

20. MacLeod, I. A. and Littlejohn, G.S. 1974. Discussion on Session 5. *Conference Settlement of Structures, Cambridge, Pentech Press, London, pp. 792 – 795.*

21. Mair, R. J., Taylor, R.N., 1997. Bored Tunneling in the urban environment. *Proc. 14th Int. Conference in Soil Mechanics and Foundation Engineering. Balkema, Amsterdam, 4; 2353 – 2385.*

22. National Coal Board, 1975. Subsidence Engineering Handbook. National Coal Board Production Dept., UK.

23. Nikolinakou, M. A., 1999. Tunneling in Urban Environment – Settlements (in Greek). Thesis in partial fulfillment of the Diploma in Civil Engineering. *National Technical University of Athens, Department of Civil Engineering, Geotechnical Division.*

24. O' Reilly, M.P., 1996, Discussion: Comments on the risk of damage to structures, *Geotechnical Aspects of Underground Construction in Soft Ground, Mair & Taylor Eds. Balkema, Rotterdam, 1996.*

25. O' Reilly, M.P. and New, B.M., 1982. Settlement above tunnels in the United Kingdom – their magnitude and prediction. *Tunneling '82, London, 173 – 181.*

26. PLAXIS, Finite Element Code for Soil and Rock Analyses – Version 7 – User's Manual, Edited by Brinkgreve R.B.J., Vermeer P.A., et al. A. A. BALKEMA / ROTTERDAM / BROOKFIELD / 1998.

27. Polshin, D. E. & Tokar, R. A., 1957, Maximum allowable non-uniform settlement of structures, *Proc., 4th International Conf. On Soil Mechanics and Foundation Engineering, 1, London, England, 402-405.*

28. Potts, D.M. & & Addenbrooke, T.I., 1996, The influence of an existing surface structure on the ground movements due to tunneling, *Geotechnical Aspects of Underground Construction in Soft Ground, Mair & Taylor Eds. Balkema, Rotterdam, 1996.*

29. Potts, D.M. & & Addenbrooke, T.I., 1997, A structure's influence on tunneling induced ground movements, *Proc. Instn Civ. Engrs Geotechnical Engineering 1997, 125, Apr., 109 – 125.*

30. Price, G., Longworth, T. I., Sullivan, P. J. E., 1994. Installation and performance of monitoring systems at the Mansion House. *Proc. Instn Civ. Engrs Geotechnical Engineering 1997*, 107, Apr., 77 - 87.

31. Rankin, W. J., 1988. Ground movements resulting from urban tunneling; Predictions and effects. *Engineering Geology of Underground Movement. Geological Society, Engineering Geology Special Publication No. 5, 79 – 92.*

32. Schanz, T., Vermeer, P.A., Bonnier, P.G., 1999. Formulation and Verification of the Hardening Soil Model. Submitted for publication to Int. J. Numer. Anal. Meth. Geomech.,

33. Simic, D. & Gittoes, G., 1996, Ground behavior and potential damage to buildings caused by the construction of a large diameter tunnel for the Lisbon Metro, *Geotechnical Aspects of Underground Construction in Soft Ground, Mair & Taylor Eds. Balkema, Rotterdam, 1996.*

34. Skempton, A. W. & MacDonald, D.H., 1956, The allowable settlement of buildings, *Proc., Inst. of Civil Engineers, Part III, 5, 727-784.*

35. Taylor, R. N., Grant R. J., 1998, Centrifuge modeling of the influence of surface structures on tunneling induced ground movements. *Tunnels and Metropolises, Volume I, Balkema 1998, pp. 261 – 266.*

36. Timoshenko, S., (1957), Strength of Materials – Part I, *D. Van Nostrand Co. Inc., London, England.*